Optimal Dynamic Strategies for Index Tracking and Algorithmic Trading

Brian Ward

Submitted in partial fulfillment of the
requirements for the degree
of Doctor of Philosophy
in the Graduate School of Arts and Sciences

Columbia University

2017

ABSTRACT

Optimal Dynamic Strategies for Index Tracking and Algorithmic Trading

Brian Ward

In this thesis we study dynamic strategies for index tracking and algorithmic trading. Tracking problems have become ever more important in Financial Engineering as investors seek to precisely control their portfolio risks and exposures over different time horizons. This thesis analyzes various tracking problems and elucidates the tracking errors and strategies one can employ to minimize those errors and maximize profit.

In Chapters 2 and 3, we study the empirical tracking properties of exchange traded funds (ETFs), leveraged ETFs (LETFs), and futures products related to spot gold and the Chicago Board Option Exchange (CBOE) Volatility Index (VIX), respectively. These two markets provide interesting and differing examples for understanding index tracking. We find that static strategies work well in the nonleveraged case for gold, but fail to track well in the corresponding leveraged case. For VIX, tracking via neither ETFs, nor futures portfolios succeeds, even in the nonleveraged case. This motivates the need for dynamic strategies, some of which we construct in these two chapters and further expand on in Chapter 4. There, we analyze a framework for index tracking and risk exposure control through financial derivatives. We derive a tracking condition that restricts our exposure choices and also define a slippage process that characterizes the deviations from the index over longer horizons. The framework is applied to a number of models, for example, Black-

Scholes model and Heston model for equity index tracking, as well as the Square Root (SQR) model and the Concatenated Square Root (CSQR) model for VIX tracking. By specifying how each of these models fall into our framework, we are able to understand the tracking errors in each of these models.

Finally, Chapter 5 analyzes a tracking problem of a different kind that arises in algorithmic trading: schedule following for optimal execution. We formulate and solve a stochastic control problem to obtain the optimal trading rates using both market and limit orders. There is a quadratic terminal penalty to ensure complete liquidation as well as a trade speed limiter and trader director to provide better control on the trading rates. The latter two penalties allow the trader to tailor the magnitude and sign (respectively) of the optimal trading rates. We demonstrate the applicability of the model to following a benchmark schedule. In addition, we identify conditions on the model parameters to ensure optimality of the controls and finiteness of the associated value functions. Throughout the chapter, numerical simulations are provided to demonstrate the properties of the optimal trading rates.

Contents

List of Figures

List of Tables

Acknowledgements

First and foremost I must thank my advisor, Tim Leung. Tim has a passion for research and Financial Engineering that immediately resonated with me upon meeting him. His research style and dedicated focus is something I strive to attain every day when I begin work. Without Tim, I would not have been successful in my Ph.D. program and I am forever grateful to him for showing me how to conduct research.

Next, I would like to thank the other members of my committee: Agostino Capponi, Ton Dieker, Hongzhong Zhang and Yuchong Zhang. I appreciate them taking the time to sit for my defense and as well as carefully reading over this thesis.

My academic career has been shaped by a number of amazing teachers, lecturers and professors. Going all the back to Commack High School, I must thank Derek Pope, Nancy Pally, Barbara Gerson and Bruce Leon for giving me my mathematical foundation. Whether it was Math Fair, AP/IB Calculus class, or the Math Team, I always found myself immersed in what I was doing/learning from them. Next, I dove deeper into the field of mathematics by studying in the Applied Mathematics and Statistics (AMS) Department at Johns Hopkins University (JHU). It was there that discovered how useful mathematics is for finance and found that I wanted to pursue a Ph.D. program while researching Financial Engineering. Amongst the many faculty who lectured me through my undergraduate and master's studies I must thank Jian Kong, Beryl Castello, John Wierman, Daniel Naiman, Donniell Fishkind, David Audley, Fred Torcaso, Avanti Athreya, and Agostino Capponi. Finally, at Columbia I had the pleasure of learning the core materials in Optimization and Stochastic Modeling from

Donald Goldfarb, Daniel Bienstock, Ward Whitt and David Yao. Their lectures gave me new insights into materials already familiar to me as well as introduced me to new branches of Operations Research in an engaging way.

I also owe gratitude to the various staff at JHU and Columbia that facilitated every step of the way and brought me to this point in my academic career. They have made sure that everything went through smoothly so I could focus on my studies and my research. From JHU I would like to thank Kristen Bechtel and Sandy Kirt. From Columbia I would like to thank Jaya Mohanty, Krupa Thakore, Adina Brooks, Jenny Mak, Lizbeth Morales, and Kristen Maynor.

A great education is nothing without friends to share it with. My colleagues at JHU and Columbia are nothing short of amazing and I'm glad to have worked with them on various projects and sharing conversations with them about courses. From Johns Hopkins I would especially thank Jordan Pryor, Matt Molisani and Ilana Bookner, whom I worked with on my first research project in MiLB Scheduling. At Columbia, I learned a lot from my fellow students: Jalaj Bhandari, Mauro Escobar, Itai Feigenbaum, Fei He, Randy Jia, Xin Li, Brian Lu, Cun Mu, and Nouri Sakr. Some of these students served as my TA in various courses and I am especially grateful to them for helping me along the way. Additionally, I spent a great deal of time learning from Allen Cheng, Kevin Guo, and Michael Hamilton. I have known Allen since we met at JHU and we will continue to work together at AQR. Kevin and I share Tim as an advisor and naturally, we have common intellectual interests. Our conversations have led to furthering of each other's projects and I know our collaboration will never end. Finally, Michael has been one of my closest friends here in the department. We shared Mudd 323 as an office space for two years and quite often, were the only two people there. In those times, our friendly banter made this Ph.D. program all the more enjoyable.

My brothers and sister have always supported every goal I have set and encouraged everything I work on. My true goal is to be like them and I owe them for setting such high

standards. My brother Steve showed me that anything can be accomplished by working hard and setting your mind to it. He is dedicated to everything he does and I have learned from him that with focus, no goal is impossible. Charles, my oldest brother, was the first person in my life to show me that mathematics could be fun and exciting. I fondly remember practicing for the Continental Math League with his help when I was in second grade. We continue to challenge each other to learn more, whether it be mathematics, statistics or programming. Finally, my sister Jen showed me how to dream big. My mom has told me many times that when Jen told her that she would like to become a medical doctor, my mom said, "I don't think we know how to do that! But let's find out." With that story in my mind, I have always set my mind to big goals, sometimes dreaming up what others would see as impossible. Achieving those goals required all of their help and support.

A mother will always be your biggest cheerleader. She is the only person in your life who has literally been cheering you on since day one. There is nothing quite like the smile on my mom's face as I tell her about something I am planning on doing, already working on, or have achieved. My mom has such a pride in me and that pride powers me through every single tough moment.

Finally, I would like to thank my girlfriend Sara Furia. We have been together for nine and a half years and she is truly my best friend. She has listened to every stressful moment, and helped keep me grounded through it all. Because of Sara, I have been able to stay calm when things seemed impossible to deal with. She always has the right thing to say to keep me going. I look forward to our life together in Stamford and all that it will bring us. Although life is unpredictable, one thing is certain: Sara will always be there by my side.

In memory of my father.

Chapter 1

Introduction

Many institutional investors seek to control their portfolio's exposure to various market factors. Asset managers, hedge funds and other investors must carefully set the exposures of their portfolio in order to provide the promised returns their clients demand. Recognizing this need, many major investment funds have issued a number of exchange-traded funds (ETFs), exchange traded notes (ETNs), and exchange traded products (ETPs) that attempt to give investors the desired exposure. In addition to these base products, investment funds also issue leveraged ETFs (LETFs). Such products promise some (possibly negative) multiple of the daily returns of a reference index or basket of other assets.

However, empirically it has been found that these products can fail to achieve their stated goals. Moreover, it is often the case that these products lose money relative to those targets. The reasons for these failures can be attributed to the static or passively dynamic strategies followed by many of the ETF providers. By passively dynamic, we mean that the strategy involves a time-deterministic allocation into various assets. Though such strategies are dynamic, they do not adapt to changing markets. Because of these issues, it is essential to empirically track and theoretically explain these observed deviations.

The markets for gaining exposure to gold and volatility provide interesting examples for understanding these deviations. Gold is often viewed by investors as a safe haven or a hedge against market turmoils, currency depreciation, and other economic or political events (see

Ghosh et al. (2004) and Baur and McDermott (2010) for empirical investigation of gold's role as a safe haven). Gold (L)ETFs are a natural investment vehicle to obtain this hedge in one's portfolio. Baur (2013) studies the cost-effectiveness of gold ETFs relative to physical gold holdings, while Ivanov (2013) studies the tracking errors for gold (as well as silver and oil) ETFs over the period from March 2009 to August 2009. Both studies find that gold ETFs are useful in tracking spot gold.

In contrast to the ease of tracking spot gold, tracking the Chicago Board Options Exchange's (CBOE's) Volatility Index (VIX) has been shown to be quite difficult. VIX ETFs are typically constructed from a portfolio of futures contracts. However, such futures based ETFs are not useful for diversification and achieving volatility exposure as demonstrated by Husson and McCann (2011) and Deng et al. (2012). In particular, the Barclay's iPath S&P 500 VIX Short-Term Futures ETN (VXX) has significant tracking error with respect to VIX. This is of course due to the tracking errors of these products. Futures based ETPs and their tracking errors are studied further by Alexander and Korovilas (2013) and Whaley (2013).

Nonetheless, exposure to VIX gives a similar hedge in that VIX rises in times of market turmoil. We illustrate the effects of having exposure to VIX by considering the 2011 U.S. credit rating downgrade by Standard and Poor's. News of a negative outlook by S&P of the U.S. credit rating broke on April 18$^{\text{th}}$, 2011.[1] A retail investor only holding the SPDE S&P 500 ETF, SPY (which *is* a tradable index tracking ETF), could have turned an unprofitable several months (100 days after the news) into a relatively stable period by investing a small fraction (10%) of his or her wealth into VIX (see Figure 1.1.) The blue time series represents the hedged portfolio utilizing VIX, while the purple time series is unhedged (100% in SPY.) On the left panel, the investment is held from the day after the above news story through a month past the official downgrade on August 5$^{\text{th}}$, 2011.[2] The hedged portfolio is stable through the downgrade and ends up with a small positive return, while the unhedged portfolio loses about 10%.

[1] See New York Times article: `http://www.nytimes.com/2011/04/19/business/19markets.html`.

[2] See: `http://www.nytimes.com/2011/08/06/business/us-debt-downgraded-by-sp.html`.

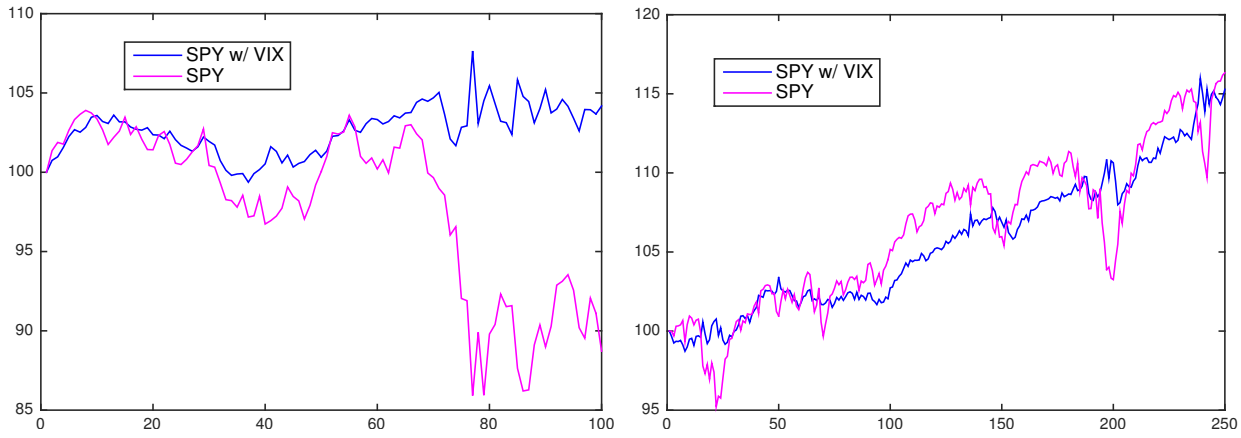

(a) April 2011 - Sept. 2011 (b) Jan. 2014 - Dec. 2014

Figure 1.1: Hedged portfolios of SPY with 10% fraction of wealth invested in VIX from April 19$^{\text{th}}$, 2011 to September 9$^{\text{th}}$, 2011 (left) and all of 2014 (right). The x-axis marks the trading day number, while the y-axis marks the price. All portfolios are initialized to \$100.

The stability of utilizing VIX can be demonstrated even when there is not much market turmoil. On the right panel of Figure 1.1 we plot the same pair of portfolios over the entire 2014 calendar year. Though both earn roughly the same 15% return, though the SPY only portfolio is more volatile than the hedged portfolio. The large drawdowns (for example on October 15$^{\text{th}}$) are met by rises in VIX thereby stabilizing the portfolio's value. This hedge motivates us to understand how to trade in such a way as to mimic the daily returns of VIX and more general indices or market exposures.

In this thesis, we study the index tracking problem through the use of derivatives contracts. We begin in Chapter 2 with an empirical study of products traded on the market related to gold. In particular, we study the spot price, gold futures and various gold (L)ETFs. There are significant price co-movements amongst these assets. Moreover, we show that static portfolios consisting of one or two futures with different maturities can effectively replicate the physical spot gold price. As for leveraged gold ETFs, their average returns tend to be lower than the corresponding multiple ($\beta \in \{3, 2, -2, -3\}$) of the spot's returns, and the under-performance worsens over a longer holding period. In order to track the leveraged benchmark, we construct a dynamic leveraged portfolio using the 1-Month futures. We demonstrate that the portfolio tracks the leveraged benchmark better than the

corresponding LETFs, and has better returns over multiple years. Chapter 2 is based on Leung and Ward (2015).

In Chapter 3, we adopt the same methodology of Chapter 2 to the market for volatility. However, the results are quite different and we find that VIX is much harder to track. Because of the mean reverting nature of VIX, VIX futures suffer strongly from roll yield losses and persistently lose money relative to the benchmark. Thus, static portfolios completely fail even in the case of tracking the unlevered benchmark. In contrast to the previous chapter, we also constructs portfolios by optimizing the coefficients with respect to another tracking criterion. But even in this case, tracking VIX with static portfolios appears completely impossible. We construct a simple myopic approach, which tracks well in simulation studies, but when backtested it does not perform well. The results of this chapter, along with the failure of static portfolios for leveraged exposure in Chapter 2 motivate the need for further exploration of dynamic strategies.

In Chapter 4, we turn our attention to dynamic strategies. We develop a general framework for understanding index tracking and exposure control using derivatives. The framework is useful for all asset classes as long as that asset class is modeled by a continuous diffusion process. The exposure control problem is an inverse problem to the dynamic hedging problem. In that problem, the goal is to dynamically trade one or more underlying assets in such a way as to replicate the price evolution of the newly created derivative. Of crucial importance in the dynamic hedging problem is the tradability of the underlying asset. In the problem that we pose in Chapter 4, the underlying and/or its driving factors may not be directly traded, but derivatives on the underlying *are* traded. We use derivatives to replicate (or more generally, control the exposure to) the underlying asset returns and the factors.

The results of Chapter 4 facilitate our understanding of the successes and failures of various (L)ETFs. In particular, we can quantify the divergence of portfolio returns from target (leveraged) returns of the index and its factors via a slippage process, so-named because it is typically negative. Moveover, we discuss how many well-known models fall into

our framework. In particular, we discuss index tracking in the context of the Black-Scholes and Heston Models, which are typically used for modeling equity prices. We also discuss the framework in the context of two models typically used for the pricing of VIX derivatives (see Grübichler and Longstaff (1996) and Mencía and Sentana (2013)). There, we use VXX as an example portfolio, and give reasons why VXX can fail to track VIX if indeed VIX follows the posited dynamics. Chapter 4 is based on Leung and Ward (2017).

In Chapter 5, we consider the low level execution of these trading strategies. This problem is itself another tracking problem, but of a different kind. In particular, the trader must choose how to use market and limit orders so as to purchase or liquidate a given asset over a finite time horizon. In this chapter, we analyze a continuous-time stochastic model for optimal execution using both order types thereby extending the foundational market impact model of Almgren and Chriss (2000). In particular, we include fill uncertainty for limit orders as well as a number of other features: a penalty for incomplete liquidation, a trade director and a speed limiter. These penalties force the algorithm to trade to full liquidation while simultaneously tailoring the sign and magnitude of the trading rates. Our key result is the solution to a stochastic optimal control problem, whose associated nonlinear HJB equation can be simplified to a system of linear ODEs. The methodology can be applied to tracking a benchmark schedule of stock holdings as well. This schedule following problem has become important to many brokerages recently as they seek to execute their clients' trades while following specific goals. The results in Chapter 5 are adapted from Bulthuis et al. (2017b), an abridged version of which was published online in RISK Magazine (see Bulthuis et al. (2017a)).

1.1 Market Mechanism

Before beginning our study, let us discuss the mechanics of the futures and equity markets that we analyze empirically in Chapters 2 and 3 and theoretically in Chapter 4. First, gold futures are exchange-traded contracts written on 100 troy ounces of gold, with a number of

available delivery dates within 6 years of any given trading date. In the US, gold futures are traded at the New York Mercantile Exchange (NYMEX). The available months include the front three months, every February, April, August and October falling within the next 23 months, and every June and December falling within the next 72 months. Trading for any specific contract terminates on the third to last business day of the delivery month.[3]

The gold ETFs and ETNs traded on the market are designed to track the spot price of gold, and are liquidly traded on exchanges. In fact, the SPDR Gold Trust ETF (GLD), is one of the most traded ETFs with an average trading volume of 7.96 million shares and market capitalization of $34.5 billion as of June 2017.[4] Besides the spot gold ETF, GLD, there are also LETFs written on gold. In the gold market, the leverage ratios that exist are are ± 2 and ± 3. Major issuers include ProShares, iShares, and VelocityShares (see Table 1.1.) For example, the VelocityShares 3x Long Gold ETN (UGLD) provides a return of 3 times the gold spot price. Furthermore, one can take a bearish position on the gold spot price by investing in an LETF with a negative leverage ratio. An example is the VelocityShares 3x Inverse Gold ETN (DGLD).

LETF	Issuer	β	Fee	Inception Date
GLD	iShares	1	0.40%	November 18$^{\text{th}}$, 2004
UGL	ProShares	2	0.95%	December 1$^{\text{st}}$, 2008
GLL	ProShares	-2	0.41%	December 1$^{\text{st}}$, 2008
UGLD	Janus	3	1.35%	October 14$^{\text{th}}$, 2011
DGLD	Janus	-3	1.35%	October 14$^{\text{th}}$, 2011

Table 1.1: A summary of the available gold (L)ETFs. For the LETFs, those with higher absolute leverage ratios, $|\beta| \in \{2, 3\}$, have higher expense fees.

In the market for volatility, VIX futures began trading on March 26$^{\text{th}}$, 2004. Naturally, they provide exposure to volatility and therefore allow for a hedge for the asymmetric volatility effect. In particular, when equity returns are low, volatility tends to be high (see e.g. Black (1976)). VIX futures have a contract multiplier of $1,000, meaning that one contract

[3]Historical quotes and contract specifics of gold futures are obtained from the CME Group `http://www.cmegroup.com/trading/metals/precious/gold_contract_specifications.html`.

[4]According to ETF Database `http://www.etfdb.com/compare/volume`.

is worth $1,000 times the quoted futures price. In fact, VIX futures were scaled down by a factor of 10 on March 26$^{\text{th}}$, 2007. At this point in time, the scaling aligned VIX futures prices to be in accordance with quoted VIX prices.[5] In terms of available maturities, initially only four existed: the front 3 months and the 6-Month contract. Two years later the CBOE began to offer more contracts including a 9 and 12-Month contract and for some time a 24-Month contract. At this point in time, the established contracts are more stable and on any given day there are between seven and nine futures contracts available for trading. These contracts always consist of the front seven through nine months.[6]

Just as in the gold market, there are (L)ETFs linked to VIX. However, such (L)ETFs do not claim to track VIX directly. Instead, the index that these (L)ETFs track (or track some possibly negative multiple of) is the S&P-500 Short Term VIX Futures Index. Thus, all (L)ETFs displayed in Table 1.2 consist of a portfolio of short term (1 or 2-Month maturity) VIX futures just as the index itself does.[7] Nonetheless it is the goal of this thesis to better understand how to properly gain exposure to volatility without being exposed to the well known losses that portfolios of futures suffer. Thus, we will be benchmarking VIX ETFs to VIX itself. In fact, in Chapter 3 we will focus our attention on benchmarking the performance of VXX, but it is useful to know there are other VIX (L)ETFS available, especially those with $\beta < 0$, given the recent downtrend in volatility.[8]

1.2 Literature Review

Tracking an index has been well studied in the literature from a number of different perspectives. For example, Bamberg and Wagner (2000) demonstrate that regression assumptions are often violated in the context of index tracking. However, they show that regression anal-

[5]Refer to `http://cfe.cboe.com/publish/CFEinfocirc/CFEIC07-003%20.pdf` for details on the rescaling.

[6]See `http://cfe.cboe.com/products/spec_vix.aspx`. The CBOE states they will list up to nine near-term months for trading.

[7]See `http://us.spindices.com/indices/strategy/sp-500-vix-short-term-index-mcap` for details on S&P-500 Short Term VIX Futures Index.

[8]See `http://www.nytimes.com/2017/05/02/business/dealbook/vix-political-risk.html`.

LETF	Issuer	β	Fee	Inception
VXX	iPath	1	0.89%	January 29$^{\text{th}}$, 2009
VIIX	Janus	1	0.89%	November 29$^{\text{th}}$, 2010
XXV	iPath	-1	0.89%	July 16$^{\text{th}}$, 2010
XIV	Janus	-1	1.35%	November 29$^{\text{th}}$, 2010
TVIX	Janus	2	1.65%	November 29$^{\text{th}}$, 2010
UVXY	ProShares	2	0.86%	October 3$^{\text{rd}}$, 2011

Table 1.2: A summary of the VIX (L)ETFs. For the LETFs ($\beta \in \{-1, 2\}$), the expense ratios are higher and for the higher value $\beta = 2$, the expense ratio is the highest.

ysis is still a useful tool in some cases, thereby indicating that static portfolios can sometimes perform well in tracking an index. Assuming a small subset of available stocks each following a Geometric Brownian Motion, Yao et al. (2006) solve a stochastic linear quadratic control problem for the optimal stock allocation that best tracks a (constant) benchmark rate of return. This can be viewed as trying to track the growth rate of, e.g. the S&P 500 using only a small fraction of its composite stocks. Primbs and Sung (2008) extend this work to include probabilistic portfolio constraints, e.g. short sale restrictions. By working in discrete time, they find the optimal allocation via semi-definite programming. A similar problem was studied by Edirisinghe (2013) from a mean-variance framework. In light of the Markowitz Portfolio Optimization approach, he considers optimizing a combination of mean and variance of the portfolio's tracking error with respect to a benchmark index. This thesis adds to the index tracking literature through the key results (see Propositions 4.1.2 and 4.1.1) in Chapter 4. There, we will discuss a continuous diffusion framework to better understand index tracking and risk exposure control using financial derivatives.

This thesis contributes to the growing literature on ETFs and their leveraged counterparts. There are a number of studies on the price dynamics of LETFs, including Cheng and Madhavan (2009), Avellaneda and Zhang (2010), and Jarrow (2010). They illustrate how the value of an LETF can erode proportional to the leverage ratio as well as the realized variance of the reference index. The volatility decay has implications for the long-term investor. Leung and Park (2016) study such an investor and determine the long-term growth

rate of utility of LETFs as well as the optimal leverage ratio for these investors. As we will see in Chapter 4, there are a number of useful derivative securities for tracking a leveraged benchmark. A natural one is the LETF option. As options traders often quote values of options in terms of their implied volatilities, it is crucial to understand the dynamics of the implied volatilities of LETF options. For work in that direction, we refer to Leung and Sircar (2015) and Leung et al. (2016b).

There are also a number of empirical studies on (L)ETFs. For equity ETFs, Rompotis (2011) applies regression to determine the tracking errors between ETFs and their stated benchmarks, and finds persistence in tracking errors over time. The horizon effect is also illustrated in the empirical study by Murphy and Wright (2010) for commodity LETFs. Guo and Leung (2015) systematically study the tracking errors of a large collection of commodity LETFs. They define a realized effective fee to capture how much an LETF holder effectively pays the issuer due to the fund's tracking errors. Furthermore, Holzhauer et al. (2013) corroborate the volatility effect by using VIX data in a linear regression of the returns. Additionally, they find that the change in the *expected* volatility is even more significant in this regression and that the volatility effect is stronger for bear LETFs than for bull LETFs. In this thesis, we find a similar effect[9] in that it is more difficult to track a negatively leveraged benchmark than a positively leveraged one. For more related studies on the empirical and theoretical price dynamics of LETFs, we refer to the book by Leung and Santoli (2016).

Many of the (L)ETFs we consider are futures based so we will be analyzing the tracking properties of futures portfolios and futures based replication of indices, with a focus on gold and VIX. For a general overview of commodity ETFs constructed with futures, see Guedj et al. (2011). Alexander and Barbosa (2008) discuss hedging strategies with futures contracts for index ETFs and compare them against some minimum variance hedge ratios. Empirical studies by Baur (2012) and Smales (2015) show that the volatility of gold spot and futures exhibits asymmetric responses to market shocks. Their studies argue that the higher

[9]We demonstrate this empirically in Chapters 2 and 3 and discuss theoretical reasons in Chapter 4.

sensitivity of gold volatility to positive shocks can be interpreted by the safe haven property of gold. We have previously mentioned some papers on VIX futures, and portfolios of VIX futures above, but we list them here for completeness. They include Husson and McCann (2011) and Deng et al. (2012) as well as Alexander and Korovilas (2013) and Whaley (2013).

The results of this thesis have practical implications for the development of trading strategies. A simple application of much of this work is to pairs trade the tracking portfolio against some (L)ETF that purports to track the (possibly leveraged) index. For instance, Triantafyllopoulos and Montana (2011) model the spread between mean-reverting pairs of gold and silver ETFs, and develop efficient algorithms for estimating the parameters of this model for trading purposes. Dunis et al. (2013) develop a genetic programming algorithm for trading gold ETFs. Leung and Li (2015) analyze the optimal sequential timing strategies for trading pairs of ETFs based on gold, gold miners, or silver. Additionally, Naylor et al. (2011) find gold and silver ETFs to be highly profitable ETFs and are able to yield highly abnormal returns based on filtering strategies. Leung et al. (2016a) study the problem of speculative investing in futures products under mean reverting models. Via a similar approach, Li (2016) analyzes the optimal trading strategies for VIX futures under mean reverting models where the mean reverting parameters are subject to regime switching. Though we do not construct such trading strategies explicitly, it is a natural extension to this work. The empirical methodology presented in Chapters 2 and 3 can be applied to nearly any asset class and Chapter 4 allows for better understanding of how profitable such a pairs trade might be.

As for our algorithmic trading model presented in Chapter 5, there are a number of related studies in the optimal execution and market making literature. The foundational studies by Bertsimas and Lo (1998) and Almgren and Chriss (2000) began the study of optimal execution from an academic perspective and our work continues this academic study. There are a number of related studies on optimal liquidation with similar basic settings as in these papers, though liquidation with both market and limit orders has only come to the forefront of the algorithmic trading literature in recent years. Cheng et al. (2017) extend the Almgren-

Chriss model to include uncertain order fills of a single order type. Chapter 5 extends this model even further to include both market and limit orders, along with additional penalties to guide the trade direction and limit order size. In the case of infinite uncertainty, our framework captures their model as a special case, with our optimal market order rate coinciding with theirs. Cartea and Jaimungal (2015) also solve an optimal execution problem with market and limit orders. Unlike our model, which is based on continuous diffusion processes, their model uses jump processes and optimal multiple stopping to determine the optimal market order placement time. They too penalize deviations from a schedule.

Tracking problems in algorithmic trading are important as practictioners seek to follow benchmark schedules over time. For a specific example of schedule following, we refer to a recent study by Cartea and Jaimungal (2016). They derive a closed-form optimal strategy that follows a volume weighted average price (VWAP) schedule. In additon, market making itself is a type of tracking problem in that the trader seeks to track a position that is low risk or potentially profitable (from future executions). Market making involves simultaneously determining the prices and quantities to buy and sell a stock. The market maker receives the spread in exchange for the risk of holding a position. Avellaneda and Stoikov (2008) apply indifference pricing techniques to find the optimal quotes for a risk-averse investor trading over a finite period. Guilbaud and Pham (2013) study a market making problem via the optimal placement of limit orders as well as using market orders to balance inventory risk. For more related studies on algorithmic trading and market microstructure, we refer to the books by Lehalle and Laruelle (2013) and by Cartea et al. (2015).

Chapter 2

Tracking Gold with Futures

In this chapter, we begin our study of index tracking with an empirical investigation of the tracking performance for spot gold of various securities whose values are tied to gold. In particular, in Section 2.1, we investigate the price relationships amongst gold LETFs, gold futures and the gold spot price. Our results show that gold futures are highly correlated amongst each other and correlated with the spot price of gold. Thus, we find that gold futures are highly effective in tracking spot gold through static portfolios and that the market traded ETF (GLD) also exhibits similar tracking performance. On the other hand, we find in Section 2.2 that leveraged gold ETFs tend to underperform their corresponding leveraged benchmark with worsening underperformance over longer holding periods. The underperformance is even worse for static portfolios of gold futures. This motivates our study of dynamic portfolios for index tracking and we analyze one such strategy in Section 2.2.3. We find that the dynamic portfolio also consistently outperforms the respective market-traded LETFs for different leverage ratios.

2.1 Gold Spot & Futures

We begin by analyzing the price dynamics of gold futures with respect to the spot. One benchmark for the spot gold price are the London Gold Fixing Indices, GOLDLNAM and GOLDLNPM. Each of these indices is only updated once per business day: 10:30 AM for GOLDLNAM, and 3:00 PM for GOLDLNPM in London times, by four members of the London Bullion Market Association (Scotia-Mocatta, Barclays Bank, HSBC, and Societe-Generale).[1] Another widely used benchmark for the gold spot price is the Gold-U.S. Dollar exchange rate (XAU-USD). It indicates the U.S. dollar amount required to buy or sell one troy ounce of gold immediately. XAU-USD is frequently updated around the clock and its closing price is available for all trading days studied from December 22$^{\text{nd}}$, 2008 through July 14$^{\text{th}}$, 2014. For these reasons, we choose XAU-USD as our benchmark for the gold spot price throughout this chapter.

In the gold futures market, the front months, such as the 1-Month and 2-Month contracts, are actively traded daily. However, other available contracts are set to expire in specific calendar months within the next few years. As such, it may not always be possible to trade 6-Month and 12-Month futures, and one may need to alternate with the nearest month. For a 6-Month futures position we assume a position which alternates between 6-Month futures and 5-Month futures and for a 12-Month futures position we assume a position which alternates between 12-Month futures and 11-Month futures. This involves simply waiting while the 6-Month futures (resp. 12-Month) futures becomes a 5-Month futures (resp. 11-Month) after one month and then rolling the position forward 2 months after the second month passes. For example, if it now January 2012 a 12-Month futures contract would be the Dec-12 contract. When February 2012 comes by, this becomes an 11-Month contract, but the Jan-13 contract is not available. Instead, we hold the position as an 11-Month futures and then in March 2012, we roll the position forward into the Feb-13 contract returning it to

[1] According to the London Bullion Market Association. See `http://www.lbma.org.uk/pricing-and-statistics`.

a 12-Month position. Throughout this chapter, we will use the 1, 2, 6, and 12-Month gold futures contracts in our regressions.

2.1.1 Price Dependency

We begin by performing linear regressions of the 1-day returns of spot gold versus the futures of maturities: 1, 2, 6, and 12-Months. Across all maturities, the linear relationships are all strong and they are quite similar. In Table 2.1, we summarize the regression results, including the slope, intercept, R^2, and root mean squared error (RMSE). The R^2 values are all greater than 80%, indicating a strong linear fit. For every maturity, the slope is close to 0.94 and the intercept is essentially zero. The slopes suggest that the price sensitivity of futures with respect to the spot is slightly less than 1 to 1. While this may suggest that the futures prices should be less volatile than the spot return, we find that the historical annual volatilities of the futures are higher: 19.261% (1-Month), 19.263% (2-Month), 19.269% (6-Month), and 19.266% (12-Month), as compared to the spot (18.374%). The fact that the regression results are almost the same among different futures suggests that the futures prices are highly positively correlated. Indeed, our calculations show that the correlation among the futures over the same period are all over 99%.

Response	Slope	Intercept	R^2	$RMSE$
1-Month	0.94314	$2.41916 \cdot 10^{-5}$	0.80947	0.00530
2-Month	0.94301	$6.20316 \cdot 10^{-5}$	0.80911	0.00530
6-Month	0.94348	$3.17973 \cdot 10^{-5}$	0.80934	0.00530
12-Month	0.94358	$-5.23334 \cdot 10^{-5}$	0.80984	0.00529

Table 2.1: A summary of the regression coefficients and measures of goodness of fit for regressing 1-day returns of 1, 2, 6 and 12-Month futures on 1-day returns of spot gold from December 22$^{\text{nd}}$, 2008 to July 14$^{\text{th}}$, 2014.

The high correlation among futures prices can also be seen from their time series. In Figure 2.1, we plot the gold price, 1-Month futures price (Jan-13 contract) and 12-Month futures price (Dec-13 contract) over the period from December 29$^{\text{th}}$, 2012 to January 1$^{\text{st}}$,

2013. Over this period the 1-Month futures and 12-Month futures prices move in parallel to one another just as the near perfect correlation would indicate. Furthermore, the gold spot price and 1-Month futures price are close, as expected. On Jan 29$^{\text{th}}$, 2013, or trading day 21 in Figure 2.1, the 1-Month futures would expire. We observe a slight discrepancy between the futures price and the spot on this date. While futures should theoretically converge to the spot price at maturity, in practice gold futures settle at their volume weighted average (VWAP) price within the last one minute.[2] The last price will be equal to the spot price at maturity, but the settlement price (which is used in marking futures positions to market) used here will be calculated by weighting this last price against its volume traded and hence need not be equal to the spot gold price.

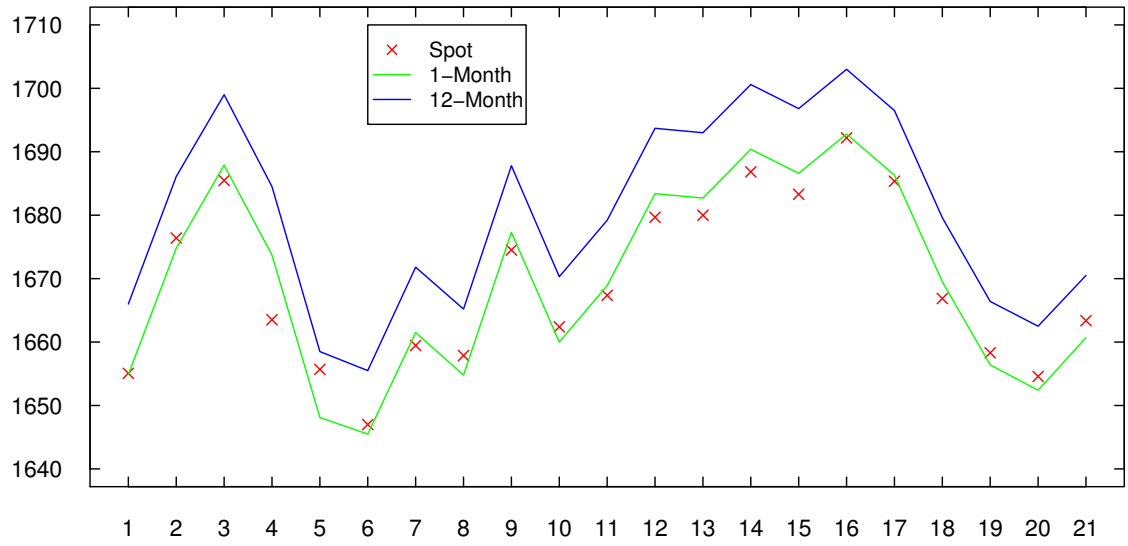

Figure 2.1: Time evolution of spot gold price, 1-Month futures price (Jan-13 contract) and 12-Month futures price (Dec-13 contract) over the period from Dec 29$^{\text{th}}$, 2012 to Jan 29$^{\text{th}}$, 2013. The two futures prices move in parallel, and the spot price trades very close to the 1-Month futures price. The x-axis marks the trading day number, while the y-axis marks the price.

In fact, the price co-movement among futures also has implications for the term structure dynamics. On a typical date in the gold market, futures prices are increasing and convex with respect to maturity as seen in Figure 2.2. Since the futures contracts tend to move in

[2]According to CME Group gold futures settlement procedures documentation, available at `http://www.cmegroup.com/trading/metals/files/daily-settlement-procedure-gold-futures.pdf`

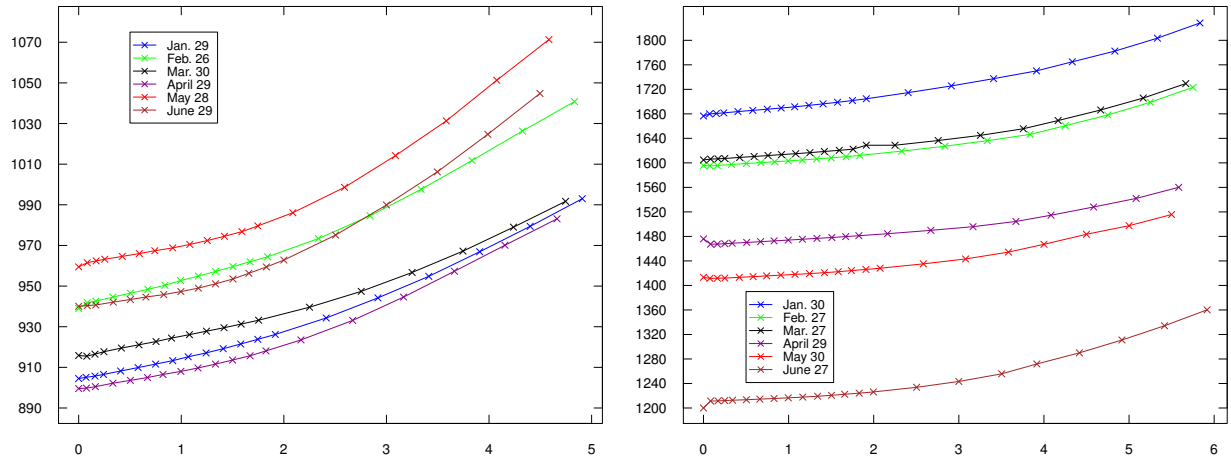

(a) Jan.-June 2009 (b) Jan.-June 2013

Figure 2.2: Term structures from Jan. to June in 2009 (left) and 2013 (right). The legend marks the date upon which the term structure is constructed (which is one day after that month's expiring contract's maturity). The x-axis marks the time-to-maturity (in years, assuming each year is precisely 252 days), while the y-axis marks the price.

parallel, this leads to almost parallel shifts in the term structure. The shape of the term structure remains almost the same over time. During both periods we can see the increasing convex feature of the gold futures market, but in 2013 there is a reduction in convexity. In 2009, the term structure generally shifts upward from January to June, while in 2013 the term structure strictly shifts downward from January to June.

Next, we compare the linear relationships for returns computed over 5, 10, and 15 trading days. Since we use disjoint time windows for return calculations, a longer holding period implies fewer data points for the regression. In Figure 2.3, we plot the regressions of 12-Month futures returns versus gold returns for both 1-day returns and 10-day returns, plotted on the same x-y axis scale. We can see the returns vary on a larger range for the 10-day returns. Spot gold has a 1-day return between -9.07% (April 15^{th}, 2014)[3] and 4.99% (January 23^{rd}, 2009), while its 10-day returns vary between -9.12% (June 6^{th}, 2013 to June 19^{th}, 2013) and 11.30% (August 5^{th}, 2011 to August 18^{th}, 2011). On the other hand, the 12-Month futures has a 1-day return between -9.40% (April 15^{th}, 2014) and 7.68% (March 19^{th}, 2009), while

[3]Gold returns plummeted on this day. See `http://mobile.nytimes.com/blogs/dealbook/2013/04/15/golds-plunge-shakes-confidence-in-a-haven/`

its 10-day returns vary between -9.16% (June 6^{th}, 2013 to June 19^{th}, 2013) and 11.30% (August 5^{th}, 2011 to August 18^{th}, 2011). Moreover, we can see that the slope is slightly higher for the 10-day returns versus the 1-day returns.

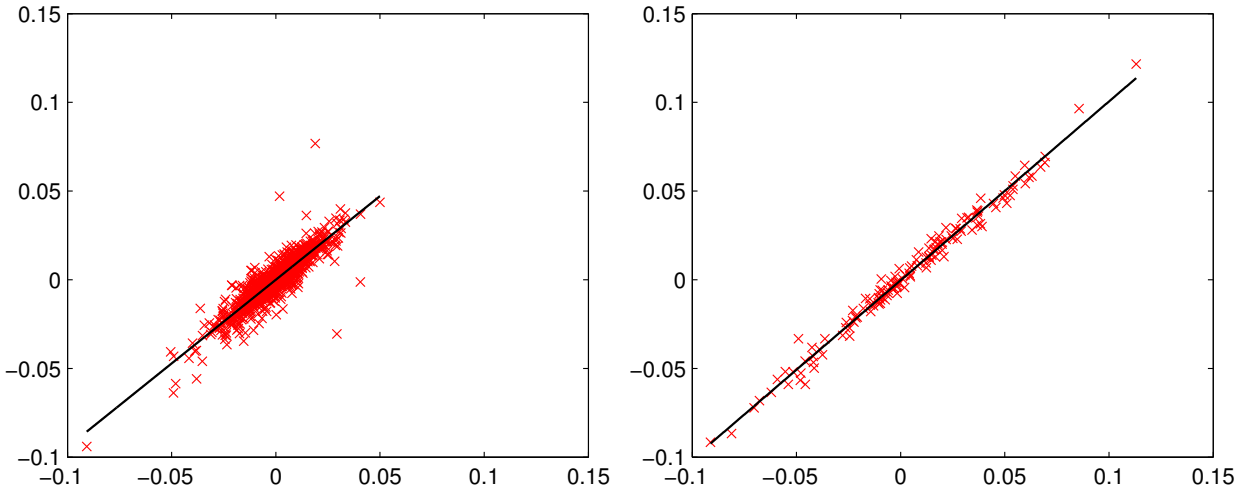

(a) 1-day Returns (b) 10-day Returns

Figure 2.3: Linear regressions of 12-Month futures returns based on 1-day returns (left) and 10-day returns (right) versus the spot gold returns. The x-axis marks the returns (decimals, not percentages) of spot gold, while the y-axis marks the returns (decimals, not percentages) of the 12-Month futures.

This is confirmed numerically and in general for the various futures contracts in Table 2.2. Here, we give the slopes for the regression of each futures return versus the gold return, while varying the holding period. We display the slopes and R^2 values from Table 2.1 for comparison. However, we do not give the intercepts for these regressions as they are all very trivial and effectively 0. We can see that the slopes approach the value 1 as the holding period is lengthened. Thus, the longer the holding period, the more closely the gold return and futures price return are to one another. In particular, the slopes for 10-day returns are all greater than 1, indicating an increased price sensitivity. Furthermore, the strength (as measured by R^2) of this linear relationship increases with increasing holding period length.

	Days	1-Month	2-Month	6-Month	12-Month
Slope	1	0.94314	0.94301	0.94348	0.94358
	5	0.99805	0.99752	0.99757	0.99715
	10	1.01075	1.01020	1.00970	1.00841
	15	0.99448	0.99461	0.99431	0.99345
R^2	1	0.80947	0.80911	0.80934	0.80984
	5	0.97154	0.97158	0.97194	0.97165
	10	0.98516	0.98530	0.98572	0.98550
	15	0.98704	0.98691	0.98725	0.98713

Table 2.2: A summary of the slopes and R^2 from the regressions of futures returns versus gold returns over different holding periods.

2.1.2 Static Replication of Gold Spot Price

In this section we consider replication of the gold spot price with a static portfolio of futures contracts. We use portfolios of either 1 or 2 futures contracts and an investment in the money market account. We seek a static portfolio that minimizes the sum of squared errors:

$$SSE = \sum_{j=1}^{n} (V_j - G_j)^2 , \tag{2.1.1}$$

where V_j is the dollar value of the portfolio on trading day j, while G_j is the dollar value of the gold spot price on trading day j.

Let k be the number of futures contracts and $\mathbf{w} := (w_0, \ldots, w_k)$ be the real-valued vector of portfolio weights. In particular, w_0 represents the weight given to the money market account. To calculate the optimal portfolio value we will choose weights historically which minimize SSE over the 5-year period December 22$^{\text{th}}$, 2008 to December 22$^{\text{th}}$, 2013. Thus, we solve the following constrained least squares optimization problem:

$$\begin{aligned} \min_{\mathbf{w} \in \mathbb{R}^{k+1}} \quad & \|\mathbf{C}\mathbf{w} - \mathbf{d}\|^2 \\ \text{s.t.} \quad & \sum_{j=0}^{k} w_j = 1. \end{aligned} \tag{2.1.2}$$

The matrix $\mathbf{C}$ contains as columns, the historical prices of the various futures contracts and the money market account,[4] and the vector, $\mathbf{d}$ contains the historical prices of spot gold. When we refer to historical prices of say, the 1-Month futures contract, we mean a position that is rolled forward every contract period. For example, for the 1-Month contract we begin with an investment of $\$1,000$ dollars and purchase as many units of 1-Month futures as possible with this sum. After that contract expires, we roll forward whatever value is left in the position into the current 1-Month futures. (Previously, this contract was the 2-Month futures at time 0.) This is similarly defined for 2-Month, 6-Month and 12-Month futures. All prices are normalized by $\$1,000$, without loss of generality, so that an investor starting with $\$1,000$ will invest $\$1,000 \cdot w_j$ into the jth futures contract and $\$1,000 \cdot w_0$ into the money market account.

We will compare our portfolios to investments in the ETF GLD, which tracks the gold spot price. To do this, we will perform an out-of-sample analysis and compare the values of $1000 invested in GLD and $1000 invested in our constructed portfolio over the period from December 23$^{\text{th}}$, 2013 to July 14$^{\text{th}}$, 2014. To measure the performance we will use the following root mean squared error for both in-sample and out-of-sample prices:

$$RMSE = \sqrt{\frac{1}{n}\sum_{j=1}^{n}\left(V_j - G_j\right)^2}. \tag{2.1.3}$$

We solve this optimization problem for ten different portfolios with one or two futures, along with the money market account. The optimal weights, and corresponding in-sample/out-of-sample RMSEs are given in Table 2.3. In general, the money market account is used minimally as the weights on the account are less than 7% in absolute value for all ten portfolios.

For all the portfolios with two futures contracts, the optimal strategy is to go long the shorter term futures contract and short the longer term futures contract, with different

[4]We use historical overnight LIBOR to construct an investment in the money market account.

weights. The sum of the two resulting weights is approximately 1. In terms of RMSE, the 1-Month futures contract appears to be the best replicating instrument of the gold spot. When it is used alone, it performs best relative to other single futures portfolios. When it is used in a pair with another futures, it performs better than any other single futures contract, and better than all other futures pairs: (2-m, 6-m), (2-m, 12-m), and (6-m, 12-m).

	Futures	w_0	w_1	w_2	$RMSE$ (in)	$RMSE$ (out)
1 Futures	1-m	−0.01071	1.01071	-	6.62989	3.34047
	2-m	−0.04835	1.04835	-	12.22148	6.12074
	6-m	−0.05030	1.05030	-	13.23663	5.33971
	12-m	−0.06842	1.06842	-	15.11103	5.71318
2 Futures	1-m, 2-m	−0.00088	1.27315	−0.27227	6.26711	2.79411
	1-m, 6-m	−0.00171	1.23899	−0.23729	6.27232	2.97602
	1-m, 12-m	−0.00021	1.19336	−0.19315	6.28735	3.00006
	2-m, 6-m	−0.04079	5.06602	−4.02523	10.27413	9.37292
	2-m, 12-m	−0.01179	2.94860	−1.93681	9.65705	7.08414
	6-m, 12-m	0.01481	4.80979	−3.82460	9.57938	4.52846

Table 2.3: A summary of the weights and in/out-of-sample RMSEs for portfolios of one and two futures contracts. For portfolios with two futures, the weight on the shorter term futures is w_1. For portfolios with a single futures, we have $w_2 = 0$. The weight assigned to the money market account is denoted by w_0.

In the sample, the RMSE values for the futures portfolios range from 6.63 to 15.11. Since these values are based on a \$1000 investment, this means the error within the sample is between 0.663% and 1.511%, which is quite low. By comparison, our calculations give a RMSE of 2.091% for the gold ETF (GLD) during December 22$^{\text{th}}$, 2008 to December 22$^{\text{th}}$, 2013. Over this longer horizon of 5 years, our portfolios track the benchmark better than GLD. However, over the shorter, out-of-sample period, December 23$^{\text{th}}$, 2013 to July 14$^{\text{th}}$, 2014, GLD appears to track spot gold slightly better. The RMSE value for GLD during this period is 0.128%, whereas our best portfolio gives a RMSE of 0.279%. In Figure 2.4, we show the time series of the optimal static portfolio with the 1-Month futures (top), and the time series for GLD. It is visible that both track the gold spot price closely over this out-of-sample period.

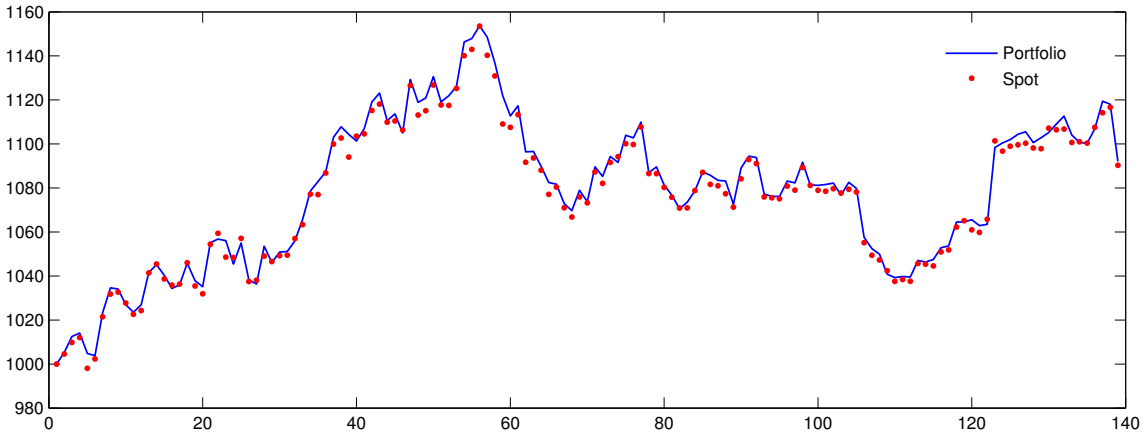

(a) Portfolio with 1-Month Futures

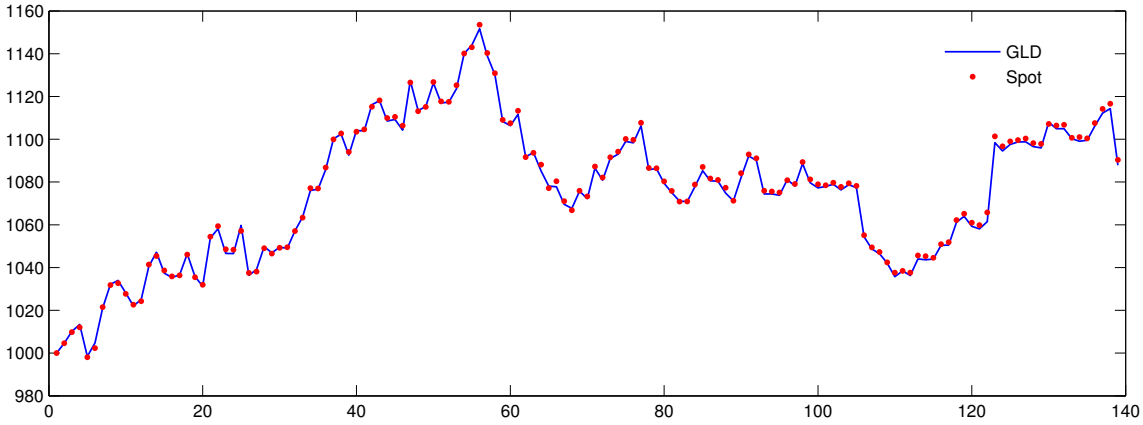

(b) GLD

Figure 2.4: Out-of-sample time series of our optimal portfolio of 1-Month futures and money market account (top) compared to the spot price, and GLD compared to the spot price (bottom). The x-axis marks the trading day number which is from December 23$^{\text{th}}$, 2013 to July 14$^{\text{th}}$, 2014, while the y-axis marks the price. All portfolios are normalized to start at \$1,000.

2.2 Leveraged ETFs

In this section we analyze the returns and tracking performances of various leveraged ETFs. From historical prices of each LETF, we conduct an estimation of the leverage ratio, and investigate the potential deviation from the target leverage ratio. Moreover, we construct a number of static portfolios with futures contracts to seek replication of some leveraged benchmarks. However, the static portfolios fail to effectively track the leveraged benchmarks. This motivates us to consider a dynamic portfolio with futures, which turns out to have a much better tracking performance.

By design, an LETF seeks to provide a constant multiple of the daily returns of an underlying index or asset. Let us denote $\beta \in \{-3, -2, +2, +3\}$ the leverage ratio stated by the LETF, and R_j the daily return of the underlying (gold spot). Ideally, the LETF value on day n, denoted by L_n, is given by

$$L_n = L_0 \cdot \prod_{j=1}^{n} (1 + \beta\, R_j). \tag{2.2.1}$$

We call this the leveraged benchmark, and examine the empirical performance of various LETFs with respect to this benchmark.

For many investors, one appeal of LETFs is that leverage can amplify returns when the underlying is moving in the desired direction. Mathematically, we can see this as follows. Rearranging (2.2.1) and taking the derivative of the logarithm, we have

$$\frac{d}{d\beta}\left(\log\left(\frac{L_n}{L_0}\right)\right) = \sum_{j=1}^{n} \frac{R_j}{1 + \beta\, R_j}. \tag{2.2.2}$$

With a positive leverage ratio $\beta > 0$, if $R_j > 0$ for all j, then $\log\left(\frac{L_n}{L_0}\right)$, or equivalently the value L_n, is increasing in β. In other words, when the underlying asset is increasing in value, a larger, positive leverage ratio is preferred. On the other hand, if $R_j < 0$ for all j, and $\beta < 0$, a more negative β increases $\log\left(\frac{L_n}{L_0}\right)$ and thus L_n. This means that when the underlying asset is decreasing in value, a more negative leverage ratio yields a higher return.

The example below illustrates the consequences of maintaining a constant leverage in an environment with non-directional movements:

Day	ETF	%-change	+2x LETF	%-change	−2x LETF	%-change
0	100	-	100		100	-
1	98	−2%	96	-4%	104	4%
2	99.96	2%	99.84	4%	99.84	−4%
3	97.96	−2%	95.85	−4%	103.83	4%
4	99.92	2%	99.68	4%	99.68	−4%
5	97.92	−2%	95.69	−4%	103.67	4%
6	99.88	2%	99.52	4%	99.52	−4%

Table 2.4: A hypothetical example of how volatility decay can lead to both a long and short leveraged ETF to losing money, even in the case of perfect daily return tracking.

Even though the ETF records a tiny loss of 0.12% after 6 days, the +2x LETF ends up with a loss of 0.48%, which is greater (in absolute value) than 2 times the return (−0.12%) of the ETF. We can see this to be the case on any day (e.g. not just the terminal date) except for day 1. For example, on day 3, the ETF has a net loss of 2.04% and the LETF has a net loss of 4.15%, which is greater (in absolute value) than 4.08% (twice the absolute value of the return of the ETF). Furthermore, it might be intuitive that that the −2x LETF should have a positive return when the ETF and LETF have negative returns: this is not true. At the terminal date, both the long and short LETFs have recorded net losses of 0.48%. Again, this occurs throughout the period as well, not just the terminal date. In addition to day 6, both the long and short LETFs as well as the ETF itself are in the black. These results are consequences of volatility decay.

Although long and short LETFs are expected to move in opposite directions daily by design, it is often possible for both LETFs to have negative cumulative returns when held over a longer horizon. Figure 2.5 shows the historical cumulative returns of the gold LETFs UGL (+2x) and GLL (−2x) from July 2013 to July 2014. From trading day 124 (January 24$^{\text{th}}$, 2014) onward, GLL has a negative cumulative return. There are points after trading date 124 where UGL also has a negative cumulative return. In fact, it starts in the black on this date and continues to have a net loss until trading date 146 (February 12$^{\text{th}}$, 2014). This occurs again a few times, another long stretch where both have a net loss is trading

date 210 (May 15th, 2014) through 233 (June 18th, 2014).This observation, though perhaps counter-intuitive at first glance, is a consequence of daily replication of leveraged returns. The value erosion tends to accelerate during periods of non-directional movements.

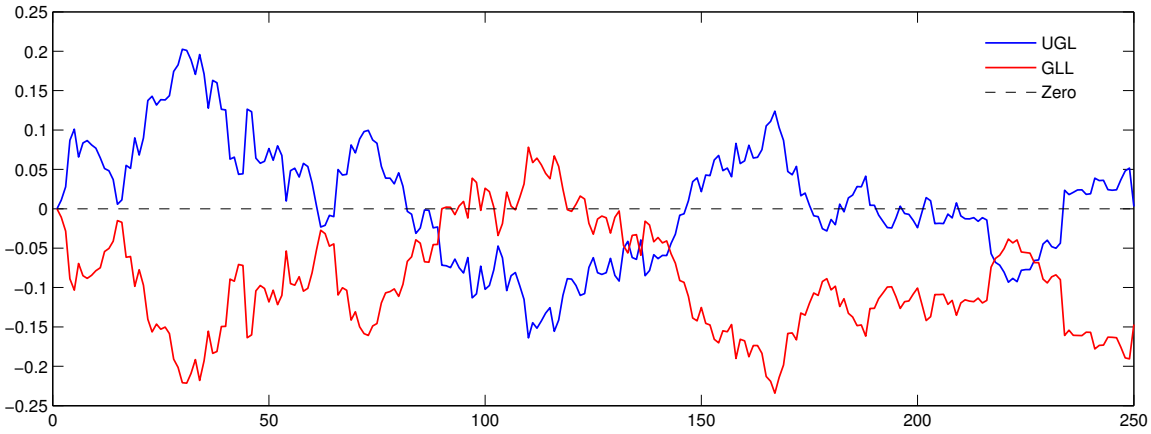

Figure 2.5: UGL (+2x) and GLL (−2x) cumulative returns from July 2013 to July 2014. Observe that both UGL and GLL can give negative cumulative returns (below the dotted line of 0%) simultaneously over several periods in time. The x-axis marks the trading day number, while the y-axis marks the cumulative return, which is initialized to 0.

2.2.1 Empirical Leverage Estimation

We conduct a regression analysis and the results are given in Table 2.5. Each slope is approximately equal to the LETF's target leverage ratio. In principle, if each (L)ETF is able to generate the desired multiple of daily returns, the slopes of the regression should be equal to the various leverage ratios. In this table, we give an additional two columns for the t-statistic and p-value for testing the hypothesis: $\{H_0 : \text{slope} = \beta\}$ vs. $\{H_1 : \text{slope} \neq \beta\}$, where, β is the target leverage ratio. We can see that each p-value is larger than 0.05 and therefore conclude that statistically, each (L)ETF does not differ from its target leverage ratio. This demonstrates to us that the (L)ETFs are performing exactly as desired, at least on a daily basis.

(L)ETF	Slope	Intercept	t-stat	p-value	R^2	$RMSE$
GLD	1.00540	$-1.64276 \cdot 10^{-5}$	1.42692	0.15382	0.98060	0.00163
UGL	2.00572	$-1.31073 \cdot 10^{-4}$	0.73319	0.46357	0.97930	0.00337
GLL	-2.00556	$-1.05504 \cdot 10^{-4}$	0.67089	0.50240	0.97673	0.00358
UGLD	2.99358	$-1.98605 \cdot 10^{-4}$	0.45211	0.65133	0.98484	0.00421
DGLD	-2.97528	$-1.69127 \cdot 10^{-5}$	0.97442	0.33019	0.95256	0.00752

Table 2.5: A summary of the regression coefficients and measures of goodness of fit for regressing 1-day returns of (L)ETFs versus spot gold. We include two additional columns for the t-statistic and p-value for testing the hypothesis that the slope equals the leverage ratio in each case.

We see also that the R^2 values for each regression are quite high, all above 95%. For a fixed $|\beta| \in \{2, 3\}$, the short LETF tends to have a higher RMSE and lower R^2 value than its corresponding long LETF. Finally, we see in general that as the leverage ratio increases in absolute value, there is a higher RMSE. One possible explanation is that the benchmark is leveraged, and this could magnify the tracking error.

Just as in Section 2.1.1, we analyze the effects of changing the holding period. In Table 2.6 we give the slopes and intercepts for the regressions of each (L)ETF's return versus the spot return while varying the holding period between 15 and 5 days. Our computations show the R^2 values are all above 95%. We can see that the slopes all approximately equal the target leverage ratio of the (L)ETF. However we notice that in general the intercepts get more negative as the holding period is lengthened. Although they are still quite small, they become more significant as the holding period increases. Our calculations show that the p-values for testing the hypothesis: $\{H_0 : \text{intercept} = 0\}$ vs. $\{H_1 : \text{intercept} \neq 0\}$ generally tend to decrease for each (L)ETF. In fact, for UGL the intercepts turn out to be statistically different from 0 (at the 5% level) for holding periods of 3, 4 and 5 days with p-values of 1.37%, 0.57% and 0.33%, respectively. This is consistent with the volatility decay discussed above. We saw there an example where over shorter periods, the LETF tracks its leverage ratio well, but over a longer period it tends to lose money when there is high volatility. The intercepts being different from 0 is akin to the volatility decay in the following sense. Over longer periods, the regressions show that we require more information than just the gold

return to predict the LETF return.

To compare the performance of the LETF versus the target multiple of the spot return, we also report in Table 2.6, the average return differential, defined by

$$\overline{RD} = \frac{1}{m}\sum_{j=1}^{m}\left(R_j^{(L)} - \beta \cdot R_j^{(G)}\right), \tag{2.2.3}$$

where m is the number of the periods, $R_j^{(L)}$ is the LETF's return over the holding period and $R_j^{(G)}$ is the spot's return over the holding period. We find this to be increasing (in absolute value) with the holding period length. That is, as we hold the LETF longer, it tends to increasingly underperform with respect to the multiple of the underlying return, on average. This is exactly the same notion described above, since over time, the volatility of the underlying causes the LETF to erode in value.

	Days	UGL	GLL	UGLD	DGLD	GLD
Slope	1	2.00572	-2.00556	2.99160	-2.96362	1.00540
	2	2.00828	-2.00395	2.92015	-3.02429	1.00477
	3	1.97770	-1.99661	2.94520	-3.06690	0.99194
	4	2.00071	-2.00908	2.97854	-3.04311	1.00206
	5	2.02081	-2.03273	2.89478	-3.07267	1.01039
Intercept ($\cdot 10^{-4}$)	1	-1.31074	-1.05505	-1.98605	-0.16913	-0.16428
	2	-2.73282	-2.28807	-4.23120	-1.81545	-0.33388
	3	-4.06417	-3.96629	-4.97993	-1.05631	-0.40843
	4	-5.44427	-4.62166	-8.08478	-2.69971	-0.66133
	5	-6.81614	-4.82805	-8.03417	-0.30766	-0.92359
$\overline{RD}$ ($\cdot 10^{-3}$)	1	-0.12892	-0.10760	-0.19673	-0.02414	-0.01439
	2	-0.26677	-0.23191	-0.43999	-0.19081	-0.02964
	3	-0.43253	-0.39265	-0.53511	-0.08462	-0.05028
	4	-0.54331	-0.47645	-0.81687	-0.27854	-0.06290
	5	-0.64076	-0.54705	-0.79183	0.07165	-0.07195

Table 2.6: A summary of the slopes and intercepts from the regressions of LETF returns versus gold returns, as well as the average return differential ($\overline{RD}$) over different holding periods.

2.2.2 Static Leverage Replication

In this section, we perform the same optimization as in Section 2.1.2. We once again seek a static portfolio of futures which minimizes SSE. Let k be the number of futures contracts and $\mathbf{w} := (w_0, \ldots, w_k)$ be the real-valued vector of portfolio weights. As before, w_0 represents the weight given to the money market account. We seek the weights which minimize SSE over the 5-year period from December 22$^{\text{th}}$, 2008 to December 22$^{\text{th}}$, 2013. Thus, we are led to the same constrained least squares optimization problem we proposed in Section 5.2.1:

$$\begin{aligned} \min_{\mathbf{w}\in\mathbb{R}^{k+1}} \quad & \|\mathbf{C}\mathbf{w} - \mathbf{L}\|^2 \\ \text{s.t.} \quad & \sum_{j=0}^{k} w_j = 1. \end{aligned} \tag{2.2.4}$$

Again, the matrix $\mathbf{C}$ contains as columns, the historical prices of the various futures contracts and the money market account. Here, the vector $\mathbf{L}$ contains the historical prices of the leveraged benchmark in (2.2.1). Without loss of generality, we normalize the prices by \$1000 so that our solution will give us a set of weights on each instrument.

We will compare the tracking error of our optimal portfolios to that of investments in the LETFs. To be able to analyze the portfolios we get by solving the optimization problem, we will perform an out-of-sample analysis over the period from December 23$^{\text{th}}$, 2013 to July 14$^{\text{th}}$, 2014 and see how \$1,000 invested in the LETFs and \$1,000 invested in our optimal portfolios perform in tracking the leveraged benchmark. To quantify the performance we use the same root mean square error

$$RMSE = \sqrt{\frac{1}{n}\sum_{j=1}^{n}(V_j - L_j)^2}, \tag{2.2.5}$$

where, V_j is the dollar value of the portfolio on trading day j, and now L_j is defined as the dollar value of the leveraged benchmark on trading day j. Now, we present the results for the optimization and in-sample/out-of-sample RMSE.

UGL(+2x)	Futures	w_0	w_1	w_2	$RMSE$ (in)	$RMSE$ (out)
1 Futures	1-m	−1.48159	2.48159	-	153.20152	41.48530
	2-m	−1.57601	2.57601	-	140.41254	49.56627
	6-m	−1.58107	2.58107	-	138.63116	47.45953
	12-m	−1.62627	2.62627	-	134.50683	48.29851
2 Futures	1-m, 2-m	−1.94496	−9.89441	12.83937	114.30949	81.36970
	1-m, 6-m	−1.91184	−8.43451	11.34634	113.67580	67.39428
	1-m, 12-m	−2.02222	−6.92791	9.95013	108.29897	67.15776
	2-m, 6-m	−1.64536	−34.26195	36.90731	126.62074	22.64952
	2-m, 12-m	−1.99096	−18.99151	21.98248	111.75046	40.92852
	6-m, 12-m	−2.24344	−35.66917	38.91260	102.86283	62.53830

Table 2.7: A summary of the weights and in/out-of-sample RMSEs for portfolios of 1 and 2 futures contracts which attempt to replicate a leveraged benchmark with $\beta = 2$. By comparison, the +2x LETF, UGL has an out-of-sample RMSE of only 5.52485.

GLL(−2x)	Futures	w_0	w_1	w_2	$RMSE$ (in)	$RMSE$ (out)
1 Futures	1-m	1.97544	−0.97544	-	152.33349	76.14381
	2-m	2.01068	−1.01068	-	155.76147	73.14698
	6-m	2.01234	−1.01234	-	156.43931	74.00595
	12-m	2.02926	−1.02926	-	158.06790	73.79237
2 Futures	1-m, 2-m	1.69510	−8.46293	7.76783	139.27436	100.10091
	1-m, 6-m	1.70510	−7.83463	7.12954	137.98773	92.21120
	1-m, 12-m	1.60773	−7.37540	6.76767	133.31705	93.11206
	2-m, 6-m	1.93900	−39.08635	38.14735	142.57324	43.40713
	2-m, 12-m	1.57681	−23.56157	22.98477	127.90630	62.10415
	6-m, 12-m	1.27887	−43.36906	43.09020	117.81839	88.35987

Table 2.8: A summary of the weights and in/out-of-sample RMSEs for portfolios of 1 and 2 futures contracts which attempt to replicate a leveraged benchmark with $\beta = -2$. By comparison, the −2x LETF, GLL has an out-of-sample RMSE of only 4.76269.

UGLD(+3x)	Futures	w_0	w_1	w_2	$RMSE$ (in)	$RMSE$ (out)
1 Futures	1-m	−3.33704	4.33704	-	555.49151	111.51133
	2-m	−3.50625	4.50625	-	529.90858	125.98635
	6-m	−3.51562	4.51562	-	526.58448	122.33175
	12-m	−3.59587	4.59587	-	518.96896	123.83019
2 Futures	1-m, 2-m	−5.18147	−44.92498	51.10645	379.11676	270.58292
	1-m, 6-m	−5.02680	−38.53507	44.56188	381.92109	213.62168
	1-m, 12-m	−5.41970	−31.91076	38.33046	366.49764	210.91245
	2-m, 6-m	−3.78077	−141.31534	146.09611	472.32904	48.04126
	2-m, 12-m	−5.12561	−79.66101	85.78662	413.19682	98.33728
	6-m, 12-m	−6.14011	−147.04408	154.18419	376.40048	185.87170

Table 2.9: A summary of the weights and in/out-of-sample RMSEs for portfolios of 1 and 2 futures contracts which attempt to replicate a leveraged benchmark with $\beta = 3$. By comparison, the +3x LETF, UGLD has an out-of-sample RMSE of only 6.08133.

DGLD(−3x)	Futures	w_0	w_1	w_2	$RMSE$ (in)	$RMSE$ (out)
1 Futures	1-m	2.14737	−1.14737	-	222.59075	135.67755
	2-m	2.18885	−1.18885	-	225.76707	132.14962
	6-m	2.19079	−1.19079	-	226.42907	133.16229
	12-m	2.21063	−1.21063	-	228.13706	132.91661
2 Futures	1-m, 2-m	1.82654	−9.71612	8.88958	211.09051	163.04734
	1-m, 6-m	1.83531	−9.06486	8.22955	209.75562	154.16271
	1-m, 12-m	1.70781	−8.79773	8.08992	204.41288	155.82542
	2-m, 6-m	2.10262	−46.99103	45.88841	212.78493	95.24835
	2-m, 12-m	1.63980	−29.72604	29.08624	195.74796	117.35419
	6-m, 12-m	1.24461	−55.83130	55.58669	183.42198	150.58261

Table 2.10: A summary of the weights and in/out-of-sample RMSEs for portfolios of 1 and 2 futures contracts which attempt to replicate a leveraged benchmark with $\beta = -3$. By comparison, the −3x LETF, DGLD has an out-of-sample RMSE of only 4.43718.

In contrast to the case of tracking the gold spot with futures (see Table 2.3), the static portfolios do not replicate the leveraged benchmark well here. In Tables 2.7 through 2.10, the RMSE values are quite large for all the portfolios. The minimum RMSE for any portfolio of futures trying to replicate any leveraged benchmark is 22.64952 (achieved by a portfolio of 2-Month and 6-Month futures attempting to replicate a +2x investment in gold) and by comparison the maximum RMSE for any LETF trying to replicate its respective leveraged

investment is 6.08133. (This is achieved by UGLD, which tracks a +3x investment in gold.) Unlike the unleveraged investment, the money market account is extensively used throughout the various portfolios. This is interesting but also logical. Indeed, in order to create leverage, the portfolio must either borrow if $\beta > 0$ or invest in the money market account if $\beta < 0$.

Furthermore, the optimal weights tend to lead to over/underleveraging. Since we are considering an investment in gold, the sum of the weights on the futures (which are proxy's for investment in gold) can be interpreted as the leverage on the portfolio. Since all the weights sum to 1, we can compute the approximate leverage as $1 - w_0$. For the +2x and +3x investments, these values are all larger than 2 and 3, respectively. For the −2x and −3x investments, these values are all smaller (in absolute value) than −2 and −3, respectively. Granted, these are different instruments than the spot, but we have seen in Section 2.1.1 they all move in parallel to the spot. Thus we see that the long portfolios tend to be over leveraged, while the short portfolios tend to be under leveraged.

The optimization procedure has led to some rather uneven portfolio weights. For example, the optimal portfolio of 6-Month and 12-Month futures that attempts to replicate a +3x investment in spot gold requires the following transactions at inception: borrow $6,140.11 from the money market account, short $147,044.08 in 6-Month futures and long $154,184.19 in 12-Month futures. In practice this would not be possible in the marketplace due to position limits that may be in place.

2.2.3 Dynamic Leverage Replication

To improve upon the replication in Section 2.2.2, we now consider a dynamic portfolio of one futures contract.[5] Let P_t be our portfolio value at time t. At every point in time, the portfolio invests β times the value of the fund in the futures contract in order to achieve the required leverage. To fund this investment, the portfolio must borrow from the money market account. As a result, the value of our portfolio has the following dynamics:

[5]This is in contrast to the portfolios in the previous sections wherein the value of the portfolio was constantly rolled over into the subsequent contract.

$$dP_t = \beta P_t \frac{dF_t}{F_t} - P_t(\beta - 1) r_t dt. \tag{2.2.6}$$

Here, F_t is the value of a gold futures contract at time t with a chosen maturity, e.g. 1 month, and r_t is the risk free rate at time t.

Remark 2.2.1 *For our empirical analysis, we need not specify a parametric model for the futures price. Nevertheless, if one models the futures price by the stochastic differential equation*

$$\frac{dF_t}{F_t} = \mu_t dt + \sigma_t dW_t,$$

with some stochastic drift $(\mu_t)_{t\geq 0}$ and volatility $(\sigma_t)_{t\geq 0}$, (many well-known models, including the Heston, and exponential Ornstein-Uhlenbeck models, fit within the above framework) then the log-price of the portfolio is given by

$$\log P_t = \log P_0 + \beta \log \frac{F_t}{F_0} + \frac{\beta - \beta^2}{2}\Sigma_t + (1-\beta)R_t, \tag{2.2.7}$$

where $\Sigma_t = \int_0^t \sigma_s^2 ds$ is the realized variance of F accumulated up to time t and $R_t = \int_0^t r_s ds$. Therefore, under this general diffusion model, the log-return of the portfolio is proportional to the log-return of the futures by a factor of β, but also proportional to the variance by a factor of $\frac{\beta-\beta^2}{2}$. The latter factor is negative if $\beta \notin (0,1)$, which is true for every LETF considered here.

To implement the leveraged portfolio in (2.2.6), we choose the 1-Month futures contract. Recall from Section 2.1.2 that the 1-Month futures is the most effective in replicating the spot gold price. To calculate our portfolio value on each trading day, we discretize (2.2.6) in time, using Δt equal to 1 trading day and set P_0 equal to \$1,000 as before.

To quantify our portfolio's replicating ability we will use the same root mean squared error that we used in Section 2.2.2:

$$RMSE = \sqrt{\frac{1}{n}\sum_{j=1}^{n}(P_j - L_j)^2}, \tag{2.2.8}$$

where, L_j is the value of a leveraged investment in gold and P_j is the value of our portfolio, each at trading day j. For this dynamic portfolio, there is no sample from which we will need to draw our weights or train our model in any way. Therefore we can look at any conceivable time period and compare how the LETF (L) or leveraged portfolio (P) performs using the metric in (2.2.8).

For this tracking metric, we consider the period January 3$^{\text{rd}}$, 2012 (first trading day of 2012) to July 14$^{\text{th}}$, 2014. The results are shown in the first column of Table 2.11. The portfolio RMSEs range between 0.687% and 3.291%, which are smaller than LETF RMSEs which range between 1.87% and 4.338%. Overall, we see that the portfolio RMSEs are lower than the LETF RMSEs. Indeed, we see that our dynamic portfolio is able to track the target leveraged index quite well according to the RMSE values for $\beta \in \{2, -2, 3\}$. However the tracking is not as strong for $\beta = -3$. Nonetheless, the value is quite small and not that far off from the LETF RMSE.

In Figures 2.6 and 2.7, we see the time evolution for both the dynamic portfolio and GLL compared to the -2x benchmark. It is visible that the LETF tends to underperform the benchmark and the difference worsens over time. On the other hand, the portfolio tends to stay close to the benchmark over the entire period. Though not reported here, we observe similar patterns for other gold LETFs.

In Table 2.11, we also give the annual returns for each asset for the years 2011, 2012 and 2013. For UGLD and DGLD we do not have data for the full year of 2011 (trading for these assets began on October 14$^{\text{th}}$, 2011) so we do not have annual returns for these LETFs in 2011. The dynamic portfolio returns range between -69.22% and 107.54% while the LETF returns range between -69.90% and 106.16%. Comparing each year and leverage ratio pair, we find that, except for $\beta = -3$ in 2012, our portfolio outperforms the LETF in each year. Thus, we have shown that in general, a dynamic portfolio consisting of just

one futures contract can not only more closely track the target leveraged index, but it also outperforms the respective LETF.

			Annual Returns (%)		
β	Asset	$RMSE$	2011	2012	2013
+2x	UGL	30.33	12.90	2.81	-52.31
	Portfolio	6.87	15.23	6.29	-51.83
−2x	GLL	40.12	-29.43	-16.40	67.82
	Portfolio	15.87	-27.06	-14.89	70.57
+3x	UGLD	43.38	-	0.41	-69.90
	Portfolio	12.55	-	5.29	-69.22
−3x	DGLD	18.70	-	-23.57	106.16
	Portfolio	32.91	-	-24.51	107.54

Table 2.11: A summary of the annual returns (over the periods: January 3rd, 2011 to December 31st, 2011, January 3rd, 2012 to December 31st, 2012 and January 2nd, 2013 to December 31st, 2013) and RMSE for each LETF and a dynamic portfolio of 1-Month futures and cash. RMSE values are calculated over the period January 3rd, 2012 to July 14th, 2014.

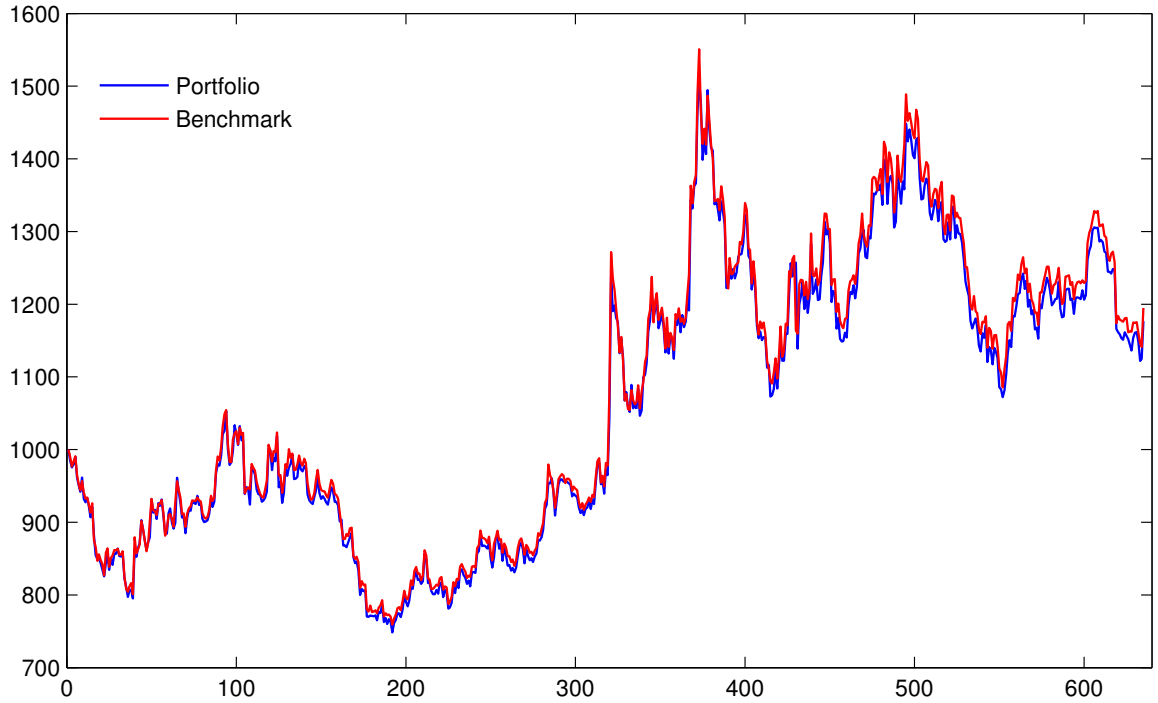

Figure 2.6: Time evolution of our dynamic portfolio of 1-Month futures and cash compared to the −2x benchmark. The time period displayed is January 3rd, 2012 to July 14th, 2014.The x-axis marks the trading day number, while the y-axis marks the price. All portfolios are initialized to start at $\$1,000$.

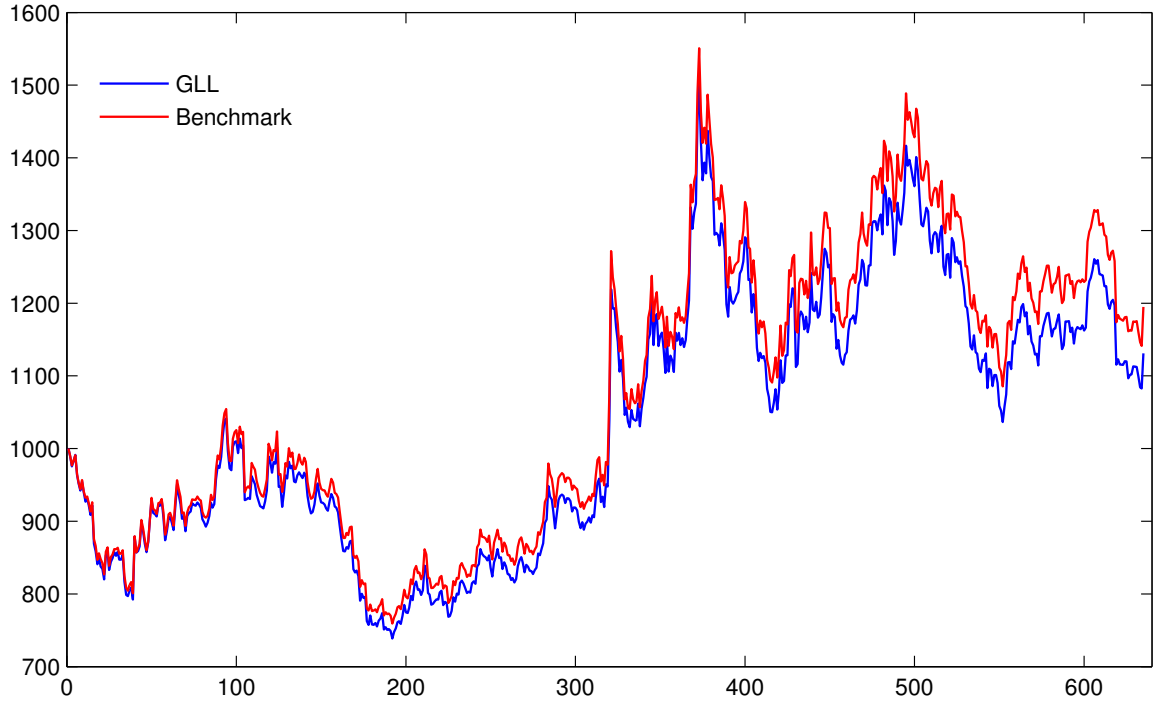

Figure 2.7: Time evolution of GLL compared to the -2x benchmark. Time period displayed is January 3$^{\text{rd}}$, 2012 to July 14$^{\text{th}}$, 2014.The x-axis marks the trading day number, while the y-axis marks the price. All portfolios are initialized to start at $\$1,000$.

Chapter 3

Tracking VIX with Futures

In this chapter, we conduct a similar analysis to that of Chapter 2, except here, we analyze products related to VIX. Our results show that VIX is quite difficult to track. Neither futures on VIX, nor the heavily traded VIX ETF, VXX, are capable of tracking VIX well. We do not even consider a leveraged position due to the negative empirical results for nonleveraged positions in VIX. In Section 3.1.3, the same optimization procedure that was performed in Sections 2.1.2 (nonleveraged) and 2.2.2 (leveraged) for gold is implemented to derive statically optimal portfolios of VIX futures to track the physical price of VIX. Due to the mean reverting nature of VIX, the optimization indicates that it is best to just hold the value of the portfolio roughly constant, since VIX futures simply do not react quickly enough to movements in spot VIX. Because of this, we consider a static portfolio by instead optimizing weights to track the daily returns (rather than physical price). Though the performance is better, it is clear that dynamic portfolios are required. Thus, we set up a discrete-time model and suggest a myopic dynamic strategy in Section 3.2. The strategy is then calibrated to data and implemented to extricate its properties in Section 3.3.

3.1 VIX Spot & Futures

We begin by analyzing the price dynamics of VIX futures and how their co-movements with spot VIX. The data for VIX futures was obtained from Quandl,[1] where historical prices for many CBOE traded futures are available. We validated the data against the data available directly from the CBOE.[2] To obtain benchmarking data for the index, VIX, we used Yahoo! Finance.[3] We tried to validate the data against the CBOE's published version of VIX historical prices but found a number of discrepancies. In fact from 2011 to 2016, the open and close prices for VIX differ on 353 and 376 days, respectively. It turns out that many of these errors are small and less than 10^{-5} in absolute value. Moreover, almost all of them are less than or equal to 0.10 in absolute value. Since we will also use VIX ETF data later on in this chapter (and the only readily available source is Yahoo! Finance) we utilize the data from Yahoo! Finance for spot VIX and expect the very minor discrepancies will not bias the results much in any direction.

After compiling, our dataset consists of the entire closing price history from March 26$^{\text{th}}$, 2004 (the first day VIX futures began trading) through January 27$^{\text{th}}$, 2017. However, we choose to analyze only the period from January 3$^{\text{rd}}$, 2011 (first trading date of 2011) through January 30$^{\text{th}}$, 2016, which is a 6-year period from 2011 to 2016. We feel that this amount of data is sufficient to avoid overfitting, and recent enough to understand the current dynamics amongst VIX spot, futures and ETFs. Unless otherwise noted, when we refer to the training set or in-sample set, we mean the 5-year period from 2011 to 2015 and when we refer to the test set or out-of-sample set, we mean the 2016 period. However, this splitting is not relevant until Sections 3.1.3 and 3.1.4, where we are develop strategies over the 2011-2015

[1] Refer to `https://www.quandl.com/collections/futures/cboe` for documentation on the available CBOE data. One can search for specific contracts at `https://www.quandl.com/data/CBOE-Chicago-Board-Options-Exchange`.

[2] CBOE publishes the historical data as well here: `http://cfe.cboe.com/data/historicaldata.aspx`. We are looking at the ticker, VX, the CBOE S&P 500 Volatility Index (VIX) Futures in this paper.

[3] See `https://finance.yahoo.com/quote/%5EVIX`. Quandl also has VIX data available, but it is sourced from Yahoo! Finance. We did however validate the Yahoo! Finance data against Quandl's version to make sure.

period and test them over the 2016 period.

Over the entire sample period from the beginning of 2011 to the end of 2016 there are 1,510 total days of data. Moreover, on any given day of the sample set there are between 7 and 9 futures contracts available. In particular, there are 15 days with only 7 futures contracts available, 278 days with only 8 futures contracts available and 1217 days with a full 9 months of contracts available.[4] It is also important to note that the contracts are *always* consecutive months (starting with the 1-Month contract) over the 2011 to 2016 time period. In other words, when there are N futures available for trading, they always consist of the N front months. As an example, if the current trading date were sometime early in January (so the January futures has not yet expired), and 7 futures contracts were available for trading, then the maturities of the futures contracts would be the months of January through July, consecutively. In our analysis, we eliminate the eighth and ninth month contract as it is not always the case that one can trade the eighth or ninth month contract. This allows us to use the full 1,510 days of day and avoid the need to eliminate the $15 + 278 = 293$ days with only 7 or 8 futures for trading.

Though we perform regressions and portfolio optimizations over this 2011 to 2016 set, we would be remiss if we did not make mention of the Credit Crisis in an empirical study of the *fear index*. Indeed the data are available to us and we do look at some interesting examples during that time period. It is also worth noting that VIX futures were rescaled by a factor of 10 on March 26$^{\text{th}}$, 2007.[5] This point in time is not part of our analysis, and we need not make any adjustments to account for it, but it is an important consideration for any future research that wishes to look at the entire period of available VIX futures data.

[4]See `http://cfe.cboe.com/products/spec_vix.aspx`. The CBOE states they will list up to 9 near-term months for trading.

[5]Refer to `http://cfe.cboe.com/publish/CFEinfocirc/CFEIC07-003%20.pdf` for details on the rescaling.

3.1.1 Return Dependency

To understand the co-movements between VIX and futures on VIX, we begin by looking at a regression of the 1-day returns of VIX futures against the corresponding 1-day returns of VIX. The results are summarized in Table 3.1 where we report the slope, intercept, R^2, and root mean squared error (RMSE) for the regression. The R^2 values are fairly strong, all exceeding 59%, corresponding to correlations in excess of 77% for each contract. Not surprisingly, the values of R^2 fall with increasing maturity. This is a fairly standard property of futures markets that closer maturities will trade closer to the spot than long-dated maturities. This is typically due to (i) the fact that futures prices tend to converge (or at least approach) spot prices as the futures approaches maturity and (ii) the fact that long dated contracts are less liquid than the short term contracts.

The slope coefficients are all statistically significant and all less than 1. This indicates the futures returns are not as reactive to spot returns and should be less volatile than the spot returns. In fact, we find the historical (annual) return volatilities are 84.27%, 61.01%, 47.11%, 39.95%, 34.86%, 31.67%, and 29.54% for the front seven month contracts. Though these values are quite large, the spot return volatility is even larger at 124.16%. Indeed, we see the futures are less volatile, confirming our expectation based on the slope coefficients.

Response	Slope	Intercept	R^2	$RMSE$
1-Month	0.60412	$-3.54216 \cdot 10^{-3}$	0.79228	0.02419
2-Month	0.42804	$-3.32786 \cdot 10^{-3}$	0.75886	0.01887
3-Month	0.32149	$-2.45114 \cdot 10^{-3}$	0.71793	0.01576
4-Month	0.26678	$-1.97891 \cdot 10^{-3}$	0.68753	0.01406
5-Month	0.22554	$-1.79483 \cdot 10^{-3}$	0.64525	0.01308
6-Month	0.20004	$-1.62159 \cdot 10^{-3}$	0.61510	0.01237
7-Month	0.18386	$-1.35468 \cdot 10^{-3}$	0.59707	0.01181

Table 3.1: A summary of the regression coefficients and measures of goodness of fit for regressing one-day returns of 1-Month through 7-Month futures on 1-day returns of spot VIX from January 3$^{\text{rd}}$, 2011 to December 30$^{\text{th}}$, 2016.

Finally, we note that the intercepts are also statistically significant and negative. This

indicates that futures prices tend to fall even if the spot price does not move. As we will see later, the term structure of VIX futures is typically an increasing function of time-to-maturity. Since the futures prices approach spot prices at maturity, as time passes, even when the spot does not move, the futures price tends to fall.

We also look at the co-movements among futures prices themselves. Here we give the correlation matrix for the daily returns of the spot as well as futures contracts for maturities 1-Month through 7-Month:

$$\begin{bmatrix} 1 & 0.890 & 0.871 & 0.847 & 0.829 & 0.803 & 0.784 & 0.773 \\ - & 1 & 0.939 & 0.916 & 0.899 & 0.874 & 0.856 & 0.848 \\ - & - & 1 & 0.985 & 0.969 & 0.947 & 0.929 & 0.920 \\ - & - & - & 1 & 0.989 & 0.973 & 0.958 & 0.951 \\ - & - & - & - & 1 & 0.989 & 0.978 & 0.971 \\ - & - & - & - & - & 1 & 0.991 & 0.984 \\ - & - & - & - & - & - & 1 & 0.990 \\ - & - & - & - & - & - & - & 1 \end{bmatrix}$$

Note that since the correlation matrix is symmetric, we only report the upper right correlations for simplicity. The first row contains the same information as the fourth column of Table 3.1. The correlations are simply the square roots of the R^2 values from the table. Notice the other rows, which indicate that correlations *amongst* the futures contracts exceed 84% and are as high as 99%. This would suggest that the futures prices move together.

Indeed the futures prices move almost in parallel. In Figure 3.1, we plot the time series of spot VIX, the 1-Month futures price (May-16 contract), and the 7-Month futures price (Nov.-16 contract) over the period from April 22$^{\text{nd}}$, 2016 (1 day after the expiration of the April-16 contract) to May 18$^{\text{th}}$, 2016 (the expiration date of the May-16 contract). Notice that the spot, 1-Month futures price and 7-Month futures price all move together. However, the moves in the spot are larger than moves in the futures prices. We observe that the spot and futures prices move often move in the same direction, but the futures prices do not move

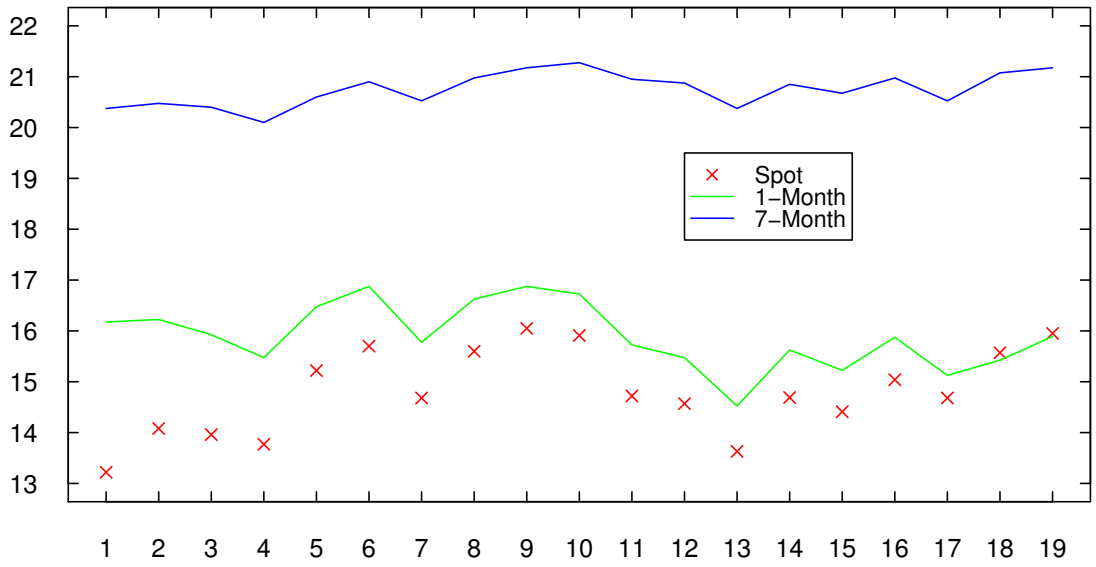

Figure 3.1: Time evolution of VIX, 1-Month futures price (May-16 contract) and 7-Month futures price (Nov.-16 contract) over the period from April 22$^{\text{nd}}$, 2016 to May 18$^{\text{th}}$, 2016. The x-axis marks the trading day number, while the y-axis marks the price.

1 for 1 with the spot. As one might expect, this effect is more pronounced for the 7-Month contract, which barely moves over the period. For example, from trading day 4 to 5, we have a large up move in VIX of \$1.45 which is only met by an increase of \$1.00 by the 1-Month contract and an increase of \$0.50 by the 7-Month contract.

Notice also that there is a slight discrepancy between the 1-Month futures price at maturity (the final trading day) and the spot price. In theory, futures prices should converge to the spot price. However, settlement rules/procedures as well as market frictions to trade the spot can substantially limit this convergence.[6]

To better understand the dynamics amongst futures and the spot, we can look at the term structure, which is a plot of the futures price against the time-to-maturity of the contract. In Figure 3.2, we plot the term structure of VIX futures as observed at several different time points throughout the first 6 months of 2016 (left) and 2009 (right). Typically, the term

[6]See Pavlova and Daigler (2008) for an empirical study of the non-convergence of VIX futures as well as `https://cfe.cboe.com/products/settlement_vix.aspx` for a description of VIX derivatives' settlement procedures. See also Guo and Leung (2017) for a theoretical study of the implications of exchange set settlement rules on the pricing/non-convergence of agricultural futures.

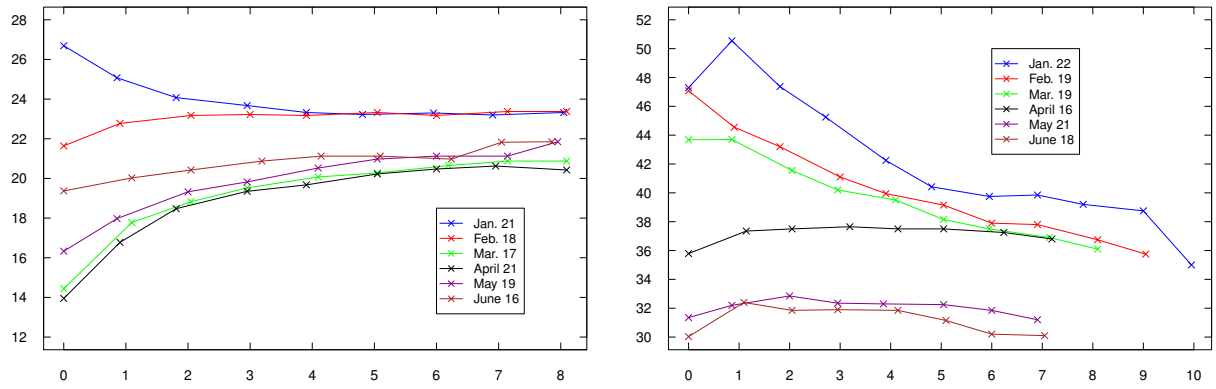

(a) Jan.-June 2016 (b) Jan.-June 2009

Figure 3.2: Term structures from Jan. to June in 2016 (left) and 2009 (right). The legend marks the date upon which the term structure is constructed. These dates are 1 day after maturity of that month's futures contract. The x-axis marks the time-to-maturity (in months) and assumes each month is exactly 21 (= 252/12) days, while the y-axis marks the price.

structure forms an increasing and concave function of time-to-maturity. On the left, we see this is the case for many different different months. However, in January 2016, VIX spiked as did expectations of future volatility.[7] When this happens, the term structure of VIX futures tends to invert and become a decreasing and convex function of time-to-maturity. In fact, many models for VIX dynamics lead to term structures that necessarily possess these shape properties (either increasing/concave or decreasing/convex).[8] In these models, when there is a spike in spot VIX above its long run average level, the term structure inverts. This indicates long term expectations that volatility will fall. This is seen prominently in the aftermath of the financial crisis. On the right of Figure 3.2, we plot the term structures in early 2009. One notices the high levels for the prices of VIX futures. During this chaotic period, the term structures do not fall into the usual patterns. For example in April (black) we notice the term structure is increasing in spite of the spot being at a historically high

[7]One can find a discussion of trends in volatility in late January in the following article: `https://tickertape.tdameritrade.com/options/2016/01/volatility-high-early-2016-42727`.

[8]Grübichler and Longstaff (1996) model VIX with a Cox-Ingersoll-Ross process. In that case $dV_t = \mu(\theta - V_t)dt + \sigma\sqrt{V_t}dW_t$. When V_t is below θ, the long term mean, the term structure is increasing and concave and when it is above θ, the term structure is decreasing and convex. The same is true under the Ornstein-Uhlenbeck Model, $dV_t = \mu(\theta - V_t)dt + \sigma dW_t$ (see Uhlenbeck and Ornstein (1930)). See Leung and Li (2016) for further discussion of mean-reverting models and optimal trading of futures under such models.

level. This term structure does not follow the increasing and concave shape, as it dips back down for the longest dated futures. A similar shape occurs in May and June.

3.1.2 Long-Term Dependency

Next, we look at the longer term tracking performance by analyzing the linear relationships for returns over longer holding periods. We remark that we use *disjoint* intervals of various lengths when we compute the returns. Thus, for the longer horizons we have fewer data points, but even for the 30-day horizon we have approximately 50 data points. In Figure 3.3, we plot the regressions of 1-Month futures returns versus gold returns for both 1-day returns (left) and 10-day returns (right), plotted on the same x-y axis scale. The red x's mark pairs of returns, while the black line is the best fit line. Notice the large range of the returns, even for the futures. We observe the 10-day returns are much larger and consequently more volatile. However, for both holding periods, the futures returns are less volatile than the corresponding spot returns. More precisely we find that the 1-day returns of the spot vary between -26.96% and 50%, while for the 10-day returns they vary between -39.76% and 148.06% (i.e. the longer holding period has more volatile returns). On the other hand for the 1-Month futures, the 1-day returns vary between -20.81% and 35.83%, while the 10-day returns vary between -36.91% and 88.89% (i.e. futures returns are less volatile than respective spot returns).

In the plot, the slope is slightly higher for the 10-day returns as compared to the 1-day returns. Moreover, for the 1-day returns the scatter plot is more tightly bound to the best fit line indicating a better fit than on the 10-day returns. However, this pattern does not hold in general. There is no discernible pattern in either the R^2 values or the slope coefficients as the holding period is lengthend. We give an example for 3-Month futures in Figure 3.4. The points form a cloud with no pattern of increasing or decreasing predictive power (as measured by R^2) or leverage necessary to replicate the spot returns. (Leverage can be measured by the reciprocal of the slope.)

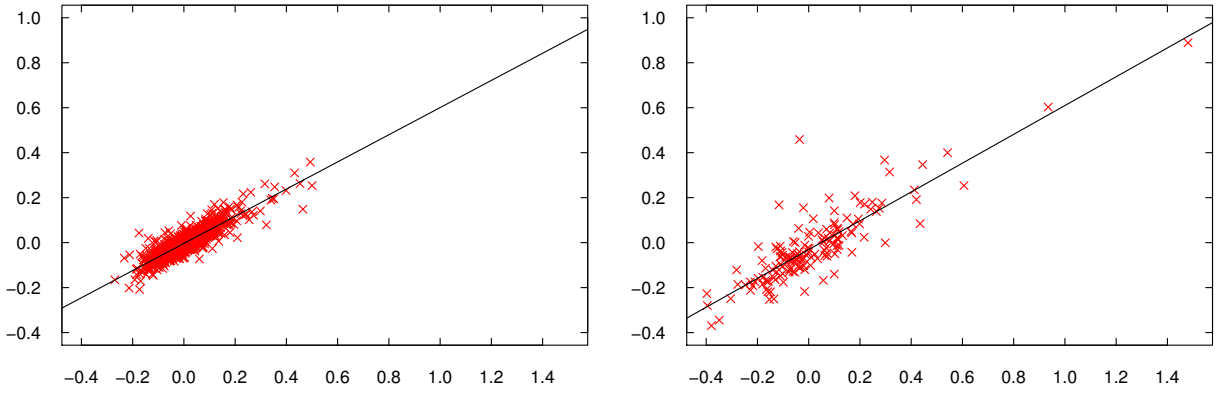

(a) 1-Day Returns (b) 10-Day Returns

Figure 3.3: Linear regressions of 1-Month futures returns vs. spot VIX returns based on 1-day returns (left) and 10-day returns (right). The x-axis marks the returns (decimals, not percentages) of spot VIX, while the y-axis marks the returns (decimals, not percentages) of the 1-Month futures.

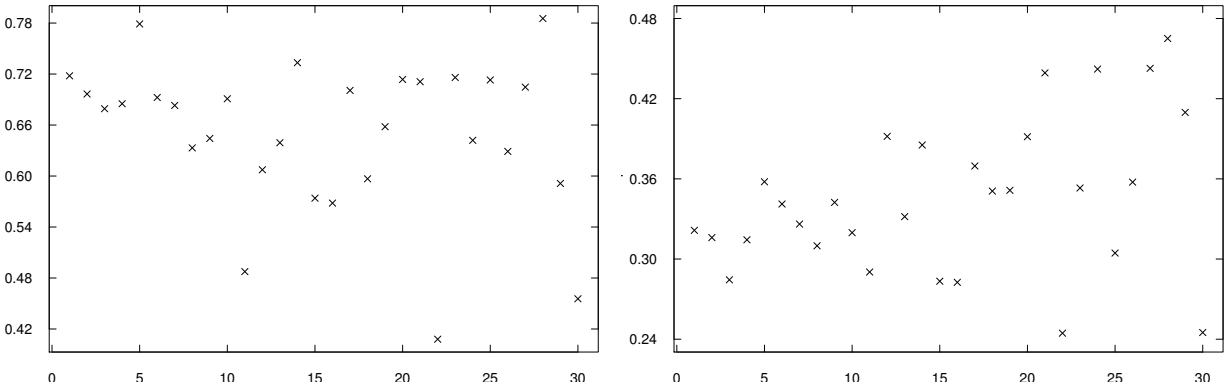

(a) R^2 (b) Slope

Figure 3.4: The R^2 (left) and slopes (right) for regressions of 3-Month futures returns against spot returns with increasing holding period. We vary holding period from 1 day up to 30 days. There are no strong patterns in these statistics as the holding period is lengthened. The x-axis marks the holding period length (in trading days), while the y-axis marks the statistic.

On the other hand, if we fix the holding period and increase the maturity of the contract, we see a decrease in predictive power and a decrease in slope. (Thus, an increase in leverage necessary to replicate the spot.) We demonstrate this for a number of different holding periods (1, 5, 10 and 15 days) in Table 3.2. In the top half, we display the slope coefficients for the regressions of futures returns against spot returns and in the bottom half, we display the R^2 values. By looking across the rows in either half, one notices a decrease in the reported

statistic. This reaffirms our earlier observation that the spot is more closely tracked by short-term futures than long term futures. Indeed, over a 15 day period, the results indicate that about 1.61x leverage is required to track the spot with just 1-Month futures vs. 7.21x leverage for the 7-Month futures.[9] The latter amount is a substantial amount of leverage that may not be feasible in the marketplace.

	Days	1-Month	2-Month	3-Month	4-Month	5-Month	6-Month	7-Month
Slope	1	0.60412	0.42804	0.32149	0.26678	0.22554	0.20004	0.18386
	5	0.66818	0.47056	0.35782	0.29102	0.24411	0.21911	0.19908
	10	0.64067	0.42413	0.31974	0.25444	0.20624	0.18455	0.16690
	15	0.62179	0.37305	0.28340	0.21815	0.17129	0.15280	0.13880
R^2	1	0.79228	0.75886	0.71793	0.68753	0.64525	0.61510	0.59707
	5	0.83197	0.82479	0.77897	0.73825	0.69743	0.67324	0.64888
	10	0.75004	0.74992	0.69093	0.62952	0.56175	0.54031	0.51936
	15	0.66338	0.63884	0.57394	0.48795	0.39504	0.37570	0.35219

Table 3.2: A summary of the slopes and R^2 from the regressions of futures returns versus VIX returns over different holding periods.

It is not completely visible in Figure 3.3, but the intercept is lower and continues to be statistically significant. This reinforces what we saw earlier: futures tend to underperform and lose money relative to the spot returns. What we are seeing here is that this underperformance worsens over longer horizons. To see this more generally, in Figure 3.5, we plot the intercepts for the regressions of returns of 1-Month futures (black), 3-Month futures (red) and 6-Month futures (blue) across many different holding periods (from 1 day up to 30 days). There is a clear decreasing trend in the intercepts: they continue to become more and more negative as the holding period is lengthened. We remark that all intercepts (as well as the slopes from earlier) reported here are statistically significicant at the 1% significance level. Thus, a statistically significant discrepancy exists and continues to worsen as holding period is lengthened.

[9]These are obtained by computing the reciprocals of the slopes, which are 0.622, and 0.139, respectively.

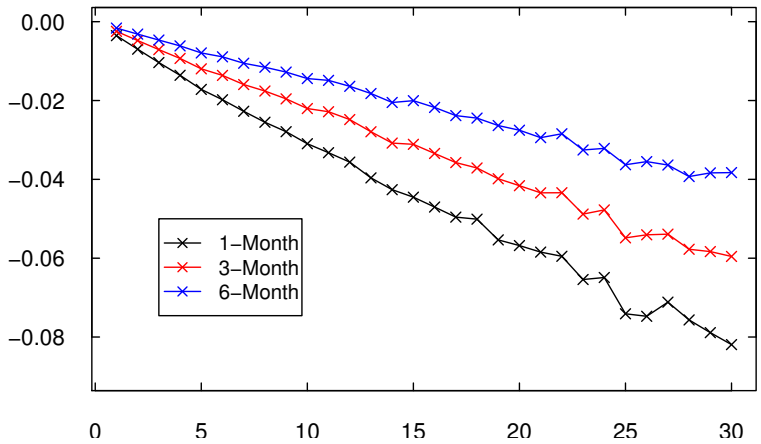

Figure 3.5: The intercepts for regressions of futures returns against spot returns with increasing holding period. We display the results for 1-Month, 3-Month and 6-Month futures. The x-axis marks the holding period length (in trading days), while the y-axis marks the intercept for the regression.

3.1.3 Static Physical Replication

We now turn our attention to replicating the spot price. In this section, we consider static positions including 1 or more futures contracts. By a static position in the futures contract, we mean a position is constantly rolled over into the next futures contract. For example, a static investment of $\$P_0$ in 1-Month futures would work as follows. First, purchase P_0/F_0 units of the current 1-Month contract and hold it until maturity. The position's value at that time can be denoted by P_1. Then, one uses this final value to purchase what was previously (e.g. at time 0) the 2-Month futures, but is now the 1-Month futures and hold *that* contract to maturity. This process continues onward, indefinitely. We do not allow cash injections to keep the number of units constant, but instead allow the number of units of futures to vary over time. This makes the position completely self-financing. The static position described here, starting on January 3$^{\text{rd}}$, 2011 with \$100 will be called the value of the 1-Month futures contract. One can analogously define the 2-Month, 3-Month, etc. values as positions that always maintain all money in 2-Month, 3-Month, etc. contracts.

We construct a portfolio consisting of the various futures contracts whose value on day j is denoted by P_j. The value of spot VIX on day j is denoted V_j. Then we seek a static

portfolio of historical futures and cash account investment that minimizes the sum of squared errors:

$$SSE = \sum_{j=1}^{n} (V_j - G_j)^2, \tag{3.1.1}$$

where n is the number of trading days.

Let k be the number of futures contracts and $\mathbf{w} := (w_0, \ldots, w_k)$ be the real-valued vector of portfolio weights. In particular, w_0 represents the weight given to the money market account. To calculate the optimal portfolio value we will choose weights historically which minimize SSE over the training set from 2011 to 2015. Thus, we solve the following constrained least squares optimization problem:

$$\begin{aligned} \min_{\mathbf{w} \in \mathbb{R}^{k+1}} \quad & \|\mathbf{C}\mathbf{w} - \mathbf{d}\|^2 \\ \text{s.t.} \quad & \sum_{j=0}^{k} w_j = 1. \end{aligned} \tag{3.1.2}$$

The matrix $\mathbf{C}$ contains as columns, the historical values of the various futures contracts and the money market account,[10] and the vector, $\mathbf{d}$ contains the historical prices of spot VIX. These prices are normalized by \$100, without loss of generality, so that an investor starting with \$100 will invest $\$100 \cdot w_j$ into the jth futures contract and $\$\ 100 \cdot w_0$ into the money market account. For the futures portfolios, we consider only four positions: 1-Month, 2-Month, 6-Month and 7-Month. The portfolios are all possible subsets of these contracts, of which there are $2^4 - 1 = 15$ (subtract 1 because we do not look at the portfolio using no futures). Using all 7 available futures and their $2^7 - 1 = 127$ subsets would be untenable and obscure the analysis. The four contracts selected here represent the shortest and longest dated maturities that are available in the VIX futures market on every day of both the in-sample and out-of-sample period.

[10] We use historical overnight LIBOR to construct an investment in the money market account. This is available from Quandl as well: `https://www.quandl.com/data/FRED/USDONTD156N-Overnight-London-Interbank-Offered-Rate-LIBOR-based-on-U-S-Dollar`. However, the data feed stops in November of 2016. Therefore, we get the data from the Federal Reserve Bank of St. Louis: `https://fred.stlouisfed.org/series/USDONTD156N`, which is actually the source Quandl obtains the data from.

We report the results of the optimization in Table 3.3. The value of w_0 always represents the weight on the cash account. The other values of w_i are ordered so that if $i < j$ then w_i represents the weight on a nearer term contract than w_j. For example, in row 6 we are considering a portfolio of 1-Month and 6-Month futures. Thus, w_1 is the weight on 1-Month futures, while w_2 represents the weight on 6-Month futures. The Root Mean Squared Errors (RMSE) values are computed by first dividing the sum of squared errors in (3.1.1) by the number of trading days (1,258 for the in-sample period and 252 for the out-of-sample period) and taking the square root:

$$RMSE := \sqrt{\frac{SSE}{n}}. \tag{3.1.3}$$

Since our portfolio is initialized to \$100, we can interpret RMSE as being the average percentage deviation (across either the in-sample or out-of-sample period) that the portfolio value is from the spot price.

The RMSE values are quite large, indicating that our portfolios are unable to track VIX well. To benchmark our performance we compare the portfolios to the most popular VIX ETF, VXX. The in-sample RMSE for VXX is 72.05%, while the out-of-sample value is 21.97%. The values indicate our portfolios perform significantly better in-sample than does VXX and only slightly better in a few cases out-of-sample. VXX performs poorly due to the longer sample. As soon as VXX has away from VIX, even if it tracks the returns well,[11] it cannot return to the dollar value of VIX. On the other hand, our portfolio has been optimized to stay near VIX during the in-sample period.

That being said, the resulting strategies are quite counterintuitive. One notices barely any (net long) use of the futures constracts, especially for portfolios of 1 or 2 futures only. Consider the 1-Month only portfolio. It invests only 15.2% of wealth in the value of the 1-Month futures contract. The remaining 84.8% is held in cash. This is because the optimization is (in some sense) forward looking in the period. It considers all at once the values VIX will take over the in-sample period. In particular, there is a high degree of mean rever-

[11] Indeed it does this fairly well. See Section 3.1.4.

sion in VIX and thus, holding the portfolio value at the average level of VIX over the period is preferrable as getting closer at every point in time is simply not possible with futures. Notice also the high degree of leveraging being done with the portfolios of 3 or 4 futures. It appears that the optimization is overfitting to the time period by constructing such large and oppositely signed weights.

Futures	w_0	w_1	w_2	w_3	w_4	$RMSE$ (in)	$RMSE$ (out)
1-m	0.848	0.152	-	-	-	30.724	23.345
2-m	0.857	0.143	-	-	-	31.153	26.074
6-m	0.811	0.189	-	-	-	31.026	28.840
7-m	0.777	0.223	-	-	-	30.835	28.616
1-m, 2-m	0.932	2.114	−2.046	-	-	27.741	19.521
1-m, 6-m	0.917	0.345	−0.262	-	-	30.576	17.197
1-m, 7-m	0.840	0.137	0.022	-	-	30.722	23.819
2-m, 6-m	0.757	−0.203	0.446	-	-	30.960	32.971
2-m, 7-m	0.669	−0.252	0.582	-	-	30.627	33.518
6-m, 7-m	0.492	−2.146	2.654	-	-	29.801	27.021
1-m, 2-m, 6-m	0.453	3.770	−5.615	2.392	-	23.404	22.174
1-m, 2-m, 7-m	0.341	3.745	−5.095	2.009	-	22.414	24.742
1-m, 6-m, 7-m	0.229	1.979	−11.066	9.858	-	22.960	61.713
2-m, 6-m, 7-m	0.359	2.449	−11.032	9.224	-	27.437	37.218
1-m, 2-m, 6-m, 7-m	0.225	3.292	−3.151	−5.548	6.183	21.492	44.222

Table 3.3: Optimal portfolio weights/performance measures for portfolios of VIX futures for tracking the dollar value of VIX. Porfolios utilize any subset of the 1-Month, 2-Month, 6-Month and 7-Month contract.

We plot spot VIX, the ETF VXX, and the optimal out-of-sample portfolio in Figure 3.6. One notices that the optimal portfolio is relatively flat. It holds most of its value (91.7%) in cash and is long 1-Month futures (34.5%) and short 6-Month futures (26.2%.) It is not reactive to the spot movements. On the other hand VXX is more reactive to the spot price movements, but quickly diverges from spot VIX and is unable to recover. By the end of the in-sample period, VXX has fallen to \$3.44, and for out-of-sample period, it has fallen to \$29.89. The optimal portfolio does not lose this much money but rather stays roughly constant at VIX's average level over both periods. Neither appears a perfect surrogate for trading VIX and therefore we consider alternative methods to constructing portfolios of

futures to track VIX.

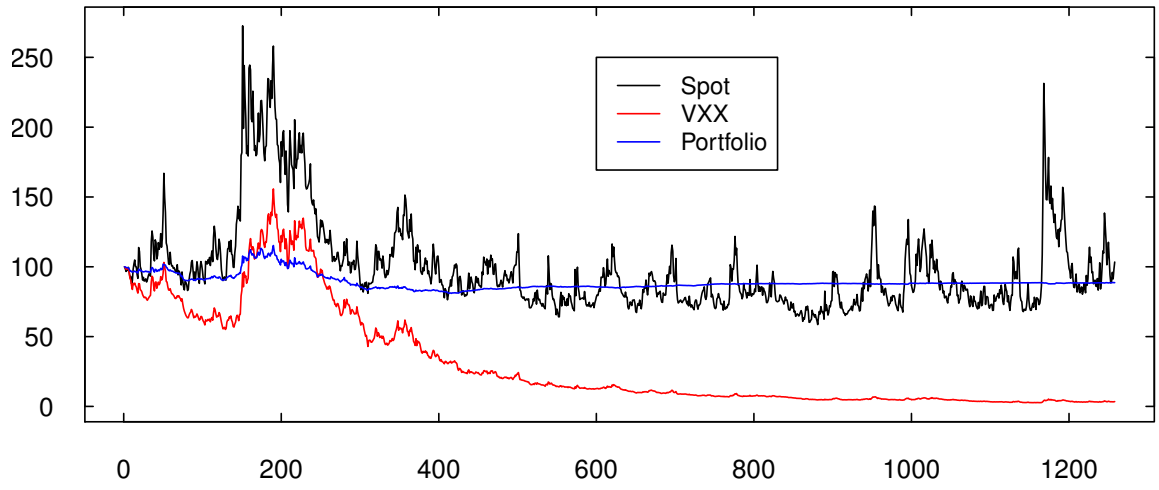

(a) In-Sample

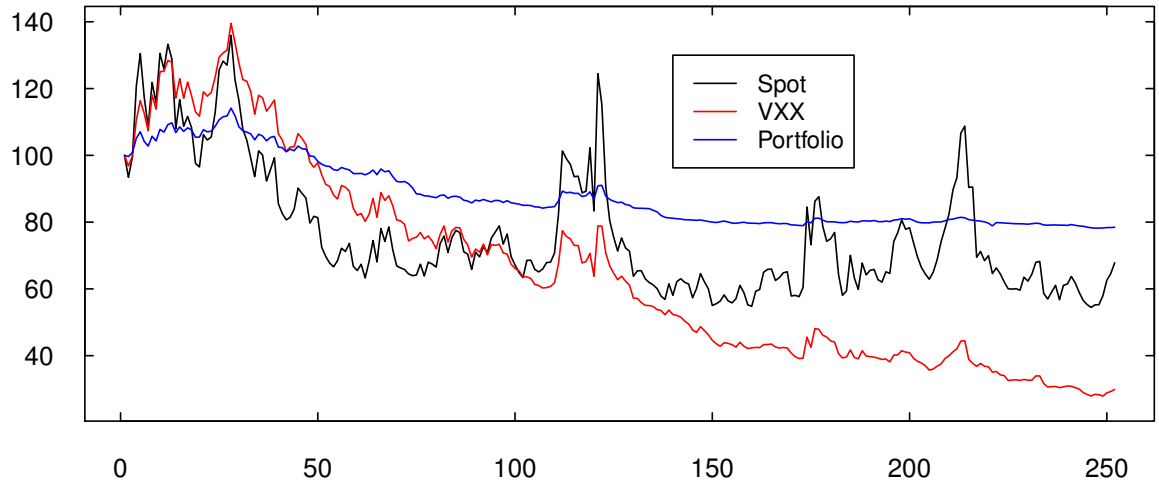

(b) Out-of-Sample

Figure 3.6: Time series of spot VIX, the ETF VXX and the optimal VIX dollar value tracking portfolio both in (a) and out-of (b) sample. The x-axis marks the trading day number, while the y-axis marks the price. All prices are normalized to start at $100.

3.1.4 Static Return Replication

Based on the results of Section 3.1.3, we find that directly the tracking the physical value of VIX is quite difficult. The resulting strategies for futures based portfolios found it optimal to simply hold the portfolio value constant. Moreover, VXX had substantial discrepancies that were unrecoverable over the longer term period. On the other hand, VXX *does* well

in tracking the returns of VIX relative to our portfolios. If we instead compute the RMSE value on the returns (rather than the physical price), we find in-sample VXX has a return RMSE of 4.63% as compared to 7.51% for our best[12] portfolio. Those values are 4.55%, and 7.21%, respectively for the out-of-sample period.

The goal of the previous section was to investigate the possibility of tracking the dollar value of VIX using a futures portfolio. Were that the case, we would have necessarily matched the returns on each day as well. (Otherwise, we could not have matched the dollar value.) The opposite need not have held true: it is possible for the returns to be close to VIX returns while the physical values still diverge. This is clearly evidenced in the above paragraph whence VXX more closely matches the returns than our portfolio does, but more poorly tracks the physical price of VIX than our portfolio does. Though matching the returns need not force the prices to match closely, we set this as our optimization goal in this section as appears to be more likely that we can match the returns rather than physical prices.

We set up a similar optimization problem as we solved in Section 3.1.3:

$$\begin{aligned} \min_{\mathbf{w}\in\mathbb{R}^{k+1}} \quad & \|\mathbf{B}\mathbf{w}-\mathbf{y}\|^2 \\ \text{s.t.} \quad & \sum_{j=0}^{k} w_j = 1. \end{aligned} \tag{3.1.4}$$

The matrix $\mathbf{B}$ contains as columns, the returns of the various futures contracts and the money market account,[13] and the vector, $\mathbf{y}$ contains the historical returns of spot VIX.

Our performance metric continues to be the RMSE defined in (3.1.3), but this time for the returns. However, we do remark that the weighted returns (as computed by $\mathbf{B}\mathbf{w}^*$) are *not* the true portfolio returns. In fact, those are the returns if the strategy is dynamic and constantly maintains the weights in each futures contract, but we emphasize here that we

[12]Best here still refers to the optimal out-of-sample portfolio from the previous section and not best by the new statistic we are reporting here.

[13]This is just historical overnight LIBOR. See `https://www.quandl.com/data/FRED/USDONTD156N-Overnight-London-Interbank-Offered-Rate-LIBOR-based-on-U-S-Dollar`. Again, the data feed stops in November of 2016 and obtain the data from the Federal Reserve Bank of St. Louis: `https://fred.stlouisfed.org/series/USDONTD156N`.

employ static strategies. As a simple example, consider an investor who places %80 of her wealth in stocks and %20 in bonds. If she has \$100, and stocks rise %10, while bonds fall %5 after 1 year, her portfolio is worth $80 \cdot 1.10 + 20 \cdot 0.95 = 107$, a %7 return, which is indeed equal to $0.8 \cdot 10 + 0.2 \cdot (-5) = \%7$ (the weighted return). However, if the following year, the performance is the same, the investor's portfolio is worth $80 \cdot 1.10^2 + 20 \cdot 0.95^2 = 114.85$, for a return of $100 \cdot (114.85/107 - 1) = \%7.33$, which is *not* equal to the weighted return in that year: $0.8 \cdot 10 + 0.2 \cdot (-5) = \%7$. Though static portfolios are simple, the mechanics of their return computations are very subtle indeed so we caution the reader in interpreting the results in the rest of this section.

The results of the optimization are reported in Table 3.4. When we consider tracking the returns (rather than physical prices), the resulting portfolios are more intuitive. As our regressions indicated, leveraging futures contracts is necessary in order to track VIX returns well. For all 15 portfolios, the weight on the money market account, w_0 is negative, so that borrowing is required. In an extreme case, the 6-Month/7-Month portfolio requires a leverage of about 3 to track the VIX returns (since it borrows about 2x its value from the bank). There is a similar effect for the 6-Month only portfolio and the 7-Month only portfolio. Additionally, almost all portfolios outperform VXX in-sample (RMSE = 4.63%) as well as out-of-sample (RMSE = 4.55%). The exceptions are the 6-Month only, 7-Month only and 6-Month/7-Month portfolios. These two observations (extreme leverage and poor tracking performance) echo our previous discussion regarding the fact that the longer dated contracts are not as reactive to spot movements as the shorter dated contracts.

Futures	w_0	w_1	w_2	w_3	w_4	$RMSE$ (in)	$RMSE$ (out)
1-m	−0.317	1.317	-	-	-	3.620	3.491
2-m	−0.751	1.751	-	-	-	3.929	3.685
6-m	−2.018	3.018	-	-	-	4.926	4.659
7-m	−2.178	3.178	-	-	-	5.020	4.832
1-m, 2-m	−0.499	0.921	0.578	-	-	3.532	3.430
1-m, 6-m	−0.542	1.210	0.333	-	-	3.603	3.492
1-m, 7-m	−0.503	1.237	0.265	-	-	3.610	3.491
2-m, 6-m	−0.445	2.033	−0.588	-	-	3.903	3.607
2-m, 7-m	−0.380	2.050	−0.669	-	-	3.896	3.598
6-m, 7-m	−1.989	3.391	−0.401	-	-	4.925	4.645
1-m, 2-m, 6-m	−0.319	0.905	0.769	−0.355	-	3.522	3.400
1-m, 2-m, 7-m	−0.244	0.904	0.810	−0.470	-	3.515	3.396
1-m, 6-m, 7-m	−0.463	1.215	1.269	−1.021	-	3.592	3.494
2-m, 6-m, 7-m	−0.379	2.040	0.193	−0.854	-	3.896	3.600
1-m, 2-m, 6-m, 7-m	−0.237	0.910	0.770	0.594	−1.036	3.511	3.405

Table 3.4: Optimal portfolio weights/performance measures for portfolios of VIX futures for tracking VIX returns. Porfolios utilize any subset of the 1-Month, 2-Month, 6-Month and 7-Month contract. The reported RMSE values are for the returns of the portfolio.

Finally, we plot the resulting time series in Figure 3.7 for the lowest out-of-sample RMSE portfolio: the 1-Month/2-Month/7-Month portfolio. In terms of physical price replication, both VXX and the optimized portfolio continue to underperform, but that is not the goal of this section. Rather, we are concerned with return replication. Indeed the optimized portfolio is more reactive to spot movements and is no longer constant over the time period and the RMSE calculations demonstrate that the portfolio is tracking VIX returns well. However, with the leveraging the portfolio has eroded so far in value both in-sample and out-of-sample that it has gone negative! Though surprising, this is completely possible (see Remark 3.1.1) and is due to the leveraging and the fact that VIX futures tend to suffer substantial roll yield losses. It is interesting to note that this portfolio has the second smallest degree of leveraged amongst all 15 optimized portfolios. At inception it borrows only 24.4% of its initial value. It is at this point, quite evident that dynamic strategies are needed if one is to track VIX. We discuss one such strategy in the following section.

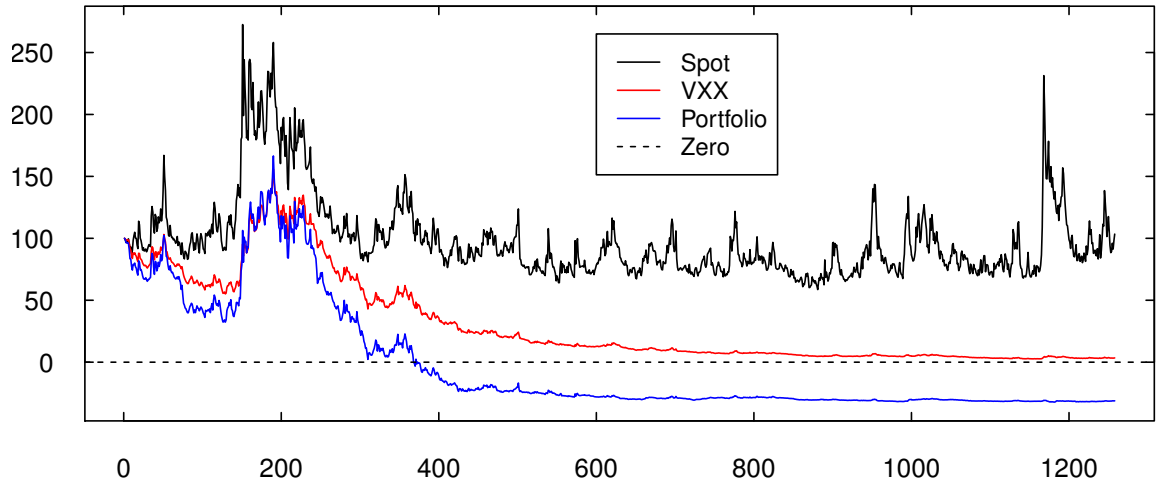

(a) In-Sample

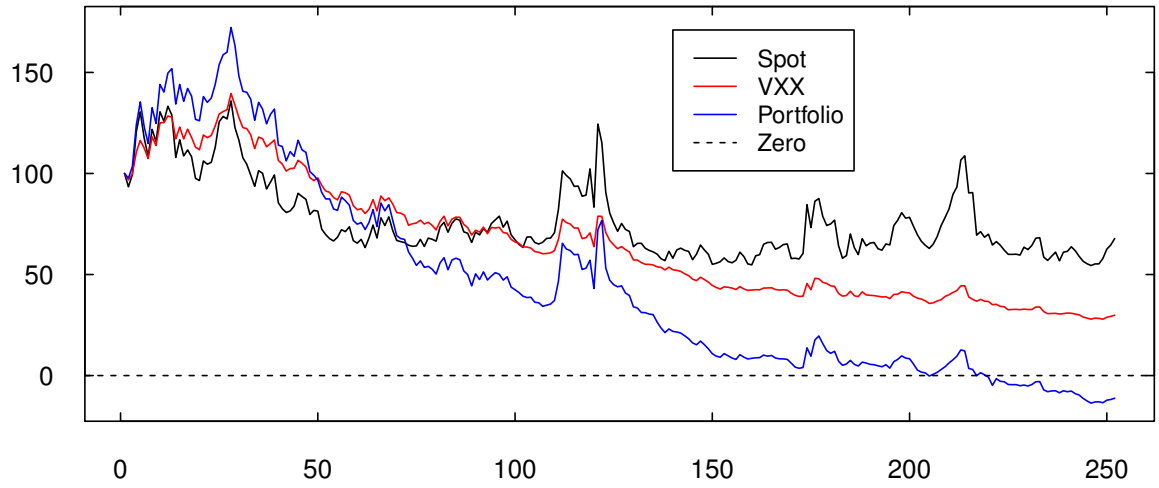

(b) Out-of-Sample

Figure 3.7: Time series of spot VIX, the ETF VXX and the optimal VIX return portfolio both in (a) and out-of (b) sample. The x-axis marks the trading day number, while the y-axis marks the price. All prices are normalized to start at \$100.

Remark 3.1.1 *To understand why the portfolio value is negative, consider the following scenario. The investor begins with* \$100 *and wishes to obtain a leveraged investment in an asset which is currently priced at* \$30*. The investor seeks a leverage ratio of* $\beta = 3$ *so borrows* \$200 *from the bank, at a (constant and annually compounded) interest rate of 4% and uses the full amount to purchase 10 units of the asset. Suppose now that after 1 year's time, the asset's value has plummeted to* \$20*. Then the investor has 10 units of the asset worth a total*

of \$200, but owes $200 \cdot 1.04 = 208$ *to the bank. The net value of his portfolio is therefore,* -8*, meaning a cash injection of \$8 is necessary just to liquidate the portfolio. This is precisely what has happened here with the optimal futures portfolio. The combination of leveraging along with the poor returns of VIX futures drove the portfolio to a negative value.*

3.2 Discrete-Time Model

In this section we develop a discrete-time model of the portfolio dynamics. By working in discrete time, we will be able to capture the daily mark to market feature that is present in futures markets. We will then find the optimal dynamic weights to allocate capital amongst two futures contracts so as to replicate the daily returns of the index.

3.2.1 Futures Portfolio

To maintain a futures position, the investor places a certain fraction of the exposure, e.g. 20% of the dollar value, on margin with the clearing agency. This amount is called the *initial margin*, while the account held with the clearing agency is called the *margin account*. The margin account is *marked-to-market* which means that if we denote the futures price for maturity T_i, as observed on day j by $f_j^{(i)}$, the margin account receives a cash flow equal to $f_j^{(i)} - f_{j-1}^{(i)}$ for each unit of long futures held at the end of day j. Moreover, if these cash flows accumulate to a substantially negative value, the margin account will fall below a level called the *maintenance margin*. In that case, the investor receives a *margin call* and must replenish the account's funds back up to the initial margin. The account will otherwise be paid the risk free rate in exchange for the collateral. In our discrete-time model, we assume for simplicity that the full amount of the exposure is held on margin. This simplifies matters as there is no need to incorporate margin calls or maintenance margins in the model.[14]

[14] In the sequel, we will derive an optimal allocation amongst futures contracts. Without any constraints, it is possible for these weights to be > 1, indicating a degree of leverage in the exposure. If that is the case, one can assume the investor is able to borrow at the risk free rate so as to post all the collateral on margin.

Each time step will be one day, which we denote by Δt.[15] Thus, the futures contracts are marked-to-market in accordance with the time step. Consequently, the investor must make all decisions for the next day's holdings based on information generated by the previous day's prices. Furthermore, the allocation between futures must be constant from day to day. The value of the investor's holdings is denoted by the discrete-time stochastic process, $\{X_j\}_{j=0}^{\infty}$, where X_0 is the (deterministic) initial wealth.

Further suppose there are N futures contracts available for trading with maturities $T_1 < ... < T_N$. Then a portfolio which holds a fraction of wealth, $w_j^{(i)}$, in the i^{th} maturity, $(i = 1, ..., N)$ will have $\frac{w_j^{(i)} X_j}{f_j^{(i)}}$ many units of futures contract of maturity T_i on day j. Let the continuously compounded risk free rate be r so that 1 dollar grows to $e^{r\Delta t}$ dollars the next day. From the above, it follows that if the portfolio of futures contracts is worth X_j on day j, then it is worth

$$X_{j+1} = X_j e^{r\Delta t} + \sum_{i=1}^{N} \frac{w_j^{(i)} X_j}{f_j^{(i)}} \left[f_{j+1}^{(i)} - f_j^{(i)} \right], \tag{3.2.1}$$

on day $j+1$. The daily return of the portfolio is given by

$$\frac{X_{j+1}}{X_j} - 1 = e^{r\Delta t} - 1 + \sum_{i=1}^{N} w_j^{(i)} \left[\frac{f_{j+1}^{(i)}}{f_j^{(i)}} - 1 \right]. \tag{3.2.2}$$

This is the sum of the risk free return for placing collateral with the exchange and the weighted average daily returns of the various futures contracts.

The value of the index we seek to track is denoted by the discrete-time stochastic process, $\{S_j\}_{j=0}^{\infty}$. We suppose the index satisfies the following equation:

$$S_{j+1} - S_j = \mu(\theta - S_j)\Delta t + g(j, S_j)\sqrt{\Delta t} Z_{j+1}, \tag{3.2.3}$$

where Z_{j+1} $(j = 0, 1, 2, ...)$ are independent and identically distributed standard normal

[15] Here, $\Delta t = \frac{1}{252}$ as there are on average 252 trading days per year.

random variables under the historical measure $\mathbb{P}$. From this equation, the daily return of the index is equal to

$$\frac{S_{j+1}}{S_j} - 1 = \frac{\mu\theta\Delta t}{S_j} - \mu\Delta t + \frac{g(j, S_j)}{S_j}\sqrt{\Delta t}Z_{j+1}. \tag{3.2.4}$$

Remark 3.2.1 *These equations are motivated by the continuous-time mean-reverting model*

$$dS_t = \mu(\theta - S_t)dt + g(t, S_t)dZ_t, \tag{3.2.5}$$

where $\mu, \theta > 0$, $g(\cdot, \cdot)$ is a generic volatility function and Z_t is a Standard Brownian Motion (SBM) under the historical measure ($\mathbb{P}$). The drift $\mu(\theta - S_t)$ indicates that when $S_t < \theta$, S_t tends to rise and when $S_t > \theta$, S_t tends to fall, hence S_t mean-reverts to θ. By instantiating $g(\cdot, \cdot)$ with a particular function, one obtains many well-known mean-reverting models. For example, when $g(t, S_t) = \sigma$, the model is called the Ornstein-Uhlenbeck Model *(see Uhlenbeck and Ornstein (1930)) and when $g(t, S_t) = \sigma\sqrt{S_t}$, the model is called the* Cox-Ingersoll-Ross Model. *(See Cox et al. (1985) as well as Grübichler and Longstaff (1996) for an application of this model to pricing futures and options on volatility.)*

We assume further that under the risk neutral measure ($\mathbb{Q}$), the index maintains the same mean-reverting property, but with different parameters. Namely,

$$dS_t = \widetilde{\mu}(\widetilde{\theta} - S_t)dt + g(t, S_t)d\widetilde{Z}_t, \tag{3.2.6}$$

where $\widetilde{\mu}, \widetilde{\theta} > 0$, g is the same volatility function as above and $\widetilde{Z}_t$ is a SBM under the risk neutral measure. Denoting by $\lambda(t, S_t)$, the market price of risk, we have

$$dZ_t = d\widetilde{Z}_t - \lambda(t, S_t)dt,$$

so that

$$\lambda(t, S_t) = \frac{\mu(\theta - S_t) - \widetilde{\mu}(\widetilde{\theta} - S_t)}{g(t, S_t)}. \tag{3.2.7}$$

This form of risk premium preserves the mean-reverting model, up to different parameter values across two measures.

It can be shown that the price of a futures contract written on S with maturity T is

$$f_t^T := f(t, S; T) = \mathbb{E}^{\mathbb{Q}}\left[S_T | S_t = S\right] = (S - \widetilde{\theta})e^{-\widetilde{\mu}(T-t)} + \widetilde{\theta}, \tag{3.2.8}$$

as long as the function $g(\cdot, \cdot)$ satisfies the condition

$$\mathbb{E}^{\mathbb{Q}}\left[\int_0^T e^{2\widetilde{\mu}\xi} g^2(\xi, S_\xi) d\xi\right] < \infty, \quad \forall\, T. \tag{3.2.9}$$

It follow from Ito's Formula that the dynamics of f_t^T are given by

$$\begin{aligned} df_t^T = dS_t e^{-\widetilde{\mu}(T-t)} + \widetilde{\mu} e^{-\widetilde{\mu}(T-t)}(S_t - \widetilde{\theta})dt &= e^{-\widetilde{\mu}(T-t)} g(t, S_t) d\widetilde{Z}_t \\ &= e^{-\widetilde{\mu}(T-t)} g(t, S_t)(\lambda(t, S_t)dt + dZ_t). \end{aligned} \tag{3.2.10}$$

The rightmost equation on the first line indicates the dynamics under the $\mathbb{Q}$, while the equation on the second line indicates the dynamics under $\mathbb{P}$.

We rewrite Equation (3.2.8), with the discrete-time index, j, as

$$f_j^{(i)} = \widetilde{\theta} + (S_j - \widetilde{\theta})e^{-\widetilde{\mu}(T_i - j\Delta t)}, \quad \forall\, j \leq \frac{T_i}{\Delta t}. \tag{3.2.11}$$

Here, T_i is the maturity (measured in years) of the i^{th} futures contract and is a multiple of Δt. The above is defined $\forall\, j \leq \frac{T_i}{\Delta t}$.[16] In order to calculate the futures return (which will be

[16]For simplicity, we assume all contracts have incepted at or before time $j = 0$. In the case of VIX futures, we are guaranteed for this not to be a problem if $N \leq 7$ and the trading horizon is less than 6 months. Of course, one can simply update the set of available futures as well and still maintain the above equations for all $j \leq \frac{T_i}{\Delta t}$.

needed for Equation (3.2.2)), it will be more useful to discretize the second line of Equation (3.2.10) as

$$f_{j+1}^{(i)} - f_j^{(i)} = e^{-\widetilde{\mu}(T_i - j\Delta t)} g(j, S_j) \left(\lambda_j \Delta t + \sqrt{\Delta t} Z_{j+1} \right), \tag{3.2.12}$$

where

$$\lambda_j := \lambda(j, S_j) = \frac{\mu(\theta - S_j) - \widetilde{\mu}(\widetilde{\theta} - S_j)}{g(j, S_j)}, \tag{3.2.13}$$

is the discrete-time-stochastic process for the market price of risk defined as above for all $j \geq 0$. For notational simplicity let us denote the time-to-maturity of the i^{th} futures contract on day j by $D_j^{(i)} := T_i - j\Delta t$. Then the daily return of the futures contract is

$$\begin{aligned} \frac{f_{j+1}^{(i)}}{f_j^{(i)}} - 1 = \frac{e^{-\widetilde{\mu} D_j^{(i)}} g(j, S_j)}{\widetilde{\theta} + \left(S_j - \widetilde{\theta} \right) e^{-\widetilde{\mu} D_j^{(i)}}} \left(\lambda_j \Delta t + \sqrt{\Delta t} Z_{j+1} \right) &= \frac{g(j, S_j)}{\widetilde{\theta} e^{\widetilde{\mu} D_j^{(i)}} + S_j - \widetilde{\theta}} \left(\lambda_j \Delta t + \sqrt{\Delta t} Z_{j+1} \right) \\ &= B_j^{(i)} \left(\lambda_j \Delta t + \sqrt{\Delta t} Z_{j+1} \right), \end{aligned} \tag{3.2.14}$$

where we have defined

$$B_j^{(i)} := \frac{g(j, S_j)}{\widetilde{\theta} e^{\widetilde{\mu} D_j^{(i)}} + S_j - \widetilde{\theta}}. \tag{3.2.15}$$

Plugging Equation (3.2.14) into Equation (3.2.2), we express the portfolio's return as

$$\frac{X_{j+1}}{X_j} - 1 = e^{r\Delta t} - 1 + \Delta t \sum_{i=1}^{N} w_j^{(i)} B_j^{(i)} \lambda_j + \sqrt{\Delta t} \sum_{i=1}^{N} w_j^{(i)} B_j^{(i)} Z_{j+1}. \tag{3.2.16}$$

3.2.2 Optimal Tracking Problem

Now, we consider replicating the daily returns of the mean reverting index described in Section 3.2.1. In discrete-time, the investor will choose weights and realize cash flows the following day. I.e. the trades and rebalancing happen at the time steps $j = 0, 1, ...$ and the

investor chooses weights dynamically so as to solve the following optimization problem:

$$\min_{w_j^{(i)}, i=1,\ldots,N} \mathbb{E}^{\mathbb{P}} \left[\left(\frac{X_{j+1}}{X_j} - \beta \frac{S_{j+1}}{S_j} + \beta - 1 \right)^2 \Big| \mathcal{F}_j \right], \tag{3.2.17}$$

where $(\mathcal{F}_j)_{j=0}^{\infty}$ is the discrete-time filtration representing information generated by prices observed as of day j. Thus, the investor seeks to minimize the expected squared deviation of her portfolio's 1-day return from the index's one-day return, adjusted by a leverage factor, β. The quantity $\beta - 1$ comes from the fact that the objective criterion in Optimization Problem (3.2.17) is a sqaured return difference. That is,

$$\frac{X_{j+1}}{X_j} - 1 - \beta \left(\frac{S_{j+1}}{S_j} - 1 \right) = \frac{X_{j+1}}{X_j} - \beta \frac{S_{j+1}}{S_j} + \beta - 1.$$

Moreover, the expectations are measured w.r.t. the historical measure, $\mathbb{P}$. This is because the investor realizes cash flows in accordance with the historical (rather than risk neutral) measure. The risk neutral measure was only necessary to write down the discrete-time futures price equation.

Remark 3.2.2 *The approach here is a myopic approach, each day working to minimize the squared deviation from the return with no regard for either previous deviations or future deviations. The strategy will necessarily be dynamic, as it is updated each day. However, it need not be optimal for the problem of finding a policy that minimizes the squared deviations of the portfolio from the index's value over the* entire *trading horizon.*

We are motivated here to track the volatility index, VIX. One ETF that tries to track VIX is VXX and it attempts to replicate VIX by holding a combination of 2 futures contracts. More specifically, VXX holds 100% of its wealth at time 0 in the 1-Month futures, and via daily rebalancing, reduces its holdings in 1-Month futures and purchases 2-Month futures. By maturity of the 1-Month futures, VXX has sold off its entire position in 1-Month futures and holds 100% of its wealth in 2-Month futures (which, at maturity *is* the 1-Month futures).

The reduction in 1-Month holdings by VXX is linear and deterministic. Our goal is to construct an adaptive strategy, which may possibly be non-linear.

Due to this motivation, we solve optimization problem (3.2.17) when $N = 2$, subject to the constraint that on each day j, we must have $w_j^{(i_1)} + w_j^{(i_2)} = 1$. We do not require impose any other restrictions on the weights. Specifically, we do not set any constraints on the sign or size of the weights and in general we will find that leveraging positions in one futures contract is required to optimally track the VIX according to Optimization Problem (3.2.17). Furthermore, we choose generic maturities, i_1 and i_2 and do not tie ourselves to portfolios consisting only of 1-Month and 2-Month futures. The following proposition gives the complete solution to (3.2.17):

Proposition 3.2.1 *Suppose the price of an index, S, satisfies Equation* (3.2.3) *and the value, X, of a portfolio of $N = 2$ futures contracts on S with maturities $T_{i_1} \neq T_{i_2}$ satisfies Equation* (3.2.1)*. Then, the solution to Optimization Problem* (3.2.17) *is given by*

$$w_j^{(i_1)} = -\frac{\alpha_0\alpha_1 + \nu_0\nu_1}{\alpha_1^2 + \nu_1^2}, \quad w_j^{(i_2)} = 1 - w_j^{(i_1)},$$

with the optimal objective function value

$$\frac{(\nu_1\alpha_0 - \nu_0\alpha_1)^2}{\alpha_1^2 + \nu_1^2},$$

where

$$\begin{aligned}
\alpha_0 &:= e^{r\Delta t} - 1 + \Delta t B_j^{(i_2)}\lambda_j - \beta\mu\Delta t\left(\frac{\theta}{S_j} - 1\right),\\
\alpha_1 &:= \Delta t\lambda_j(B_j^{(i_1)} - B_j^{(i_2)}),\\
\nu_0 &:= \sqrt{\Delta t}\left(B_j^{(i_2)} - \frac{\beta g(j, S_j)}{S_j}\right),\\
\nu_1 &:= \sqrt{\Delta t}(B_j^{(i_1)} - B_j^{(i_2)}).
\end{aligned}$$

Proof. Combining Equations (3.2.16) and (3.2.4), we compute the difference between the portfolio's return and the targeted multiple of the index's return. We have

$$\frac{X_{j+1}}{X_j} - 1 - \beta\left(\frac{S_{j+1}}{S_j} - 1\right) = e^{r\Delta t} - 1 + \Delta t \sum_{i=1}^{N} w_j^{(i)} B_j^{(i)} \lambda_j + \sqrt{\Delta t} \sum_{i=1}^{N} w_j^{(i)} B_j^{(i)} Z_{j+1} - \beta\mu\Delta t\left(\frac{\theta}{S_j} - 1\right) - \frac{\beta g(j, S_j)}{S_j}\sqrt{\Delta t} Z_{j+1}.$$

The above can be expressed in the affine form $\phi_0 + \phi_1 Z_{j+1}$, where

$$\phi_0 := e^{r\Delta t} - 1 + \Delta t \sum_{i=1}^{N} w_j^{(i)} B_j^{(i)} \lambda_j - \beta\mu\Delta t\left(\frac{\theta}{S_j} - 1\right),$$

and

$$\phi_1 := \sqrt{\Delta t} \sum_{i=1}^{N} w_j^{(i)} B_j^{(i)} - \frac{\beta g(j, S_j)}{S_j}\sqrt{\Delta t}.$$

Both ϕ_0 and ϕ_1 are stochastic and depend on j, S_j as well as the parameters of the model and futures contracts (though, we suppress their dependence here). However, they are both measurable with respect to $\mathcal{F}_j$ and Z_{j+1} is independent of $\mathcal{F}_j$. From this we can conclude that, conditional on $\mathcal{F}_j$, the return difference has a normal distribution mean ϕ_0 and variance ϕ_1^2. It follows that the conditional second moment of the return difference is

$$\left(e^{r\Delta t} - 1 + \Delta t \sum_{i=1}^{N} w_j^{(i)} B_j^{(i)} \lambda_j + \beta\mu\Delta t\left(1 - \frac{\theta}{S_j}\right)\right)^2 + \left(\sqrt{\Delta t} \sum_{i=1}^{N} w_j^{(i)} B_j^{(i)} - \frac{\beta g(j, S_j)}{S_j}\sqrt{\Delta t}\right)^2.$$

Now, set $N = 2$ and for the rest of the proof set $w \equiv w_j^{(i_1)}$ so that $w_j^{(i_2)} = 1 - w$. Then Optimization Problem (3.2.17) is equivalent to

$$\min_{w \in \mathbb{R}} \left(\alpha_0 + \alpha_1 w\right)^2 + \left(\nu_0 + \nu_1 w\right)^2, \tag{3.2.18}$$

where α_1, α_0 ν_1 and ν_0 are as defined in the statement of the proposition. As with ϕ_0 and ϕ_1, all four of these coefficients are stochastic and depend on j, S_j as well as the parameters

of the model and futures contracts, but we suppress the dependence here.

The square of a linear function is always convex and since the sum of convex function is convex, the overall optimization problem is convex. It follows then that the first order condition (when solvable) is necessary and sufficient for global optimality. Thus,

$$2\left(\alpha_0+\alpha_1 w\right)\alpha_1+2\left(\nu_0+\nu_1 w\right)\nu_1=0 \implies w^*=-\frac{\alpha_0\alpha_1+\nu_0\nu_1}{\alpha_1^2+\nu_1^2}.$$

To be certain the optimal solution exists, we require $\alpha_1 \neq 0$ and $\nu_1 \neq 0$. From the above definitions, we observe that to be the case (for both) so long as $B_j^{(i_1)} \neq B_j^{(i_2)}$. This happens if and only if

$$\frac{g(j,S_j)}{\widetilde{\theta}e^{\widetilde{\mu}D_j^{(i_1)}}+S_j-\widetilde{\theta}} \neq \frac{g(j,S_j)}{\widetilde{\theta}e^{\widetilde{\mu}D_j^{(i_1)}}+S_j-\widetilde{\theta}} \iff e^{\widetilde{\mu}D_j^{(i_1)}} \neq e^{\widetilde{\mu}D_j^{(i_2)}} \iff D_j^{(i_1)} \neq D_j^{(i_2)}.$$

This holds as long as the two futures contracts have different maturities, which is assumed here. Finally, direct substitution of w^* into the objective function, $(\alpha_0+\alpha_1 w)^2+(\nu_0+\nu_1 w)^2$, yields the optimal objective function value. ■

As a corollary to the above proposition we can give a value for the index that yields zero expected squared error.

Corollary 3.2.1 *Suppose the price of an index, S, satisfies Equation* (3.2.3) *and the value, X, of a portfolio of $N=2$ futures contracts on S with maturities $T_{i_1} \neq T_{i_2}$ satisfies Equation* (3.2.1)*. Then, the optimal objective function value is 0 for Optimization Problem* (3.2.17) *if and only if*

$$S_j=\frac{\beta\widetilde{\mu}\widetilde{\theta}}{\beta\widetilde{\mu}+\bar{r}},$$

where $\bar{r}=\frac{e^{r\Delta t}-1}{\Delta t}$.[17]

[17]Note that $\bar{r}$ is the Δt compounded equivalent interest rate to r.

Proof. The optimal objective function value is 0 for Optimization Problem (3.2.17) if and only if $\frac{\alpha_0}{\alpha_1} = \frac{\nu_0}{\nu_1}$. This is equivalent to

$$\frac{e^{r\Delta t} - 1 + \Delta t B_j^{(i_2)}\lambda_j + \beta\mu\Delta t\left(1 - \frac{\theta}{S_j}\right)}{\Delta t\lambda_j(B_j^{(i_1)} - B_j^{(i_2)})} = \frac{\sqrt{\Delta t}\left(B_j^{(i_2)} - \frac{\beta g(j,S_j)}{S_j}\right)}{\sqrt{\Delta t}(B_j^{(i_1)} - B_j^{(i_2)})}$$

or

$$\bar{r} + B_j^{(i_2)}\lambda_j + \beta\mu\left(1 - \frac{\theta}{S_j}\right) = B_j^{(i_2)}\lambda_j - \frac{\beta g(j,S_j)\lambda_j}{S_j} \iff \bar{r}S_j + \beta\mu(S_j - \theta) = -\beta g(j,S_j)\lambda_j$$

Plugging in the expression for the market price of risk this reduces to

$$\bar{r}S_j + \beta\mu(S_j - \theta) = -\beta\left[\mu(\theta - S_j) - \widetilde{\mu}(\widetilde{\theta} - S_j)\right] \iff \bar{r}S_j = \beta\widetilde{\mu}(\widetilde{\theta} - S_j).$$

This is a linear equation in S_j, with the solution $S_j = \frac{\beta\widetilde{\mu}\widetilde{\theta}}{\beta\widetilde{\mu}+\bar{r}}$. Therefore, it is equivalent that S take this value for Optimization Problem (3.2.17) to have an optimal objective function value of 0. ■

Remark 3.2.3 *The critical value is independent of of both the day on which we trade as well as the maturities of the pair of contracts used. Moreover, in Chapter 4, we will discuss dynamic strategies in continuous time under two mean reverting models. In that case, for there to be zero drift other than the desired leveraged exposure, we require* $S_t = \frac{\beta\widetilde{\mu}\widetilde{\theta}}{\beta\widetilde{\theta}+r}$*, where* r *is the* continuously compounded *risk free rate. Therefore, there is a correspondence between the trading frequency and the compounding frequency of the interest rate that appears in the critical value for perfect replication.*

3.3 Numerical Implementation

In this section, we implement the optimal strategy above. In particular, we will set the function $g(\cdot,\cdot)$ as $g(t,S_t) = \sigma\sqrt{S_t}$. As mentioned in Remark 3.2.1, when the function $g(\cdot,\cdot)$

is given as such, the associated continuous-time model is called the CIR Model (see Cox et al. (1985)). In Section 3.3.1, we discuss calibration of this model under the historical and risk neutral measures. In Section 3.3.2 we give a simulation of the strategy and discuss its properties relative to VXX.

3.3.1 Empirical Estimation

First, we consider calibration under the historical measure to obtain the parameters μ, θ, and σ. Suppose the continuous-time process S_t is driven by the CIR process

$$dS_t = \mu(\theta - S_t)dt + \sigma\sqrt{S_t}dZ_t,$$

where $\mu, \theta, \sigma > 0$ and Z_t is a SBM. Further suppose we have observed a discrete sampling of S_t as $\{S_{t_1}, ..., S_{t_n}\}$. Then, the conditional probability density of S_{t_j} at time t_j given $S_{t_{j-1}} = s_{j-1}$ with (equally spaced) time increment $\Delta t := t_j - t_{j-1}$ is given by

$$f^{CIR}(s_j|s_{j-1};\theta,\mu,\sigma) = \frac{1}{\tilde{\sigma}^2}\exp\left(-\frac{s_j + s_{j-1}e^{-\mu\Delta t}}{\tilde{\sigma}^2}\right)\left(\frac{s_j}{s_{j-1}e^{-\mu\Delta t}}\right)^{\frac{\mathfrak{q}}{2}} I_{\mathfrak{q}}\left(\frac{2}{\tilde{\sigma}^2}\sqrt{s_j s_{j-1}e^{-\mu\Delta t}}\right),$$

with the constants

$$\tilde{\sigma}^2 = \sigma^2\frac{1 - e^{-\mu\Delta t}}{2\mu}, \quad \mathfrak{q} = \frac{2\mu\theta}{\sigma^2} - 1,$$

and $I_{\mathfrak{q}}(z)$ is modified Bessel function of the first kind and of order $\mathfrak{q}$. See Cox et al. (1985).

Using the observed values $\{s_j\}_{j=1}^n$, the CIR model parameters can be estimated by max-

imizing the average log-likelihood:

$$\begin{aligned}\ell(\theta,\mu,\sigma|s_1,\ldots,s_n) &:= \frac{1}{n-1}\sum_{j=2}^{n}\ln f^{CIR}(s_j|s_{j-1};\theta,\mu,\sigma)\\ &= -2\ln(\tilde{\sigma}) - \frac{1}{(n-1)\tilde{\sigma}^2}\sum_{j=2}^{n}(s_j + s_{j-1}e^{-\mu\Delta t})\\ &\quad + \frac{1}{n-1}\sum_{j=2}^{n}\left(\frac{\mathfrak{q}}{2}\ln\left(\frac{s_j}{s_{j-1}e^{-\mu\Delta t}}\right) + \ln I_{\mathfrak{q}}\left(\frac{2}{\tilde{\sigma}^2}\sqrt{s_j s_{j-1}e^{-\mu\Delta t}}\right)\right).\end{aligned}$$

For more details on the implementation of the maximum likelihood estimation (MLE) for the CIR process, we refer to Kladivko (2007). After calibrating the model to the in-sample (January 3rd, 2011 to December 31st, 2015) data, the estimators for μ, θ, and σ are given as 10.85804, 18.80899, and 6.374804, respectively.

Now, we calibrate the model under the risk neutral measure. As the volatility does not change under this measure, we need only calibrate the parameters of the mean reversion:[18] $\widetilde{\mu}$ and $\widetilde{\theta}$. The futures price on S, with maturity T, as observed at time t is given by

$$f_t^T = (S_t - \widetilde{\theta})e^{-\widetilde{\mu}(T-t)} + \widetilde{\theta}.$$

On any given day we may observe the spot price as well as the entire term structure. Thus, in calibrating the risk neutral parameters, our data is the set of triples

$$\left\{\left(S_{t_j}, T_i, f_{t_j}^{T_i}\right) : j = 1,...,n, i = 1,...,N_j\right\},$$

where N_j is the number of futures contracts available for trading on day j, and T_i is the time-to-maturity of the i^{th} futures. Let us continue to use the shorthand notation $s_j := S_{t_j}$ as well as introduce the notation $f_j^{(i)} := f_{t_j}^{T_i}$. Then, in calibrating the parameters to the term

[18] See Remark 3.2.1; we assume the process is still a CIR process under the risk neutral.

structure on a particular day, we consider the loss function

$$L\left(\widetilde{\mu},\widetilde{\theta}|s_j\right) := \frac{1}{2N_j}\sum_{i=1}^{N_j}\left((s_j-\widetilde{\theta})e^{-\widetilde{\mu}T_i}+\widetilde{\theta}-f_j^{(i)}\right)^2.$$

To obtain a single set of parameters across all days, we average the loss function over the entire sample and minimize

$$L_{RN}(\widetilde{\mu},\widetilde{\theta}|s_1,...,s_n) := \frac{1}{n}\sum_{j=1}^{n}L\left(\widetilde{\mu},\widetilde{\theta}|s_j\right) = \frac{1}{n}\sum_{j=1}^{n}\frac{1}{2N_j}\sum_{i=1}^{N_j}\left((s_j-\widetilde{\theta})e^{-\widetilde{\mu}T_i}+\widetilde{\theta}-f_j^{(i)}\right)^2, \tag{3.3.1}$$

by choosing $\widetilde{\mu}$ and $\widetilde{\theta}$. After calibrating to the in-sample (January 3$^{\text{rd}}$, 2011 to December 31$^{\text{st}}$, 2015) data, the estimators for $\widetilde{\mu}$ and $\widetilde{\theta}$ are given as 1.389641 and 26.033725, respectively.

Remark 3.3.1 *One can also dynamically re-calibrate the parameters at the end of every day and use them to make trading decisions for the subsequent day. In principle, if the CIR model is correct the parameters should not change day to day. However, it is possible that the model could be incorrect for VIX so without adjusting the model, re-calibration is the only option. Such a dynamically re-calibrated strategy is one that utilizes the parameters obtained at the end of every day by minimizing*

$$L\left(\widetilde{\mu}_j,\widetilde{\theta}_j|s_j\right) := \frac{1}{2N_j}\sum_{i=1}^{N_j}\left((s_j-\widetilde{\theta}_j)e^{-\widetilde{\mu}_jT_i}+\widetilde{\theta}_j-f_j^{(i)}\right)^2,$$

by choosing $\widetilde{\mu}_j$ and $\widetilde{\theta}_j$ for each $j = 1, ..., n$. However, the parameters are very unstable when inferred in this manner. It may be better to consider a rolling lookback window and minimize the objective function in (3.3.1) *over time. We do not pursue that in the following section and instead keep the parameters static.*

3.3.2 Qualitative Properties of the Solution

In this section, we describe the qualitative properties of the derived optimal strategy by giving some numerical simulations. Specifically, we use the parameters derived in Section 3.3.1, and simulate the index and its corresponding futures prices using Equations (3.2.3) and (3.2.11). We can use Equation (3.2.1) to simulate the value of a dynamic portfolio as well as that of VXX. For both, we use the 1-Month and 2-Month futures since they are the nearest dated contracts and in Section 3.1 we found the nearest dated contracts to be members of many of the optimal portfolios used. When computing the value of VXX, we assume that it dynamically weights the futures contracts using a linear strategy starting at 1 and ending at 0 by the end of the contract period. For our simulations, we assume $n = 252$ trading days per year, 12 months per year and even contract cycles for the futures. This implies that each contract cycle is precisely 21 days. In this section, we only concern ourselves with directly tracking the index returns (i.e. $\beta = 1$), though the optimal strategy applies more generally.

A few typical simulations are displayed in Figure 3.8. In this figure, the simulations take place over 3 contract cycles or 63 total days. We separate the analysis into three cases. In panel (a), S starts at its (historical measure) long term level of θ. In panel (b), S starts at a value of $\frac{1}{3} \cdot \theta$. Finally, in panel (c), S starts at a value of $3 \cdot \theta$. These cases emphasize three market conditions: (a) non-directional movements in the index, (b) upward trending movements in the index and (c) downward trending movements in the index, respectively. In all cases, we see that the dynamic portfolio tracks both the index and its return quite well over the first few days. The same is true for VXX. After this time, both portfolios fall away from the index, especially in the updward trending (Figure 3.8(b)) case. However, the strategy is designed to track the returns, rather than the physical price so this is somewhat expected.

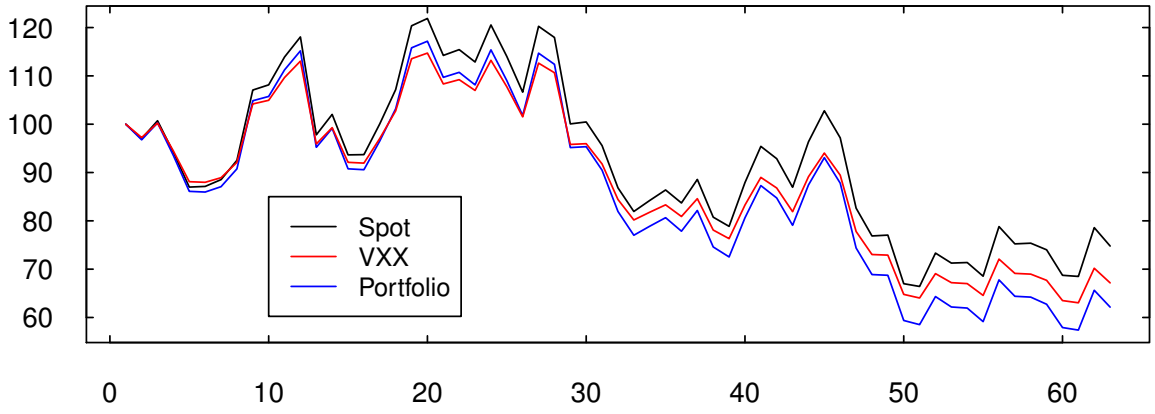

(a) $S_0 = \theta$

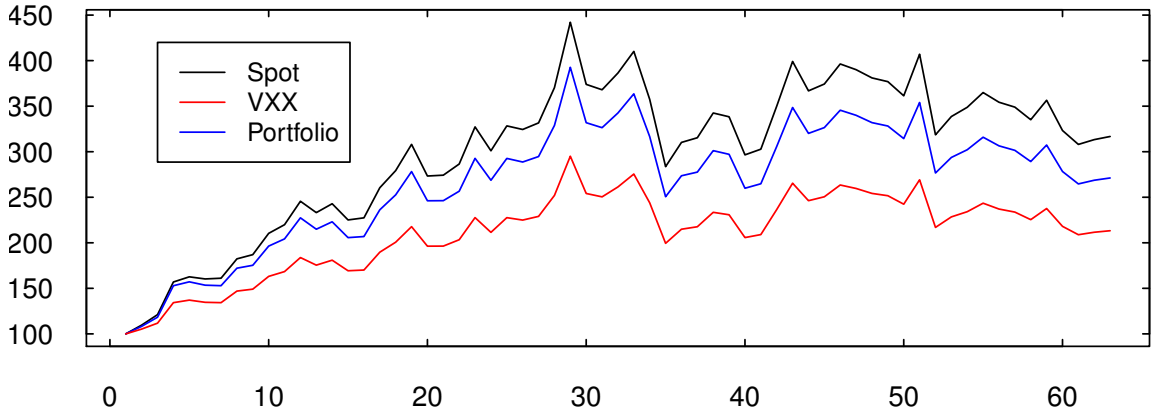

(b) $S_0 = \frac{1}{3} \cdot \theta$

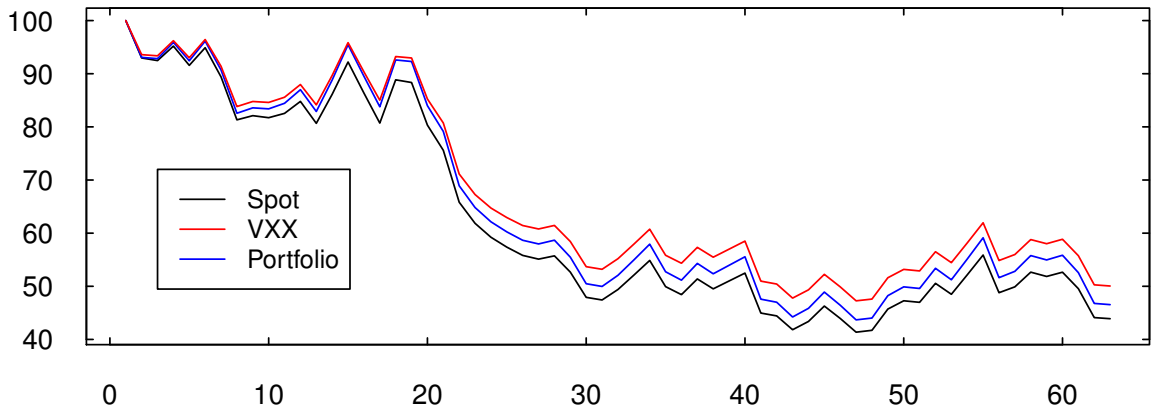

(c) $S_0 = 3 \cdot \theta$

Figure 3.8: Simulations of the index, VXX and the dynamic portfolio under 3 different scenarios: (a) non-directional movements in the index, (b) upward trending movements in the index and (c) downward trending movements in the index. The parameters are $\mu = 10.86$, $\theta = 18.81$, $\sigma = 6.38$, $\widetilde{\mu} = 1.39$, and $\widetilde{\theta} = 26.03$. Trading is over a 3 contract cycles of 21 days each. The x-axis marks the trading day, while the y-axis marks the price. All portfolios are normalized to start at \$100.

In terms of tracking error, the worst case appears to be case (a): the non-directional case. This is somewhat intuitive. The dynamic portfolio tries to predict the return of the index, and minimize the squared deviation from this return. If the index is initialized to its long-term mean, then the portfolio cannot make any prediction and so is exposed to the variation of the returns. Compare this to cases (b) and (c). In those cases (they are extreme), the index is well-below and well-above (respectively) the long-term mean. Before the index has stablized in value, the dynamic portfolio *is* able make predictions and can optimize to keep the portfolio's expected return close to the index's expected return.

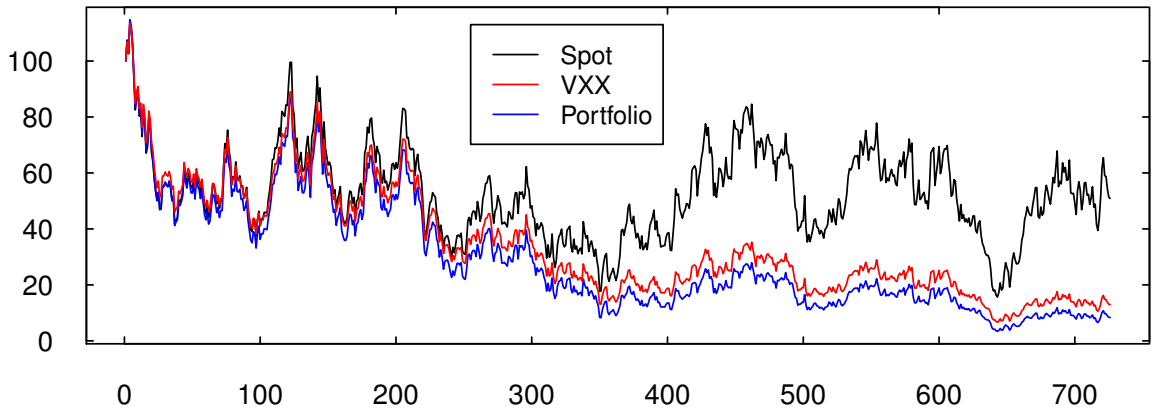

Figure 3.9: Simulation of the index, VXX and the dynamic portfolio over a 3-year (or 756 trading days) period. The parameters are $\mu = 10.86$, $\theta = 18.81$, $\sigma = 6.38$, $\widetilde{\mu} = 1.39$, $\widetilde{\theta} = 26.03$ and $S_0 = \frac{1}{2} \cdot \theta$. The x-axis marks the trading day, while the y-axis marks the price. All portfolios are normalized to start at \$100.

To emphasize the losses in the non-directional case, we plot a simulation of a longer time period in Figure 3.9. Here, the simulation occurs over 3 years (or 756 trading days) and we initialize $S_0 = \frac{1}{2} \cdot \theta$. For almost the first full year of this simulation, both VXX and the dynamic portfolio track quite well. However, after this time, the index has stablilized at its long term level.[19] Though the index continuous to mean-revert to this value, the losses on the futures portfolios continue to compound. This is true for *both*. Here, we are seeing the so-called theta-decay (time-decay) of the futures contracts. To quantify that, we compute

[19]Since this portfolio starts at \$100, the long-term value is \$50.

(in the continuous-time case for simplicity)

$$\frac{\partial f_t^T}{\partial t} = (S_t - \widetilde{\theta})e^{-\widetilde{\mu}(T-t)}\widetilde{\mu} \approx \widetilde{\mu}(\theta - \widetilde{\theta})e^{-\widetilde{\mu}(T-t)} < 0,$$

where we have set S_t to the value θ in the approximation since the index stablizes around this time. Referencing Section 3.3 for the relevant parameter values indicates that $\theta < \widetilde{\theta}$, hence $\frac{\partial f_t^T}{\partial t}$ is negative.

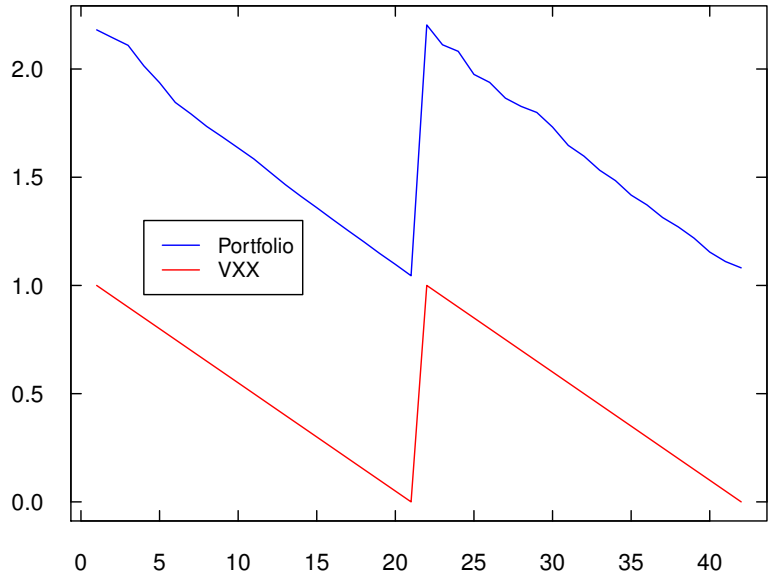

Figure 3.10: Simulation of the dynamic strategy of the portfolio and VXX over a 2 contract cycle time period (or 42 trading days). The parameters are $\mu = 10.86$, $\theta = 18.81$, $\sigma = 6.38$, $\widetilde{\mu} = 1.39$, $\widetilde{\theta} = 26.03$ and $S_0 = \theta$. The x-axis marks the trading day, while the y-axis marks the weight on 1-Month futures.

As for the strategy, we give an example in Figure 3.10 over a 2 contract cycle time period (or 42 trading days). Interestingly, the dynamic strategy is quite linear falling from a little over 2 in value to 1 by maturity. This indicates that the strategy is also short %100 of its value in 2-Month futures rising to 0% by maturity of the 1-Month futures. For comparison, we also plot the strategy of VXX, which is linear from 1 to 0 over each contract cycle.

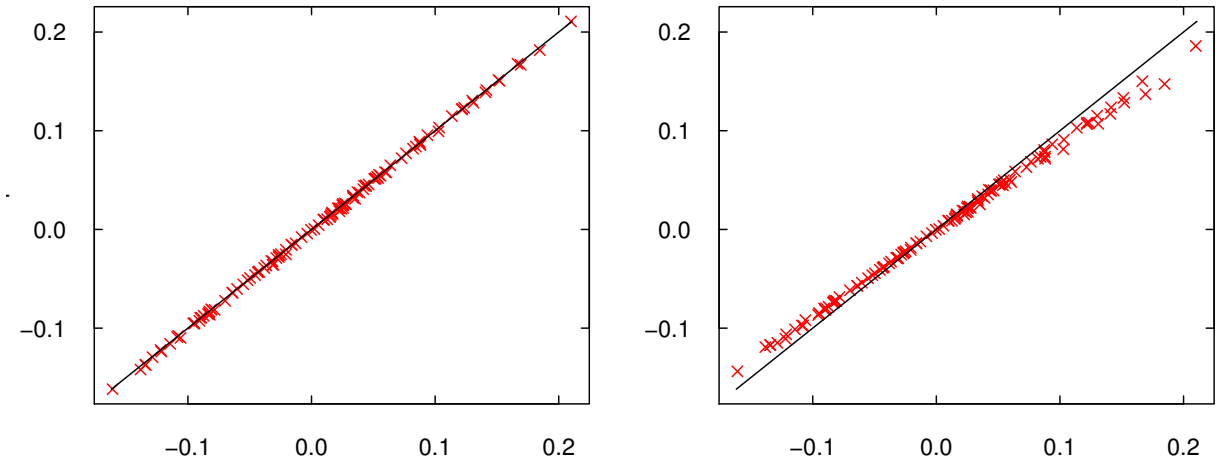

(a) Dynamic Portfolio (b) VXX

Figure 3.11: Scatterplot of the returns of the dynamic portfolio (left) and VXX (right) vs. the VIX. The parameters are $\mu = 10.86$, $\theta = 18.81$, $\sigma = 6.38$, $\widetilde{\mu} = 1.39$, $\widetilde{\theta} = 26.03$, and $S_0 = \theta$. Trading is over 126 trading days (6 contract cycles). The x-axis marks the index returns (decimals, not percentages), while the y-axis marks the dynamic portfolio/VXX returns (decimals, not percentages).

Statistic	Dynamic Portfolio	VXX
Slope	1.00292	0.87338
SE(Slope)	$1.64076 \cdot 10^{-3}$	$2.94771 \cdot 10^{-3}$
Intercept	$-8.55136 \cdot 10^{-4}$	$-10.15242 \cdot 10^{-4}$
SE(Intercept)	$1.29794 \cdot 10^{-4}$	$2.33183 \cdot 10^{-4}$
R^2	0.99967	0.99860

Table 3.5: Optimal portfolio weights/performance measures for portfolios of VIX futures for tracking VIX returns. Porfolios utilize any subset of the 1-Month, 2-Month, 6-Month and 7-Month contract. The reported RMSE values are for the returns of the portfolio.

To see that the dynamic portfolio tracks the returns of VIX better than VXX, we display a simulated return scatterplot in Figure 3.11. For this figure, another 126 trading days (6 contract cycles) were simulated. Panel (a) shows the scatterplot of the returns of the dynamic portfolio vs. the returns of VIX, while panel (b) gives the scatterplot of the returns of VXX vs. the returns of VIX. Both plots have the same x-y axis scale for easy comparison. We also superimpose (in black) the line $y = x$. One notices that for the dynamic portfolio, the returns pairs are closer to the line $y = x$ indicating that the portfolio returns closely

match the returns of VIX. On the other hand, for VXX the returns are further from this line and the slope appears to be less than 1 in value. In fact, both statements are statistically significant. This can be verified from the regression results in Table 3.5. The p-value for testing the null hypothesis $H_0 : \{\text{slope} = 1\}$ for the regression of the dynamic portfolio returns vs. VIX returns is equal to 0.078, which is greater than many standard significance levels. The corresponding test for VXX has a p-value of $6.521 \cdot 10^{-76}$.

Finally, we note that even though both regressions have an R^2 greater than 99%, the R^2 value for the dynamic portfolio exceeds that of VXX. Though these R^2 values would indicate a nearly perfect linear relationship, they do not imply the portfolios can perfectly replicate the physical dollar value of VIX. In fact, the RMSE values for the difference in prices over the time horizon are 12.097 for the dynamic portfolio and 14.828 for VXX. Thus, on average, the time series are between \$12 and \$15 from the index they are trying to track. Many time series of the prices have already been displayed so we do not overburden the reader with another, but the results are qualitatively the same for this simulation: the two portfolios are far from the index by the end of the trading horizon and in fact are substantially lower in value than the index. This indicates that without a perfect linear relationship between the returns of a dynamic futures portfolio and the returns of an index, the dynamic futures portfolio cannot perfectly track the price of an index.

Chapter 4

Dynamic Index Tracking

In this chapter, we develop a methodology for index tracking and risk exposure control using financial derivatives. From the empirical observations in Chapters 2 and 3, we learned that static portfolios of futures are unable to correctly track both spot gold and VIX. In those chapters, we constructed some dynamic strategies that helped reduce the tracking errors. Here, we seek to understand the properties of these dynamic strategies under a general diffusion framework for index tracking and risk exposure control. Section 4.1 we set up the index tracking problem and derive our key results. Specifically, in Section 4.1.1, we present a the continuous-time diffusion framework for the price evolution of a market index and its driving factors. The index and/or its factors may be not directly tradable. Nonetheless, the investor seeks to precisely set the exposure to each of the factors. Section 4.1.2 derives a condition relating the achievable exposures and in the special case of constant exposure, we give an intuitive expression for the portfolio value. This involves a process we call the slippage process that reveals how the portfolio return deviates from the targeted return. In our multi-factor setting, the portfolio's realized slippage depends not only on the realized variance of the index (as is standard in the literature), but also on the realized covariance among the index and factors. Finally, in Sections 4.2 and 4.3, we apply our methodology under a number of different models for equity index tracking and volatility index tracking, respectively.

4.1 Continuous-Time Tracking Problem

We present our tracking methodology in a continuous-time multi-factor diffusion framework, which encapsulates a number of different models for financial indices and market factors. Derivatives portfolios are constructed to achieve a pre-specified exposure, and their price dynamics are examined. In particular, we compare the strategies using only futures to those using other derivatives, such as options, for tracking and exposure control.

4.1.1 Price Dynamics

In the background, we fix a probability space $(\Omega, \mathcal{F}, \mathbb{Q})$, where $\mathbb{Q}$ is the risk-neutral probability measure inferred from market derivatives prices. Throughout, we assume a constant risk-free interest rate $r \geq 0$. Consider an index S, along with $d \geq 0$ exogenous observable stochastic factors $\{Y^{(i)}\,;\, i = 1, \ldots, d\}$, which satisfy the following system of stochastic differential equations (SDEs):

$$dS_t = \widetilde{\gamma}_t^{(0)} dt + \sigma_t^{(0,0)} dB_t^{\mathbb{Q},0} + ... + \sigma_t^{(0,d)} dB_t^{\mathbb{Q},d}, \tag{4.1.1}$$

$$dY_t^{(i)} = \widetilde{\gamma}_t^{(i)} dt + \sigma_t^{(i,0)} dB_t^{\mathbb{Q},0} + ... + \sigma_t^{(i,d)} dB_t^{\mathbb{Q},d}, \qquad i = 1, ..., d. \tag{4.1.2}$$

Here, $B_t^{\mathbb{Q}} := (B_t^{\mathbb{Q},0}, ..., B_t^{\mathbb{Q},d})$, $t \geq 0$, is a $(d+1)-$dimensional standard Brownian Motion (SBM) under $\mathbb{Q}$. We assume that S_t and $Y_t^{(i)}$, $i = 1, ..., d$, are all strictly positive processes, and consider a Markovian framework whereby the coefficients are functions of t, S_t, and $Y_t^{(i)}$, $i = 1, \ldots, d$, defined by

$$\widetilde{\gamma}_t^{(i)} := \widetilde{\gamma}^{(i)}(t, S_t, Y_t^{(1)}, ..., Y_t^{(d)}), \quad i = 0, ..., d,$$

$$\sigma_t^{(i,j)} := \sigma^{(i,j)}(t, S_t, Y_t^{(1)}, ..., Y_t^{(d)}), \quad i = 0, ..., d,\ j = 0, ..., d.$$

Equivalently, we can write the SDEs more compactly in matrix form as

$$dM_t = \widetilde{\gamma}_t dt + \Sigma_t dB_t^{\mathbb{Q}},$$

where $M_t := (S_t, Y_t^{(1)}, ..., Y_t^{(d)})$ is a vector. The drift vector is $\widetilde{\gamma}_t := (\widetilde{\gamma}_t^{(0)}, \widetilde{\gamma}_t^{(1)}, ..., \widetilde{\gamma}_t^{(d)})$, and the $(d+1) \times (d+1)$ volatility matrix Σ_t, has the entry $(\Sigma_t)_{i,j} = \sigma_t^{(i,j)}$ for each i, j.

Remark 4.1.1 *The risk-neutral pricing measure, $\mathbb{Q}$ is an equivalent martingale measure with respect to the historical probability measure $\mathbb{P}$. The associated numeraire is the cash account, so all traded security prices are discounted martingales. Under the original measure, $\mathbb{P}$, the market evolves according to*

$$dM_t = \gamma_t dt + \Sigma_t dB_t^{\mathbb{P}},$$

where $B_t^{\mathbb{P}}$ is a $(d+1)-$dimensional SBM under $\mathbb{P}$. The measures $\mathbb{P}$ and $\mathbb{Q}$ are connected by the market price of risk vector $\lambda_t := \Sigma_t^{-1}(\gamma_t - \widetilde{\gamma}_t)$. That is,

$$dB_t^{\mathbb{P}} = dB_t^{\mathbb{Q}} - \lambda_t dt. \tag{4.1.3}$$

While our framework includes both complete and incomplete market models, we always assume that a risk-neutral measure has been chosen a priori and satisfies (4.1.3)*. Since all our results and strategies are derived and stated* pathwise *(see Propositions 4.1.1 and 4.1.2), there is no need to revert from measure $\mathbb{Q}$ back to $\mathbb{P}$.*

Let us denote by $c_t^{(k)} := c^{(k)}(t, S_t, Y_t^{(1)}, ..., Y_t^{(d)})$, for $k = 1, ..., N$, $t \in [0, T_k]$, the price processes of N European-style derivatives written on S, with respective terminal payoff functions $h^{(k)}(s, y_1, ..., y_d)$ to be realized at time T_k.[1] At time $t \leq T_k$, the no-arbitrage price

[1]We allow the payoff to depend on the factors themselves. For example, consider a spread option on an equity index S and another correlated index Y. This amounts to setting $d = 1$, and viewing Y as an index, and specifying the option payoff $h(s, y) = (s - y)^+$.

of the kth derivative is given by

$$c^{(k)}(t, S_t, Y_t^{(1)}, ..., Y_t^{(d)}) = \mathbb{E}^{\mathbb{Q}}\left[e^{-r(T_k-t)}h^{(k)}(S_{T_k}, Y_{T_k}^{(1)}, ..., Y_{T_k}^{(d)})\big|S_t, Y_t^{(1)}, ..., Y_t^{(d)}\right]. \quad (4.1.4)$$

The infinitesimal relative return of the kth derivative can be expressed as

$$\frac{dc_t^{(k)}}{c_t^{(k)}} = C_t^{(k)}dt + D_t^{(k)}\frac{dS_t}{S_t} + E_t^{(k,1)}\frac{dY_t^{(1)}}{Y_t^{(1)}} + ... + E_t^{(k,d)}\frac{dY_t^{(d)}}{Y_t^{(d)}}, \quad (4.1.5)$$

where we have defined

$$C_t^{(k)} := r - \frac{\widetilde{\gamma}_t^{(0)}}{c_t^{(k)}}\frac{\partial c^{(k)}}{\partial S} - \frac{\widetilde{\gamma}_t^{(1)}}{c_t^{(k)}}\frac{\partial c^{(k)}}{\partial Y^{(1)}} - ... - \frac{\widetilde{\gamma}_t^{(d)}}{c_t^{(k)}}\frac{\partial c^{(k)}}{\partial Y^{(d)}}, \quad (4.1.6)$$

$$D_t^{(k)} := \frac{S_t}{c_t^{(k)}}\frac{\partial c^{(k)}}{\partial S}, \quad (4.1.7)$$

$$E_t^{(k,i)} := \frac{Y_t^{(i)}}{c_t^{(k)}}\frac{\partial c^{(k)}}{\partial Y^{(i)}}, \quad i = 1, ..., d. \quad (4.1.8)$$

The first coefficient, $C_t^{(k)}$, is the drift of the kth derivative, $D_t^{(k)}$ is the price elasticity of the kth derivative with respect to the underlying index, and $E_t^{(k,i)}$ is the price elasticity of the kth derivative with respect to the ith factor. The full derivation of (4.1.5) can be found in Appendix A.1.

To track an index, the investor seeks to construct a portfolio and precisely set the portfolio's drift and exposure coefficients with respect to the index and its driving factors. As we will discuss next, these portfolio features will be expressed as a linear combination of the above price elasticities. Therefore, to attain the desired exposures, the strategy is derived by solving a linear system over time.

4.1.2 Tracking Portfolio Dynamics

Fix a trading horizon $[0, T]$, with $T \leq T_k$, for all $k = 1, ..., N$. We construct a self-financing portfolio, $(X_t)_{0\leq t\leq T}$, utilizing N derivatives with prices given by (4.1.4). The portfolio

strategy is denoted by the vector $w_t := (w_t^{(1)}, \ldots, w_t^{(N)})$, for $0 \leq t \leq T$ so that $X_t w_t^{(k)}$ is the cash amount invested in the kth derivative at time t for $k = 1, \ldots, N$. Therefore, the amount $X_t - \sum_{k=1}^{N} X_t w_t^{(k)}$ is invested at the risk-free rate r at time t. Given such strategies, the dynamics of X are

$$\begin{aligned}\frac{dX_t}{X_t} &= \sum_{k=1}^{N} w_t^{(k)} \frac{dc_t^{(k)}}{c_t^{(k)}} + r\left(1 - \sum_{k=1}^{N} w_t^{(k)}\right) dt \\ &= \left(r + \sum_{k=1}^{N} w_t^{(k)} \left(C_t^{(k)} - r\right)\right) dt + \left(\sum_{k=1}^{N} w_t^{(k)} D_t^{(k)}\right) \frac{dS_t}{S_t} + \sum_{i=1}^{d} \left(\sum_{k=1}^{N} w_t^{(k)} E_t^{(k,i)}\right) \frac{dY_t^{(i)}}{Y_t^{(i)}}.\end{aligned} \tag{4.1.9}$$

The three terms in (4.1.9) represent respectively the portfolio drift, exposure to the index, and exposures to the d factors. Suppose that the investor has chosen (i) a drift process $(\alpha_t)_{0 \leq t \leq T}$, (ii) dynamic exposure coefficient $(\beta_t)_{0 \leq t \leq T}$ with respect to the returns of S, and (iii) dynamic exposure coefficients $(\eta_t^{(1)})_{0 \leq t \leq T}, ..., (\eta_t^{(d)})_{0 \leq t \leq T}$ with respect to the d factors. Such coefficients must be adapted to the filtration in order to be attainable, but of course they may simply be constant. Then, in order to match the coefficients as desired, we must choose the strategies so as to solve the following linear system:

$$\begin{pmatrix} \alpha_t - r \\ \beta_t \\ \eta_t^{(1)} \\ ... \\ \eta_t^{(d)} \end{pmatrix} = \begin{pmatrix} C_t^{(1)} - r & ... & C_t^{(N)} - r \\ D_t^{(1)} & ... & D_t^{(N)} \\ E_t^{(1,1)} & ... & E_{t,1}^{(N,d)} \\ & ... & \\ E_t^{(1,d)} & ... & E_t^{(N,d)} \end{pmatrix} \begin{pmatrix} w_t^{(1)} \\ ... \\ w_t^{(N)} \end{pmatrix}. \tag{4.1.10}$$

However, we observe from (4.1.6)-(4.1.8) that $C_t^{(k)}$, $D_t^{(k)}$ and $E_t^{(k,i)}$ satisfy

$$C_t^{(k)} - r + \frac{\widetilde{\gamma}_t^{(0)}}{S_t} D_t^{(k)} + \frac{\widetilde{\gamma}_t^{(1)}}{Y_t^{(1)}} E_t^{(k,1)} + ... + \frac{\widetilde{\gamma}_t^{(d)}}{Y_t^{(d)}} E_t^{(k,d)} = 0, \tag{4.1.11}$$

for each k. Therefore, the rows of the coefficient matrix on the right hand side of (4.1.10) are *linearly dependent*. We arrive at the following proposition:

Proposition 4.1.1 *A necessary condition for the derivatives portfolio in* (4.1.9) *to have drift* α_t*, and exposure coefficients* $(\beta_t, \eta_t^{(1)}, ..., \eta_t^{(d)})$ *with respect to* $(S_t, Y_t^{(1)}, ..., Y_t^{(d)})$ *defined in* (4.1.1) *and* (4.1.2) *for* $0 \leq t \leq T$ *is*

$$\alpha_t - r + \frac{\widetilde{\gamma}_t^{(0)}}{S_t}\beta_t + \frac{\widetilde{\gamma}_t^{(1)}}{Y_t^{(1)}}\eta_t^{(1)} + ... + \frac{\widetilde{\gamma}_t^{(d)}}{Y_t^{(d)}}\eta_t^{(d)} = 0, \tag{4.1.12}$$

for all $t \in [0, T]$.

We call condition (4.1.12) the **tracking condition**. For the general diffusion framework above, the left hand side of (4.1.12) is stochastic over time. It is possible to exactly control the exposures as desired almost surely if (4.1.12) holds pathwise. In some special cases, the tracking condition (4.1.12) becomes a deterministic equation relating the (achievable) exposure coefficients of the factors and the index. However, one cannot expect this in general.

Instead, suppose the dynamic exposure coefficients $(\beta_t, \eta_t^{(1)}, ..., \eta_t^{(d)})$ are pre-specified by the investor a priori, then the tracking condition (4.1.12) indicates that the associated portfolio must be subject to a stochastic portfolio drift

$$\alpha_t = r - \frac{\widetilde{\gamma}_t^{(0)}}{S_t}\beta_t - \frac{\widetilde{\gamma}_t^{(1)}}{Y_t^{(1)}}\eta_t^{(1)} - ... - \frac{\widetilde{\gamma}_t^{(d)}}{Y_t^{(d)}}\eta_t^{(d)}. \tag{4.1.13}$$

In other words, the investor cannot freely control the target drift and all market exposures simultaneously in this general diffusion framework. Indeed, we take this point of view in our examples to be discussed in the following sections, and investigate the impact of controlled exposures on the portfolio dynamics. More generally, the tracking condition tells us that amongst the $d + 2$ sources of evolution for the portfolio (drift, and $d + 1$ market variables), we can only select coefficients for $d + 1$ of them (unless the above condition happens to hold for that particular model.)

The tracking condition (4.1.12) implies that the linear system for the tracking strategies has (at least) one redundant equation. We effectively have a $(d+1)$-by-N system, so using $N > d+1$ derivatives is unnecessary and yields infinitely many portfolios having the same desired path properties. However, using exactly $N = d+1$ derivatives leads to a unique strategy and gives the desired path properties.

Remark 4.1.2 *We have explained one source of redundancy that exists in* any *diffusion model. However, other potential redundancies can arise depending on the derivative types and their dependencies on the index and factors. In fact, it is possible that the chosen set of derivatives does not allow the resulting system to have a unique solution. To see this, we provide an example in the Heston Model in Section 4.2.2 (see Example 4.2.1). This is remedied by including a new derivative type in the portfolio (see Example 4.2.2).*

Given that the index and factor exposure coefficients are constant and that the tracking condition holds, we can derive the portfolio dynamics explicitly and illustrate a stochastic divergence between the portfolio return and targeted return.

Proposition 4.1.2 *Given constant exposure coefficients, i.e.* $\beta_t = \beta$, $\eta_t^{(1)} = \eta_1, \ldots, \eta_t^{(d)} = \eta_d$, $\forall t \in [0,T]$, *and a strategy* $(w_t^{(1)}, \ldots, w_t^{(N)})_{0\le t\le T}$ *that solves system* (4.1.10) *, then the portfolio value defined in* (4.1.9) *admits the expression*

$$\frac{X_u}{X_t} = \left(\frac{S_u}{S_t}\right)^{\beta} \prod_{i=1}^{d} \left(\frac{Y_u^{(i)}}{Y_t^{(i)}}\right)^{\eta_i} e^{\int_t^u Z_v dv}, \tag{4.1.14}$$

for all $0 \le t \le u \le T$, *where* S, *and* $(Y^{(1)}, ..., Y^{(d)})$ *satisfy* (4.1.1) *and* (4.1.2), *and*

$$\begin{aligned} Z_t := \alpha_t &+ \frac{1}{2}\beta(1-\beta)\sum_{j=0}^{d}\left(\frac{\sigma_t^{(0,j)}}{S_t}\right)^2 + \frac{1}{2}\sum_{i=1}^{d}\sum_{j=0}^{d}\eta_i(1-\eta_i)\left(\frac{\sigma_t^{(i,j)}}{Y_t^{(i)}}\right)^2 \\ &- \beta\sum_{i=1}^{d}\sum_{j=0}^{d}\eta_i\frac{\sigma_t^{(i,j)}}{Y_t^{(i)}}\frac{\sigma_t^{(0,j)}}{S_t} - \sum_{i=1}^{d}\sum_{l=i+1}^{d}\sum_{j=0}^{d}\eta_i\eta_l\frac{\sigma_t^{(i,j)}}{Y_t^{(i)}}\frac{\sigma_t^{(l,j)}}{Y_t^{(l)}}. \end{aligned} \tag{4.1.15}$$

Proof. Applying Ito's formula, we write down the SDEs for $d\log(S_t)$ and $d\log(Y_t^{(i)})$, for each i:

$$d\log(S_t) = \frac{dS_t}{S_t} - \frac{1}{2}\sum_{j=0}^{d}\left(\frac{\sigma_t^{(0,j)}}{S_t}\right)^2 dt, \tag{4.1.16}$$

$$d\log(Y_t^{(i)}) = \frac{dY_t^{(i)}}{Y_t^{(i)}} - \frac{1}{2}\sum_{j=0}^{d}\left(\frac{\sigma_t^{(i,j)}}{Y_t^{(i)}}\right)^2 dt. \tag{4.1.17}$$

Next we multiply $d\log(S_t)$ by β and each $d\log(Y_t^{(i)})$ by η_i respectively, and add these all together with the term $\alpha_t dt$ to obtain

$$\alpha_t dt + \sum_{j=1}^{d}\eta_j d\log(Y_t^{(j)}) + \beta d\log(S_t) = \frac{dX_t}{X_t} - \frac{1}{2}\sum_{i=1}^{d}\sum_{j=0}^{d}\eta_i\left(\frac{\sigma_t^{(i,j)}}{Y_t^{(i)}}\right)^2 dt - \frac{1}{2}\beta\sum_{j=0}^{d}\left(\frac{\sigma_t^{(0,j)}}{S_t}\right)^2 dt. \tag{4.1.18}$$

Now, apply Ito's formula to $\log(X_t)$, we have

$$\frac{dX_t}{X_t} = d\log(X_t) + \frac{1}{2}\left(\frac{dX_t}{X_t}\right)^2.$$

Applying this to (4.1.18), we get

$$\begin{aligned}&\alpha_t dt + \sum_{j=1}^{d}\eta_j d\log(Y_t^{(j)}) + \beta d\log(S_t)\\ &\quad= d\log(X_t) + \frac{1}{2}\left(\frac{dX_t}{X_t}\right)^2 - \frac{1}{2}\sum_{i=1}^{d}\sum_{j=0}^{d}\eta_i\left(\frac{\sigma_t^{(i,j)}}{Y_t^{(i)}}\right)^2 dt - \frac{1}{2}\beta\sum_{j=0}^{d}\left(\frac{\sigma_t^{(0,j)}}{S_t}\right)^2 dt.\end{aligned} \tag{4.1.19}$$

Since there exists strategy $(w_t)_{0\le t\le T}$ that solves (4.1.10), the portfolio in (4.1.9) satisfies the SDE

$$\frac{dX_t}{X_t} = \alpha_t dt + \beta\frac{dS_t}{S_t} + \sum_{i=1}^{d}\eta_i\frac{dY_t^{(i)}}{Y_t^{(i)}}. \tag{4.1.20}$$

By squaring (4.1.20), we have

$$\begin{aligned}\frac{1}{2}\left(\frac{dX_t}{X_t}\right)^2 &= \frac{1}{2}\beta^2\left(\frac{dS_t}{S_t}\right)^2 + \frac{1}{2}\sum_{i=1}^{d}\eta_i^2\left(\frac{dY_t^{(i)}}{Y_t^{(i)}}\right)^2 + \sum_{i=1}^{d}\beta\eta_i\frac{dY_t^{(i)}}{Y_t^{(i)}}\frac{dS_t}{S_t} + \sum_{i=1}^{d}\sum_{l=i+1}^{d}\eta_i\eta_l\frac{dY_t^{(i)}}{Y_t^{(i)}}\frac{dY_t^{(l)}}{Y_t^{(l)}} \\ &= \frac{1}{2}\beta^2\sum_{j=0}^{d}\left(\frac{\sigma_t^{(0,j)}}{S_t}\right)^2 dt + \frac{1}{2}\sum_{i=1}^{d}\sum_{j=0}^{d}\eta_i^2\left(\frac{\sigma_t^{(i,j)}}{Y_t^{(i)}}\right)^2 dt + \beta\sum_{i=1}^{d}\sum_{j=0}^{d}\eta_i\frac{\sigma_t^{(i,j)}}{Y_t^{(i)}}\frac{\sigma_t^{(0,j)}}{S_t}dt \\ &\quad + \sum_{i=1}^{d}\sum_{l=i+1}^{d}\sum_{j=0}^{d}\eta_i\eta_l\frac{\sigma_t^{(i,j)}}{Y_t^{(i)}}\frac{\sigma_t^{(l,j)}}{Y_t^{(l)}}dt \\ &= \alpha_t dt + \frac{1}{2}\beta\sum_{j=0}^{d}\left(\frac{\sigma_t^{(0,j)}}{S_t}\right)^2 dt + \frac{1}{2}\sum_{i=1}^{d}\sum_{j=0}^{d}\eta_i\left(\frac{\sigma_t^{(i,j)}}{Y_t^{(i)}}\right)^2 dt - Z_t dt, \end{aligned} \tag{4.1.21}$$

where Z_t is defined in (4.1.15). Next, substituting (4.1.21) into (4.1.19) and rearranging, we obtain the link between the log returns of the portfolio and those of the index and factors:

$$d\log(X_t) = \sum_{j=1}^{d}\eta_j d\log(Y_t^{(j)}) + \beta d\log(S_t) + Z_t dt. \tag{4.1.22}$$

Upon integrating (4.1.22) and exponentiating, we obtain the desired result. ■

We call the stochastic process Z_t in (4.1.15) the **slippage process** as it is typically negative and describes the deviations of the portfolio returns from the targeted returns. In particular, taking the logarithm in (4.1.14) gives us the relationship between the portfolio's log return and the log returns of the index and each of the factors over any given period $[t, u]$, namely,

$$\log\left(\frac{X_u}{X_t}\right) = \beta\log\left(\frac{S_u}{S_t}\right) + \sum_{j=1}^{d}\eta_i\log\left(\frac{Y_u^{(i)}}{Y_t^{(i)}}\right) + \int_t^u Z_v dv.$$

The first two terms indicate that the portfolio's log return is proportional to the log returns of the index and its driving factors, with the proportionality coefficients being equal to the desired exposure. However, the portfolio's log return is subject to the integrated slippage process.

Integrating the square of the volatility of the index yields the *realized variance*. As such, the portfolio value, X, is akin to the price process of an LETF (see e.g. Avellaneda and Zhang (2010)) in continuous time, except that X also controls the exposure to various factors in addition to maintaining a fixed leverage ratio β w.r.t. S. Our framework allows for a multidimensional model, so the portfolio value and the realized slippage depend not only on the realized variances of the underlying factors, but also the *realized covariances* between the index and factors.

Remark 4.1.3 *If we apply the notations, $Y_t^{(0)} \equiv S_t$ and $\eta_0 \equiv \beta$, then the portfolio value simplifies to*

$$\frac{X_T}{X_t} = \prod_{i=0}^{d} \left(\frac{Y_T^{(i)}}{Y_t^{(i)}} \right)^{\eta_j} e^{\int_t^T Z_u du},$$

and the slippage process admits a more compact expression

$$Z_t = \alpha_t + \frac{1}{2} \sum_{i=0}^{d} \sum_{j=0}^{d} \eta_i (1 - \eta_i) \left(\frac{\sigma_t^{(i,j)}}{Y_t^{(i)}} \right)^2 - \sum_{i=0}^{d} \sum_{l=i+1}^{d} \sum_{j=0}^{d} \eta_i \eta_l \frac{\sigma_t^{(i,j)}}{Y_t^{(i)}} \frac{\sigma_t^{(l,j)}}{Y_t^{(l)}}.$$

Example 4.1.1 *If there is no additional stochastic factor ($d = 0$), then we have*

$$\frac{X_T}{X_t} = \left(\frac{S_T}{S_t} \right)^{\beta} e^{\int_t^T Z_u du},$$

and

$$Z_t := \alpha_t + \frac{1}{2} \beta (1 - \beta) \left(\frac{\sigma_t^{(0,0)}}{S_t} \right)^2, \tag{4.1.23}$$

where $\sigma_t^{(0,0)}$ can depend on t and S_t as in the general local volatility framework. As such, the slippage process does not involve a covariance term, but it reflects the volatility decay, which is well documented for leveraged ETFs with an integer β (see e.g. Avellaneda and Zhang (2010) and Leung and Santoli (2016)). As seen in (4.1.23)*, there is an erosion of the portfolio (log-)return that is proportional to the realized variance of the index whenever $\beta \notin [0, 1]$.*

Example 4.1.2 *If $d = 1$, i.e. one exogenous market factor Y along with the index S, we have*

$$\frac{X_T}{X_t} = \left(\frac{S_T}{S_t}\right)^{\beta} \left(\frac{Y_T}{Y_t}\right)^{\eta} e^{\int_t^T Z_u du},$$

and

$$Z_t := \alpha + \frac{1}{2}\beta(1-\beta)\left(\frac{\sigma_t^{(S)}}{S_t}\right)^2 + \frac{1}{2}\eta(1-\eta)\left(\frac{\sigma_t^{(Y)}}{Y_t}\right)^2 - \beta\eta\frac{\sigma_t^{(S,Y)}}{S_t Y_t}, \tag{4.1.24}$$

where

$$\sigma_t^{(S)} := \sqrt{\left(\sigma_t^{(0,0)}\right)^2 + \left(\sigma_t^{(0,1)}\right)^2},$$
$$\sigma_t^{(Y)} := \sqrt{\left(\sigma_t^{(1,0)}\right)^2 + \left(\sigma_t^{(1,1)}\right)^2},$$
$$\sigma_t^{(S,Y)} := \sigma_t^{(1,0)}\sigma_t^{(0,0)} + \sigma_t^{(1,1)}\sigma_t^{(0,1)}.$$

Here, $\sigma_t^{(S)}$, $\sigma_t^{(Y)}$, and $\sigma_t^{(S,Y)}$, are functions of t, S_t, and Y_t, as in the Local Stochastic Volatility framework. In addition to the value erosion proportional to the realized variance of the index (second term in (4.1.24)), there is another realized variance decay term for the exogenous factor (third term in (4.1.24)). Indeed it will be negative whenever the Y-exposure coefficient $\eta \notin [0,1]$. Beyond the realized variance of the index and the factor, there is also a term in the slippage process which accounts for the realized covariance between the index and factor (final term in (4.1.24)). It is negative if $\sigma_t^{(S,Y)}$, β, and η are all positive, reflecting another source of value erosion relative to the desired log return.

4.1.3 Portfolios with Futures

Futures contracts are also useful instruments for index tracking.[2] The price of a futures contract of maturity T_k[3] at time $t \le T_k$ is given by

$$f_t^{(k)} := f^{(k)}(t, S_t, Y_t^{(1)}, ..., Y_t^{(d)}) = \mathbb{E}^{\mathbb{Q}}\left[S_{T_k} \middle| S_t, Y_t^{(1)}, ..., Y_t^{(d)}\right]. \tag{4.1.25}$$

[2]See e.g. Alexander and Barbosa (2008) for a discussion on the empirical performance of minimum variance hedging strategies using futures contracts against an index ETF.

[3]Despite the identical notation, the maturities of the futures can be different from those in Section 4.1.2.

The Feynman-Kac formula implies that the price must satisfy

$$\frac{\partial f^{(k)}}{\partial t}+\widetilde{\gamma}_t^{(0)}\frac{\partial f^{(k)}}{\partial S}+\widetilde{\gamma}_t^{(1)}\frac{\partial f^{(k)}}{\partial Y^{(1)}}+...+\widetilde{\gamma}_t^{(d)}\frac{\partial f^{(k)}}{\partial Y^{(d)}}+\frac{1}{2}\operatorname{Tr}\left[\Sigma^{\intercal}\nabla^2 f^{(k)}\Sigma\right]=0, \tag{4.1.26}$$

with the terminal condition$f(T_k,s,y_1,...,y_d)=s$ for all vectors $(s,y_1,...,y_d)$ with strictly positive components. By (4.1.26) and Ito's formula, we get

$$\begin{aligned}df_t^{(k)}=&\left(-\widetilde{\gamma}_t^{(0)}\frac{\partial f^{(k)}}{\partial S}-\widetilde{\gamma}_t^{(1)}\frac{\partial f^{(k)}}{\partial Y^{(1)}}-...-\widetilde{\gamma}_t^{(d)}\frac{\partial f^{(k)}}{\partial Y^{(d)}}\right)dt+\frac{\partial f^{(k)}}{\partial S}dS_t\\&+\frac{\partial f^{(k)}}{\partial Y^{(1)}}dY_t^{(1)}+...+\frac{\partial f^{(k)}}{\partial Y^{(d)}}dY_t^{(d)}.\end{aligned}$$

Now consider a self-financing portfolio $(X_t)_{t\geq 0}$ utilizing N futures of maturities $T_1,T_2,...,T_N$ over a trading horizon $T\leq T_k$ for all k. Denote by $(u_t^{(k)})_{0\leq t\leq T}$, $k=1,...,N$ a generic adapted strategy such that, at time t, the cash amount $u_t^{(k)}X_t$ is invested in the kth futures contract.[4] Assuming that the futures contracts are continuously marked to market, the portfolio value evolves according to

$$\begin{aligned}\frac{dX_t}{X_t}&=\sum_{k=1}^{N}u_t^{(k)}\frac{df_t^{T_k}}{f_t^{(k)}}+rdt.\\&=\left(r+\sum_{k=1}^{N}u_t^{(k)}F_t^{(k)}\right)dt+\sum_{k=1}^{N}u_t^{(k)}G_t^{(k)}\frac{dS_t}{S_t}+\sum_{i=1}^{d}\sum_{k=1}^{N}u_t^{(k)}H_t^{(k,i)}\frac{dY_t^{(i)}}{Y_t^{(i)}},\end{aligned} \tag{4.1.27}$$

where coefficients are defined by

$$F_t^{(k)}:=-\frac{\widetilde{\gamma}_t^{(0)}}{f_t^{(k)}}\frac{\partial f^{(k)}}{\partial S}-\frac{\widetilde{\gamma}_t^{(1)}}{f_t^{(k)}}\frac{\partial f^{(k)}}{\partial Y^{(1)}}-...-\frac{\widetilde{\gamma}_t^{(d)}}{f_t^{(k)}}\frac{\partial f^{(k)}}{\partial Y^{(d)}}, \tag{4.1.28}$$

$$G_t^{(k)}:=\frac{S_t}{f_t^{(k)}}\frac{\partial f^{(k)}}{\partial S}, \tag{4.1.29}$$

$$H_t^{(k,i)}:=\frac{Y_t^{(i)}}{f_t^{(k)}}\frac{\partial f^{(k)}}{\partial Y^{(i)}},\quad i=1,...,d. \tag{4.1.30}$$

Comparing (4.1.28) to (4.1.6), we notice that $F_t^{(k)}$ has no r term.

[4]It is costless to establish a futures position, so no borrowing is involved.

Again suppose the investor selects a dynamic exposure coefficient $(\beta_t)_{0\leq t\leq T}$ with respect to the returns of S, as well as dynamic exposure coefficients for each factor return, $(\eta_t^{(1)},\ldots,\eta_t^{(d)})_{0\leq t\leq T}$. Suppose further that the investor chooses a target dynamic drift $(\alpha_t)_{0\leq t\leq T}$. In order for the portfolio to attain these desired path properties, we must solve the following linear system

$$\begin{pmatrix} \alpha_t - r \\ \beta_t \\ \eta_t^{(1)} \\ \ldots \\ \eta_t^{(d)} \end{pmatrix} = \begin{pmatrix} F_t^{(1)} & \ldots & F_t^{(N)} \\ G_t^{(1)} & \ldots & G_t^{(N)} \\ H_t^{(1,1)} & \ldots & H_t^{(N,1)} \\ & \ldots & \\ H_t^{(1,d)} & \ldots & H_t^{(N,d)} \end{pmatrix} \begin{pmatrix} u_t^{(1)} \\ \ldots \\ u_t^{(N)} \end{pmatrix}.$$

The definitions of $F_t^{(k)}$, $G_t^{(k)}$, and $H_t^{(k,i)}$ in (4.1.28)-(4.1.30) imply that

$$F_t^{(k)} + \frac{\widetilde{\gamma}_t^{(0)}}{S_t} G_t^{(k)} + \frac{\widetilde{\gamma}_t^{(1)}}{Y_t^{(1)}} H_t^{(k,1)} + \ldots + \frac{\widetilde{\gamma}_t^{(d)}}{Y_t^{(d)}} H_t^{(k,d)} = 0, \tag{4.1.31}$$

for each k. It follows that the rows of the linear system are linearly dependent. Thus, for the system to be consistent we must require that

$$\alpha_t - r + \frac{\widetilde{\gamma}_t^{(0)}}{S_t}\beta_t + \frac{\widetilde{\gamma}_t^{(1)}}{Y_t^{(1)}}\eta_t^{(1)} + \ldots + \frac{\widetilde{\gamma}_t^{(d)}}{Y_t^{(d)}}\eta_t^{(d)} = 0, \tag{4.1.32}$$

for all $t \in [0,T]$. As it turns out, this is the same tracking condition in Proposition 4.1.1, so the ensuing discussion applies to the current case with futures as well. However, the tracking strategies associated with futures can be significantly different from those with other derivatives.

4.2 Equity Index Tracking

In this section we discuss two prominent equity derivatives pricing models captured by our framework and present the tracking conditions and strategies.

4.2.1 Black-Scholes Model

We consider tracking using derivatives on an underlying index S under the Black-Scholes model, so there is no additional exogenous factors ($d = 0$). Under the risk-neutral measure, the index follows

$$dS_t = rS_t dt + \sigma S_t dB_t^{\mathbb{Q}}, \tag{4.2.1}$$

where $B_t^{\mathbb{Q}}$ is a SBM and $\sigma > 0$ is the volatility parameter. Then, applying Proposition 4.1.1, the tracking condition under the Black-Scholes model is simply

$$\alpha_t = r(1 - \beta_t), \qquad 0 \leq t \leq T. \tag{4.2.2}$$

A few remarks are in order. First, a zero exposure ($\beta_t = 0$) implies that the portfolio grows at the risk free rate ($\alpha_t = r$). If $\beta_t = 1$, then $\alpha_t = 0$, which means that perfect tracking of S is possible with no excess drift. This portfolio is a full investment in the index via some derivative. According to the tracking condition (4.2.2), if $\beta_t > 1$, then $\alpha_t < 0$. This indicates that borrowing is required in order to leverage the underlying returns. Moreover, we have $\alpha_t > r$ as long as $\beta_t < 0$. Hence, by shorting the index, one achieves a drift above the risk-free rate. For any value of β_t between 0 and 1, the strategy is trading off an investment in the money market account and the underlying index (via a derivative security).

Now suppose for the rest of this subsection that the drift and exposure coefficient are constant, namely, $\alpha_t \equiv \alpha$ and $\beta_t \equiv \beta$. More specifically, the investor specifies the exposure to S by setting the value of β so that condition (4.2.2) implies the fixed drift $\alpha = r(1 - \beta)$. By combining Proposition 4.1.2 with condition (4.2.2), the portfolio value can be expressed

explicitly as

$$X_t = X_0 \left(\frac{S_t}{S_0}\right)^{\beta} e^{(r+\frac{\beta\sigma^2}{2})(1-\beta)t}, \tag{4.2.3}$$

or equivalently, in terms of log-returns

$$\log\left(\frac{X_t}{X_0}\right) = \beta \log\left(\frac{S_t}{S_0}\right) + (r + \frac{\beta\sigma^2}{2})(1-\beta)t.$$

In particular, the slippage process is a constant, given by

$$Z_t = (r + \frac{\beta\sigma^2}{2})(1-\beta).$$

It is also quadratic concave in β. It follows that the slippage is non-negative for $\beta \in [-2r\sigma^{-2}, 1]$, and is strictly negative otherwise. Therefore, for constant exposure coefficient β outside (resp. inside) of the interval, $[-2r\sigma^{-2}, 1]$, the log-return of the tracking portfolio is lower (resp. higher) than the corresponding multiple (β) of the index's log-return.

To better understand the slippage, we take $r = 0.05$ and $\sigma = 0.2$. Then, for any $\beta \notin [-2.5, 1]$, the tracking portfolio's log-return falls short of the respective multiple of the index's log-return. To illustrate this, we display in Figure 4.1 the simulated sample paths of the portfolio values, along with their respective benchmark (whose log return is equal to the respective multiple of the index's log return), for $\beta \in \{-1, 2, 3\}$. As expected, when $\beta = 2$ or 3, the portfolio underperforms compared to the benchmark. In contrast, the portfolio outperforms the benchmark when $\beta = -1 \in [-2.5, 1]$.

The associated strategy achieving such path properties requires the use of at least $d+1 = 1$ derivative. Using exactly 1 leads to a unique strategy. To find the unique strategy, we can (without loss of generality) solve the corresponding equation in (4.1.10) to get $w_t = \beta/D_t$. Let us compare the tracking strategies using call options and futures contracts. First, consider a call on the index with expiration date T_c and strike K. The price of such an option is given

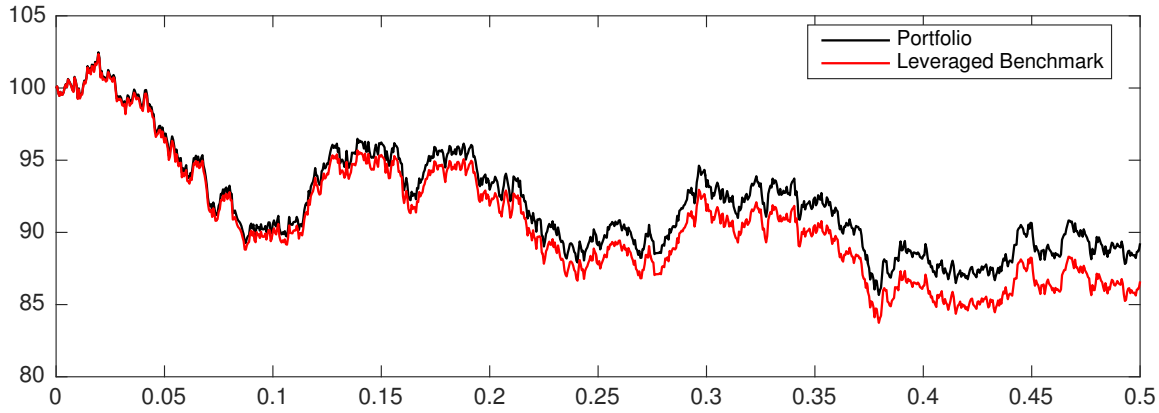

(a) $\beta = -1$

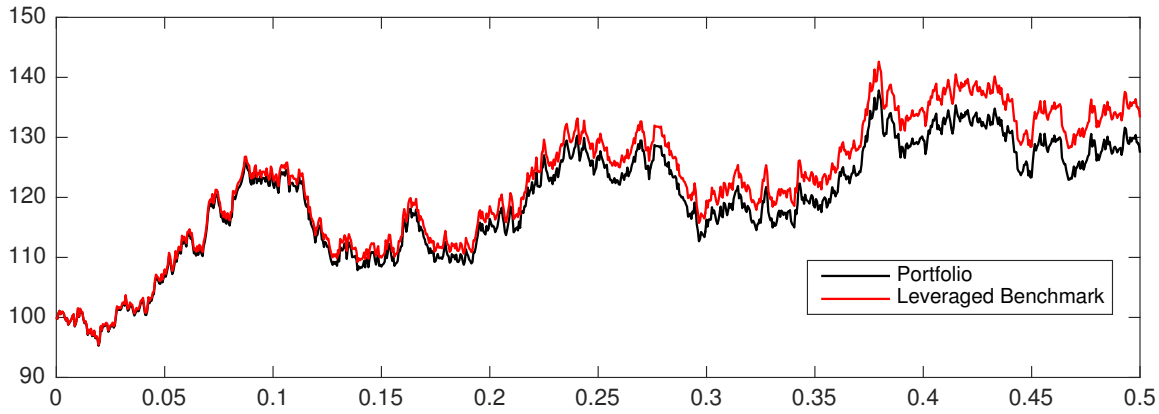

(b) $\beta = 2$

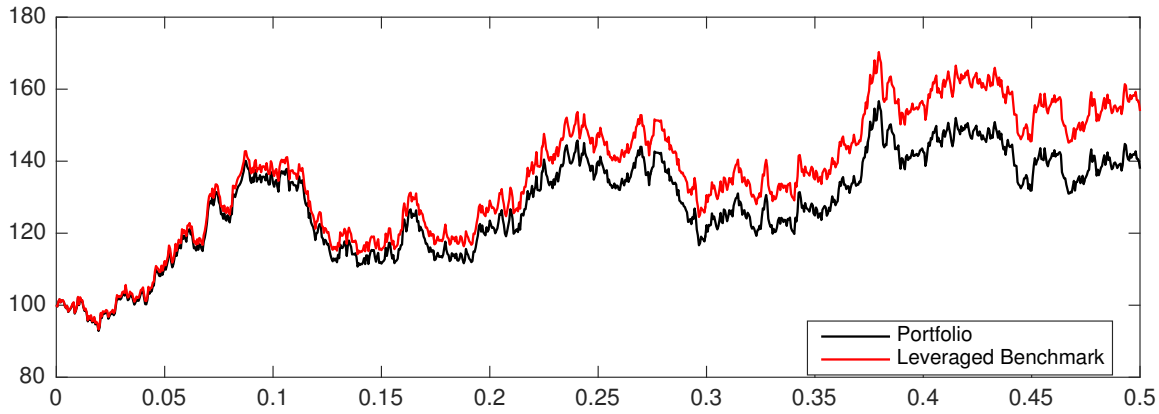

(c) $\beta = 3$

Figure 4.1: Sample paths of portfolio values (in \$) compared to their benchmarks for (a) $\beta = -1$, (b) $\beta = 2$, and (c) $\beta = 3$ under the Black-Scholes model. Parameters: $X_0 = 100$, S_0, $r = 0.05$, $\sigma = 0.2$, and $T = 0.5$. The benchmark is defined such that its log-return is equal to β times the index's log-return, with an initial value of \$100. The x-axis marks the time in years, while the y-axis marks the portfolio value.

by the Black and Scholes (1973) formula

$$c_t := c(t, S_t) = S_t N\left(d_+(t, S_t)\right) - Ke^{-r(T_c-t)} N\left(d_-(t, S_t)\right),$$

where

$$d_\pm(t, S_t) = \frac{\log\left(S_t/K\right) + (r \pm \frac{\sigma^2}{2})(T_c - t)}{\sigma\sqrt{T_c - t}}, \quad N(x) = \int_{-\infty}^{x} \frac{1}{\sqrt{2\pi}} e^{-\frac{u^2}{2}} du.$$

Therefore, to obtain an exposure coefficient of β to the index returns, requires holding

$$\frac{w_t X_t}{c_t} = \frac{\beta X_0}{S_0} \left(\frac{S_t}{S_0}\right)^{\beta-1} e^{(r+\frac{\beta\sigma^2}{2})(1-\beta)t} \frac{1}{N\left(d_+(t, S_t)\right)} \tag{4.2.4}$$

units of call option at time t.

The price of a futures written on S with maturity T_f is given by $f_t := f(t, S_t) = S_t e^{r(T_f-t)}$ for $t \leq T_f$. Therefore, to achieve an exposure with coefficient β requires holding

$$\frac{w_t X_t}{f_t} = \frac{\beta X_0}{S_0} \left(\frac{S_t}{S_0}\right)^{\beta-1} e^{(r+\frac{\beta\sigma^2}{2})(1-\beta)t - r(T_f-t)}. \tag{4.2.5}$$

contracts at time t.

To gain further intuition, let us compare the above strategies when the investor seeks a *unit exposure* ($\beta = 1$) with respect to S. The corresponding futures and options holdings are, respectively,

$$\frac{X_0}{S_0} e^{-r(T_f-t)} \qquad \text{and} \qquad \frac{X_0}{S_0 N\left(d_+(t, S_t)\right)}.$$

First, these strategies can be viewed as the reciprocal of the associated delta hedge. Under this model, both calls and futures allow for perfect tracking of S, since $\beta = 1$ implies that $\alpha = 0$. However, the two strategies are very different.

With a call option, the strategy is stochastic, depending crucially on the index dynamics. In Figure 4.2(a), we display the hedging strategies for call options of strikes $K \in \{40, 50, 60\}$

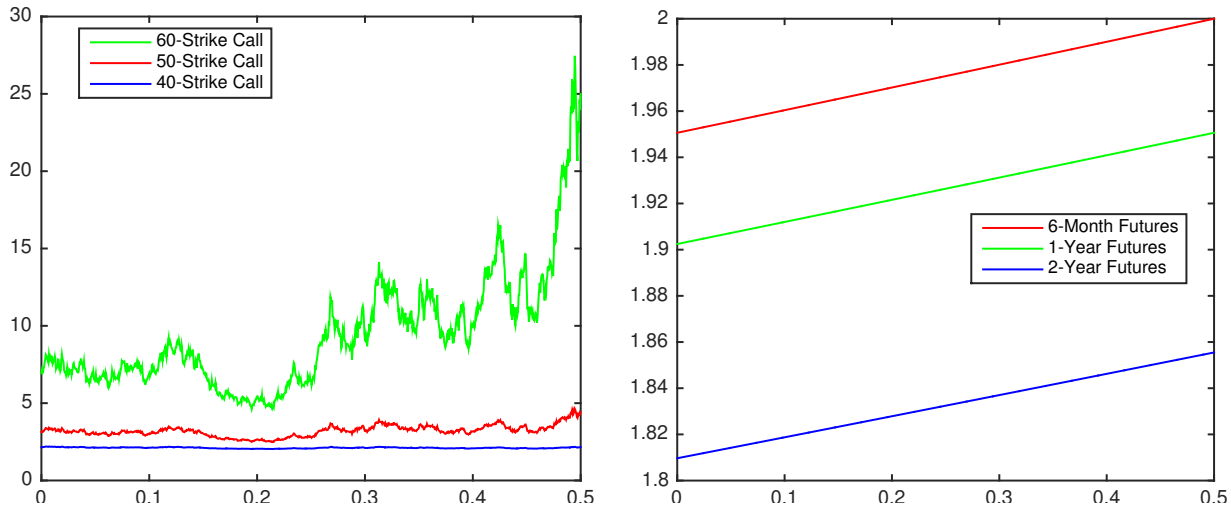

(a) Options (b) Futures

Figure 4.2: Simulation of $\beta = 1$ tracking strategies when using (a) call options of various strikes $K \in \{40, 50, 60\}$ and $T_c = 0.5$, and (b) futures contracts of various maturities $T_f \in \{0.5, 1, 2\}$ under the Black-Scholes model. Parameters: $S_0 = 50$, $X_0 = 100$, $r = 0.05$, $\sigma = 0.2$, and $T = 0.5$. For the ease of comparison, the strategies are based on sample path of the reference index used in Figure 4.1. The x-axis marks the time in years, while the y-axis marks the number of units of derivative required.

with a common maturity equal to the end of the trading horizon (6 months). The fluctuation of each strategy depends on the moneyness of the option. When $S_t >> K$, $N(d_+(t, S_t))$ is close to 1 and movements in the call price mimic those in the underlying equity index. As a result, the strategy is roughly constant over time as shown by the bottom path in Figure 4.2(a). In contrast, if the option used is deep out-of-the-money ($S_t << K$), then $N(d_+(t, S_t))$ is close to 0, meaning that the investor needs to hold many units of this call, whose per-unit price is almost zero in such a scenario, to gain sufficient direct exposure to the index S. Consequently, small movements can lead to very large changes in the holdings over time (see the top path in Figure 4.2).

For the futures, even though the contract value is stochastic, the strategy is time-deterministic with position becomes increasingly long exponentially over time at the risk-free rate. In Figure 4.2(a), we compare the positions corresponding to the futures contracts with different maturities, and notice that tracking with a shorter-term futures requires more units of futures in the portfolio.

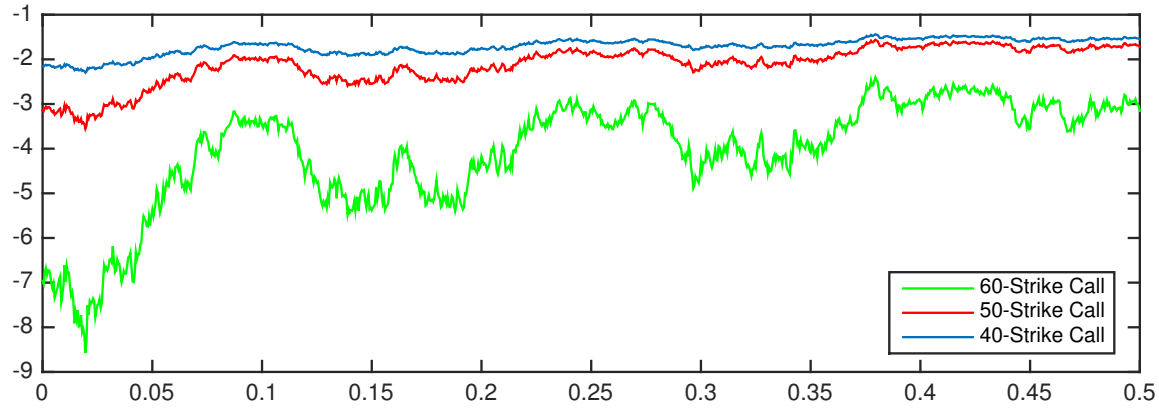

(a) Options

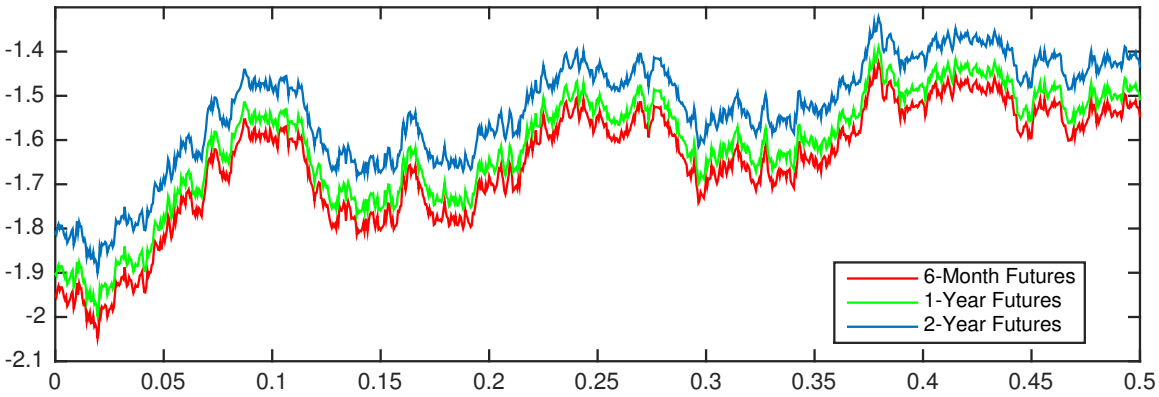

(b) Futures

Figure 4.3: Simulation of $\beta = -1$ tracking strategies for (a) call options of various strikes ($K \in \{40, 50, 60\}$ and $T_c = 0.5$) and (b) futures contracts of various maturities ($T_f \in \{0.5, 1, 2\}$). Parameters are $S_0 = 50$, $X_0 = 100$, $r = 0.05$, $\sigma = 0.2$ and $T = 0.5$. For the ease of comparison, the strategies are based on sample path of the reference index used in Figure 4.1. The x-axis marks the time in years, while the y-axis marks the number of units of derivative required.

Figure 4.3 displays the strategies for "inverse tracking" portfolios with exposure coefficient $\beta = -1$. As expected, short positions are used, but the option strategy is most (resp. least) stable when the option is most in (resp. out of) the money ($K = 40$). The futures strategy is no longer time-deterministic, though the position still shows an increasing trend towards maturity. In fact, the stochastic futures strategy is now proportional to S^{-2}, as seen in (4.2.5) when $\beta = -1$. Comparing across maturities, the shortest-term (resp. longest-term) futures has the most (least) short position, but the position remains negative for all maturities.

4.2.2 Heston Model

We now discuss the tracking problem under the Heston (1993) model for the equity index. Under the risk-neutral measure, the dynamics of the reference index and stochastic volatility factor are given by

$$\begin{aligned} dS_t &= rS_t dt + \sqrt{Y_t} S_t dB_t^{\mathbb{Q},0} \\ dY_t &= \widetilde{\kappa}(\widetilde{\theta} - Y_t)dt + \nu\big(\rho\sqrt{Y_t} dB_t^{\mathbb{Q},0} + \sqrt{1-\rho^2}\sqrt{Y_t} dB_t^{\mathbb{Q},1}\big), \end{aligned}$$

where $B_t^{\mathbb{Q},0}$ and $B_t^{\mathbb{Q},1}$ are two independent SBMs and $\rho \in (-1, 1)$ is the instantaneous correlation parameter. The stochastic volatility factor Y is not traded and is driven by a Cox-Ingersoll-Ross (CIR) process. If we assume the Feller condition $2\widetilde{\kappa}\widetilde{\theta} \geq \nu^2$ (see Feller (1951)) and $Y_0 > 0$, then Y stays strictly positive at all times almost surely under the risk-neutral measure.

Under the Heston Model, the tracking condition (4.1.12) becomes

$$\alpha_t = r(1 - \beta_t) - \widetilde{\kappa}\left(\frac{\widetilde{\theta}}{Y_t} - 1\right)\eta_t, \qquad 0 \leq t \leq T.$$

The portfolio is subject to the stochastic drift α_t which does not vanish as long as $\eta_t \neq 0$ and $\beta_t \neq 1$. Therefore, perfect tracking is not achievable.

Let us set the coefficients to be constant, i.e. $\beta_t = \beta$ and $\eta_t = \eta$ for all $t \in [0, T]$. In

the Heston Model, a portfolio generally needs at least $d+1=2$ derivatives to control risk exposure with respect to the two sources of randomness. We solve for the index exposure β and factor exposure η from the 2×2 system:

$$\begin{pmatrix} \beta \\ \eta \end{pmatrix} = \begin{pmatrix} D_t^{(1)} & D_t^{(2)} \\ E_t^{(1)} & E_t^{(2)} \end{pmatrix} \begin{pmatrix} w_t^{(1)} \\ w_t^{(2)} \end{pmatrix}.$$

The second superscript is suppressed on the factor elasticities since there is only one exogenous factor here. By a simple inversion, the portfolio weights are

$$w_t^{(1)} = \frac{\beta E_t^{(2)} - \eta D_t^{(2)}}{D_t^{(1)} E_t^{(2)} - D_t^{(2)} E_t^{(1)}}, \qquad w_t^{(2)} = \frac{-\beta E_t^{(1)} + \eta D_t^{(1)}}{D_t^{(1)} E_t^{(2)} - D_t^{(2)} E_t^{(1)}}. \tag{4.2.6}$$

Of course, this solution is only valid if

$$D_t^{(1)} E_t^{(2)} \neq D_t^{(2)} E_t^{(1)}. \tag{4.2.7}$$

For instance, using two European call (or put) options on S with different strikes can lead to the trading strategy that generates the desired exposure associated with the given coefficients β and η. However, issues may arise when only futures are used, as we will discuss next.

Example 4.2.1 *Using two futures on S, with maturities $T_f^{(k)}$ $(k=1,2)$, the corresponding portfolio weights are given by*

$$u_t^{(1)} = \frac{\beta H_t^{(2)} - \eta G_t^{(2)}}{G_t^{(1)} H_t^{(2)} - G_t^{(2)} H_t^{(1)}}, \quad \textit{and} \quad u_t^{(2)} = \frac{-\beta H_t^{(1)} + \eta G_t^{(1)}}{G_t^{(1)} H_t^{(2)} - G_t^{(2)} H_t^{(1)}}, \tag{4.2.8}$$

provided that $G_t^{(1)} H_t^{(2)} \neq G_t^{(2)} H_t^{(1)}$.[5] *Since the futures prices are $f_t^{T_k} = S_t e^{r(T_f^{(k)}-t)}$, for $k=$*

[5] Again, the second superscript is suppressed on the factor elasticities since there is only one exogenous factor here.

$1, 2$, *the elasticities (see* (4.1.29)-(4.1.30)*) simplify to*

$$G_t^{(k)} = \frac{S_t}{f_t^{T_f^{(k)}}} \frac{\partial f^{T_f^{(k)}}}{\partial S} = 1, \quad \textit{and} \quad H_t^{(k)} = \frac{Y_t}{f_t^{T_f^{(k)}}} \frac{\partial f^{T_f^{(k)}}}{\partial Y} = 0.$$

However, this means that $G_t^{(1)} H_t^{(2)} = G_t^{(2)} H_t^{(1)} = 0$*, so the strategy in* (4.2.8) *is not well defined. Hence, it is generally impossible to construct a futures portfolio that generates the desired exposure with respect to both the index and stochastic volatility factor for any non-zero coefficients* β *and* η*.*

As shown in Example 4.2.1, in order to gain exposure to S and Y, the derivative need to have a non-zero sensitivity with respect to Y. If the investor does not seek exposure to Y (i.e. $\eta = 0$), then she only needs a single futures on S to obtain the corresponding volatility-neutral portfolio. Next, we show that by including a futures on Y we obtain a tracking portfolio that can generate any desired exposure to S and Y.

Example 4.2.2 *The Heston model can be viewed as a joint model for the market index and volatility index. The CIR process has also been used to model the volatility index due to their common mean-reverting property (see Grübichler and Longstaff (1996) and Mencía and Sentana (2013), among others). Suppose there exist a futures on the market index* S *as well as a futures on the volatility index* Y*, and consider a dynamic portfolio of these two futures contracts. We use the superscript* 1 *to indicate the futures on the index (of maturity* T_f*) and the superscript* 2 *to indicate the futures on the variance process (of maturity* T_y*). The prices of the* T_f*-futures on* S *and the* T_y*-futures on* Y *are respectively given by*

$$f_t^{T_f} = S_t e^{r(T_f - t)} \quad \textit{and} \quad g_t^{T_y} = Y_t e^{-\widetilde{\kappa}(T_y - t)} + \widetilde{\theta}(1 - e^{-\widetilde{\kappa}(T_y - t)}).$$

The relevant price elasticities are

$$G_t^{(1)} = 1, \quad H_t^{(1)} = 0, \quad G_t^{(2)} = 0, \quad \textit{and} \quad H_t^{(2)} = \frac{Y_t}{g_t^{T_y}} e^{-\widetilde{\kappa}(T_y - t)}.$$

The strategy $(u_t^{(1)}, u_t^{(2)})$ *achieving the exposure with coefficients* β *and* η *is found from the system:*

$$\begin{pmatrix} \beta \\ \eta \end{pmatrix} = \begin{pmatrix} G_t^{(1)} & G_t^{(2)} \\ H_t^{(1)} & H_t^{(2)} \end{pmatrix} \begin{pmatrix} u_t^{(1)} \\ u_t^{(2)} \end{pmatrix}.$$

The system admits a unique solution, yielding the portfolio weights:

$$u_t^{(1)} = \beta, \quad \textit{and} \quad u_t^{(2)} = \eta + \eta \frac{\widetilde{\theta}}{Y_t} \left(e^{\widetilde{\kappa}(T_y - t)} - 1 \right).$$

Interestingly, the portfolio weight $u_t^{(1)}$ *(resp.* $u_t^{(2)}$*) depends only on* β *(resp.* η*).*

Finally, we discuss the slippage process under the Heston model. Applying Proposition 4.1.2, we obtain

$$Z_t = r - r\beta - \widetilde{\kappa} \left(\frac{\widetilde{\theta}}{Y_t} - 1 \right) \eta + \frac{1}{2}\beta(1-\beta)Y_t + \frac{1}{2}\eta(1-\eta)\frac{\nu^2}{Y_t} - \beta\eta\nu\rho. \tag{4.2.9}$$

The term $\frac{1}{2}\beta(1-\beta)Y_t$ in (4.2.9) indicates that the current slippage Z_t depends on the instantaneous variance Y of the index S. Similarly, the term $\frac{1}{2}\eta(1-\eta)\frac{\nu^2}{Y_t}$ reflects the dependence of the slippage on the instantaneous variance of the stochastic volatility Y. As in the Black-Scholes case, for $\eta \notin [0,1]$, this term is negative. The final term $-\beta\eta\nu\rho$ is the instantaneous covariance between the index and the stochastic volatility. Since $\nu > 0$, the term is positive whenever $\beta\eta\rho < 0$. This happens either when (i) all three are negative, or (ii) exactly 1 is negative. Since equity returns and volatility are typically negatively correlated[6] ($\rho < 0$), so going long on both the index and stochastic volatility ($\beta, \eta > 0$) can generate positive returns. This covariance term can offset some losses due to volatility decay.

[6]This phenomenon is called *asymmetric volatility* and was first observed by Black (1976).

4.3 Volatility Index Tracking

In this section, we discuss tracking of the volatility index, VIX, under two continuous-time models. These models were first applied to pricing volatility futures and options by Grübichler and Longstaff (1996) and Mencía and Sentana (2013), among others. We expand their analysis to understand the tracking performance of VIX derivatives portfolios and VIX ETFs.

4.3.1 CIR Model

The volatility index, denoted by S in this section, follows the CIR process:[7]

$$dS_t = \widetilde{\kappa}\left(\widetilde{\theta} - S_t\right)dt + \sigma\sqrt{S_t}dB_t^{\mathbb{Q}}, \tag{4.3.1}$$

with constant parameters $\widetilde{\kappa}, \widetilde{\theta}$, and $\sigma > 0$. If we assume the Feller condition $2\widetilde{\kappa}\widetilde{\theta} \geq \sigma^2$ (see Feller (1951)) and $S_0 > 0$, then S stays strictly positive at all times almost surely. We omit the second superscript on the SBM $B_t^{\mathbb{Q}}$ since there is only one SBM in this model.

Under the CIR model, the tracking condition from (4.1.12) becomes

$$\alpha_t = r - \beta_t\widetilde{\kappa}\left(\frac{\widetilde{\theta}}{S_t} - 1\right), \tag{4.3.2}$$

for all $t \in [0, T]$. Therefore, for any given exposure coefficient β_t, there is a non-zero stochastic drift depending on the inverse of S_t. In particular, if $\beta_t \equiv 0$, then $\alpha_t \equiv r$ and we recover the risk free rate by eliminating exposure to the volatility index. Next, suppose $\beta_t \equiv 1$ for a 100% exposure to the volatility index. Then, the stochastic drift takes the form

$$\alpha_t = \frac{\left(\widetilde{\kappa} + r\right)S_t - \widetilde{\kappa}\widetilde{\theta}}{S_t}, \tag{4.3.3}$$

[7] Or the square root (SQR) process in the terminology of Grübichler and Longstaff (1996).

which is negative (resp. positive) whenever S_t is below (resp. above) the critical level $\frac{\widetilde{\kappa}\widetilde{\theta}}{\widetilde{\kappa}+r}$. In addition, if $r = 0$, then the critical value is equal to $\widetilde{\theta}$.[8] Then, as S_t mean-reverts to $\widetilde{\theta}$, the drift is on average equal to 0, but is stochastic nonetheless.

Remark 4.3.1 *More generally suppose that $\beta_t \equiv \beta$, a constant. Then the stochastic drift is given by*

$$\alpha_t = \frac{(r + \beta\widetilde{\kappa})S_t - \beta\widetilde{\kappa}\widetilde{\theta}}{S_t}, \tag{4.3.4}$$

which is negative (resp. positive) whenever S_t is below (resp. above) the critical level $\frac{\beta\widetilde{\kappa}\widetilde{\theta}}{r+\beta\widetilde{\kappa}}$. Compare this to the critical value in discrete time for mean reverting models derived in Corollary 3.2.1. As mentioned in Remark 3.2.3, there is a correspondence between the trading frequency and the compounding frequency of the interest rate in the critical value for zero error.

Furthermore, according to Proposition 4.1.2, the slippage process given any constant $\beta \in \mathbb{R}$ in the CIR Model is given by

$$Z_t = r - \beta\widetilde{\kappa}\left(\frac{\widetilde{\theta}}{S_t} - 1\right) + \frac{1}{2}\beta(1-\beta)\frac{\sigma^2}{S_t}.$$

The second term reflects the mean reverting path behavior of S. And since $\widetilde{\theta}$ is the long-run mean of S_t, this term is expected to stay around zero over time, though the deviation from zero is proportional to $\beta\widetilde{\kappa}$. The last term involves the variance of the volatility index, $\frac{\sigma^2}{S_t}$, and is strictly negative for $\beta \notin [0, 1]$, leading to value erosion. Lastly, we observe that Z_t is an affine function of ${S_t}^{-1}$, which is an inverse CIR process. The moments and other statistics of such a process are well known (see Ahn and Gao (1999)), so this form will be useful for understanding the distribution and computing expectations of Z_t.

Since there are $d = 0$ factors outside of the volatility index, $d + 1 = 1$ derivatives allow for a unique tracking strategy. Specifically, we study the dynamics of portfolios of futures

[8] Alternatively, we can assume $\widetilde{\kappa} >> r$ so that $\frac{\widetilde{\kappa}}{\widetilde{\kappa}+r} \approx 1$ and the critical value is approximately $\widetilde{\theta}$.

written on S. For any maturity T, the futures price is

$$f_t^T := f(t,S,T) = \mathbb{E}^{\mathbb{Q}}\left[S_T | S_t = S\right] = (S-\widetilde{\theta})e^{-\widetilde{\kappa}(T-t)} + \widetilde{\theta}. \tag{4.3.5}$$

In Figure 4.4 we display two term structures of VIX futures on two different dates, calibrated to the CIR model. The term structure can be either increasing concave or decreasing convex (see e.g. Li (2016) and Chapter 5 of Leung and Li (2016)). While the good fits further suggest that the CIR Model is a suitable model for VIX, we remark that there exist examples of irregularly shaped VIX term structures and calibrated model parameters often change over time. This motivates us to investigate the tracking problem under a more sophisticated VIX model in the next section.

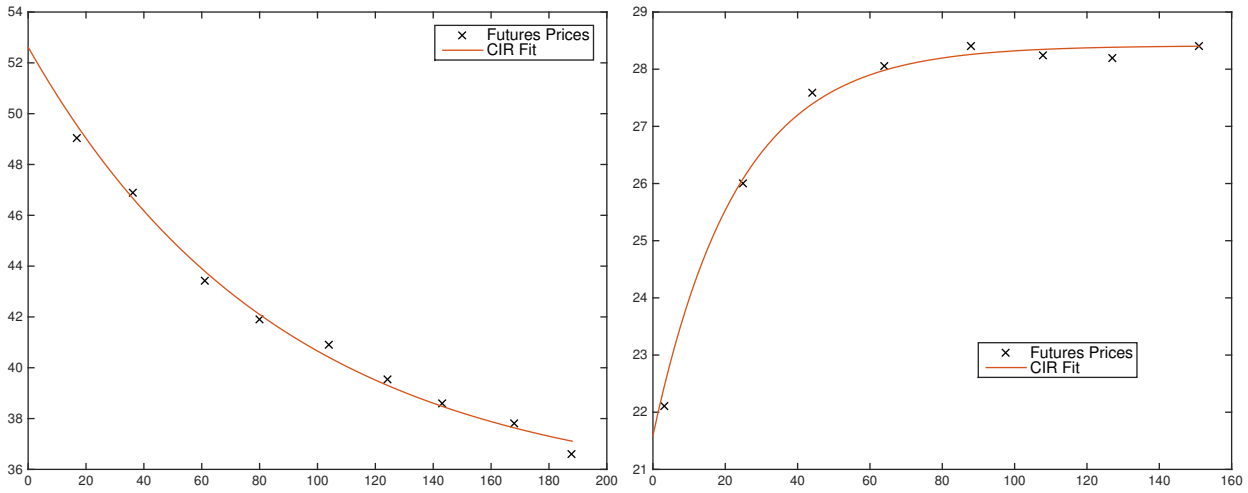

(a) Feruary 23rd, 2009 (b) December 11th, 2009

Figure 4.4: Term structure of VIX futures as observed on (a) Feb. 23rd, 2009 and (b) December 11th, 2009 along with the calibrated CIR/SQR term structure model. The term structure has changed from decreasing convex to increasing concave. The x-axis marks the time-to-maturity in days, while the y-axis marks the price.

The futures trading strategy is given by

$$u_t = \beta + \frac{\beta\widetilde{\theta}}{S_t}\left(e^{\widetilde{\kappa}(T-t)} - 1\right). \tag{4.3.6}$$

Of course, one may set $\beta = 1$ to seek direct exposure to the volatility index. A number

of VIX ETFs/ETNs attempt to gain direct exposure to VIX (e.g. VXX) by constructing a futures portfolios with time-deterministic weights. The following example elucidates how and to what extent such an exchange-traded product falls short of this goal.

4.3.2 Comparison to VXX

Let us consider a portfolio of futures with a time-deterministic strategy. Its value evolves according to

$$\frac{dV_t}{V_t} = u(t)\frac{df_t^{T_{i(t)}}}{f_t^{T_{i(t)}}} + (1-u(t))\frac{df_t^{T_{i(t)+1}}}{f_t^{T_{i(t)+1}}} + rdt, \tag{4.3.7}$$

where $i(t) := \min\{i : T_{i-1} < t \leq T_i\}$, $T_0 := 0$, and the portfolio weight for the T_i-futures is

$$u(t) := \frac{T_{i(t)} - t}{T_{i(t)} - T_{i(t)-1}}. \tag{4.3.8}$$

This is the strategy employed by the popular VIX ETN, iPath S&P 500 VIX Short-Term Futures ETN (VXX). The strategy starts by investing 100% in the 1-Month VIX futures contract, and decreases its holding linearly from 100% to 0% while the weight on the 2-Month contract increases linearly from 0% to 100%.

Figure 4.5 illustrates such a portfolio with simulated index prices. Specifically, we plot the VIX in red, and the VXX price in blue over one month. The component futures prices (1 and 2-Month) are plotted in green and purple (respectively). Compared to the VIX, the VXX is significantly less volatile. This can be confirmed analytically since

$$\left(\frac{dV_t}{V_t}\right)^2 = \left(\frac{u(t)}{S_t + \widetilde{\theta}(e^{\widetilde{\kappa}(T_{i(t)}-t)} - 1)} + \frac{1-u(t)}{S_t + \widetilde{\theta}(e^{\widetilde{\kappa}(T_{i(t)+1}-t)} - 1)}\right)^2 (dS_t)^2 < \left(\frac{dS_t}{S_t}\right)^2,$$

where the inequality is due to $\widetilde{\kappa}(T_j - t) > 0$ so that $\widetilde{\theta}\left(e^{\widetilde{\kappa}(T_j-t)} - 1\right) > 0$ for any j as well as $0 \leq u(t) \leq 1$. The strategy employed by VXX never leverages any single futures contract.

On the other hand, our portfolio *does* lever the futures contracts to the inequality above

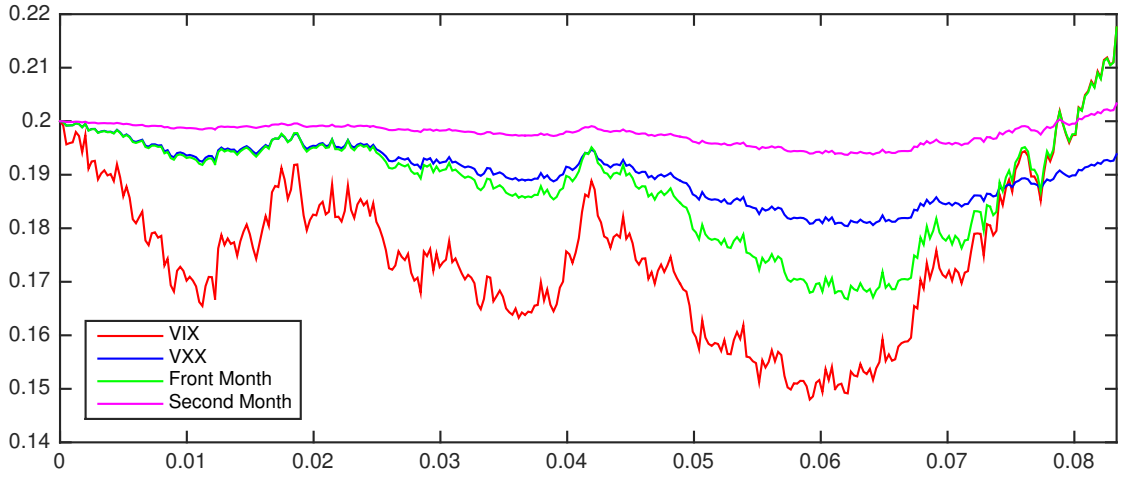

(a) One Month

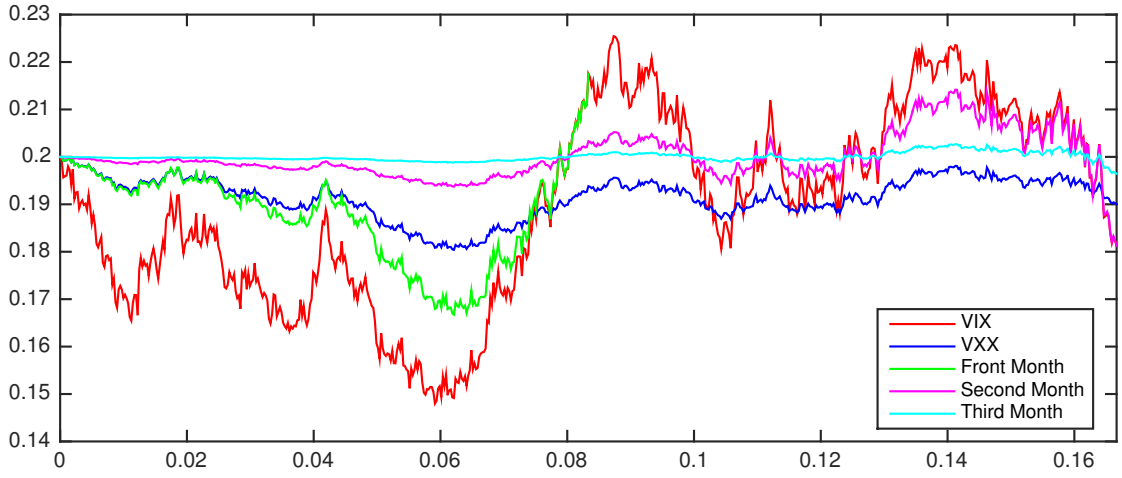

(b) Two Months

Figure 4.5: Simulation of VXX along with VIX and the two futures contracts VXX holds over (a) 1 month ($T = 1/12$) and (b) 2 months ($T = 2/12$) under the SQR model. Panel (b) is an extension of the simulation in Panel (a). Parameters are $S_0 = 0.2$, $\widetilde{\kappa} = 20$, $\widetilde{\theta} = 0.2$ and $\nu = 0.4$. The x-axis marks the time in years, while the y-axis marks the price.

need not hold for the dynamic portfolio. We demonstrate this in Figure 4.6, which gives another simulation of VIX, VXX and this time we add in the dynamic portfolio targeting $\beta = 1$. Compared to VXX, the dynamic portfolio is more reactive to changes in VIX. To further understand the differences amongst VXX and the $\beta = 1$ dynamic portfolio, Figure 4.7 displays two scatterplots of the annualized returns: the dynamic portfolio returns vs. VIX returns (top) and VXX returns vs. VIX returns (bottom). On both plots, the line $y = x$ is superimposed in black for comparison. The dynamic portfolio, while not tracking VIX perfectly, generates highly similar returns as VIX, and is visibly much closer to VIX than VXX.

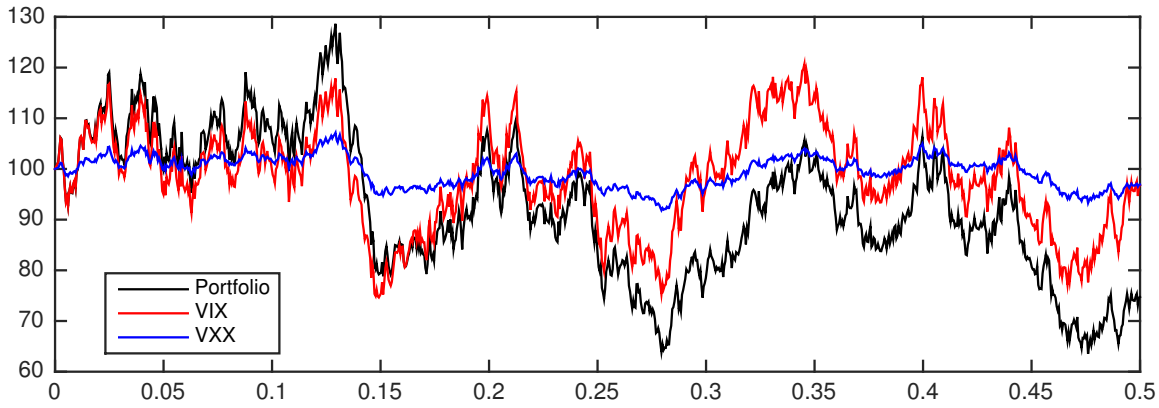

Figure 4.6: Sample paths of VIX, VXX, and the dynamic portfolio with $\beta = 1$ over a 6-month period ($T = 0.5$). Parameters are $S_0 = 0.2$, $\widetilde{\kappa} = 20$, $\widetilde{\theta} = 0.2$, and $\nu = 0.4$. All values are normalized to start at \$100. The x-axis marks the time in years, while the y-axis marks the price.

Given the VXX strategy (or any other strategy), we can infer from the SDE of the portfolio (see (4.3.7)) the corresponding drift (the dt term) and exposure to S (coefficient of dS_t/S_t), which we denote by $\alpha_t^{(V)}$ and $\beta_t^{(V)}$, respectively. As a point of reference, if a portfolio tracks VIX one-to-one perfectly, then we have $\beta_t^{(V)} = 1$ and $\alpha_t^{(V)} = 0$. As our earlier discussion following Equation (4.3.3) indicates, this perfect tracking is impossible, but we still wish to illustrate how much VXX deviates from VIX in terms of the implied values of $\alpha_t^{(V)}$ and $\beta_t^{(V)}$.

Let us denote T_1 and T_2 as the maturities for the 1-Month and 2-Month futures, respectively. With the portfolio weights in (4.3.8), we find from the portfolio's SDE (4.3.7)

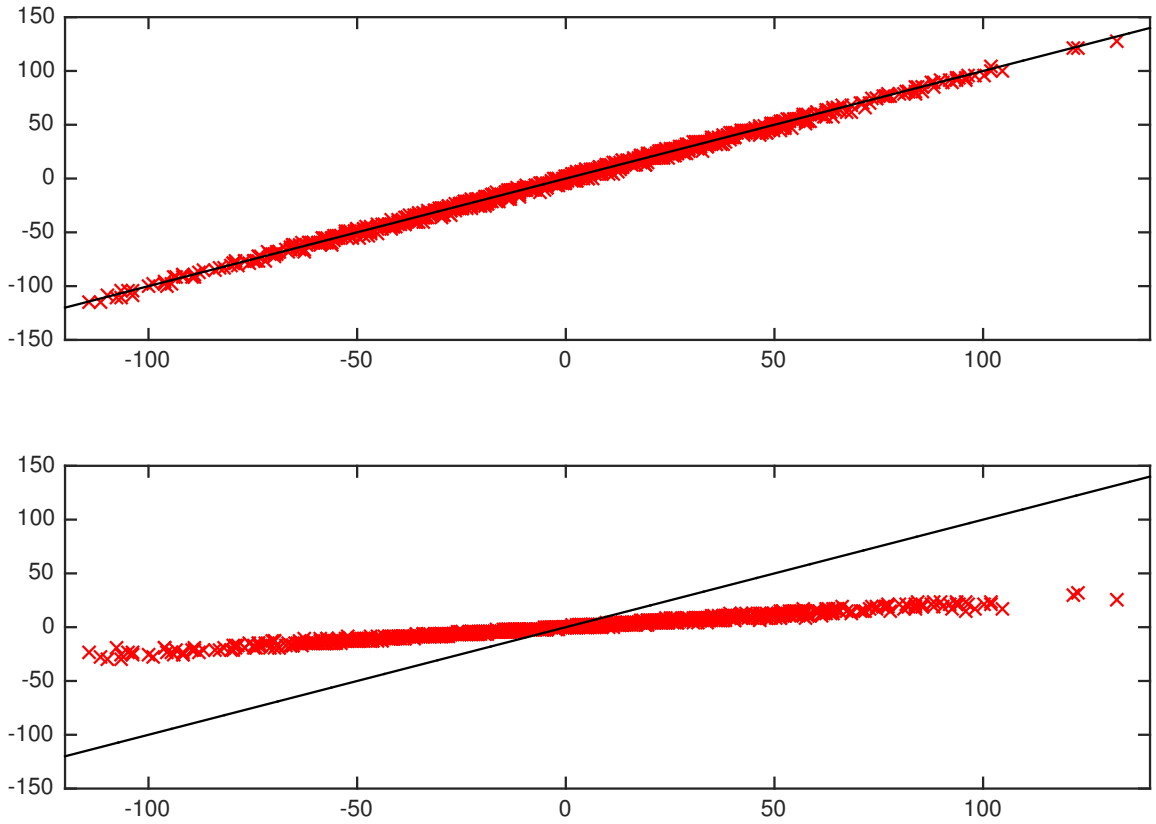

Figure 4.7: Scatter plots of the annualized returns for the simulation in Figure 4.6. On top, we plot the dynamic portfolio returns vs. VIX returns and on the bottom, we plot VXX returns vs. VIX returns. On both plots, a solid straight line with slope 1 is a drawn for visual comparison. The x-axis marks the returns (annualized percentages) of VIX, while the y-axis marks the returns (annualized percentages) of the dynamic portfolio (top) or VXX (bottom).

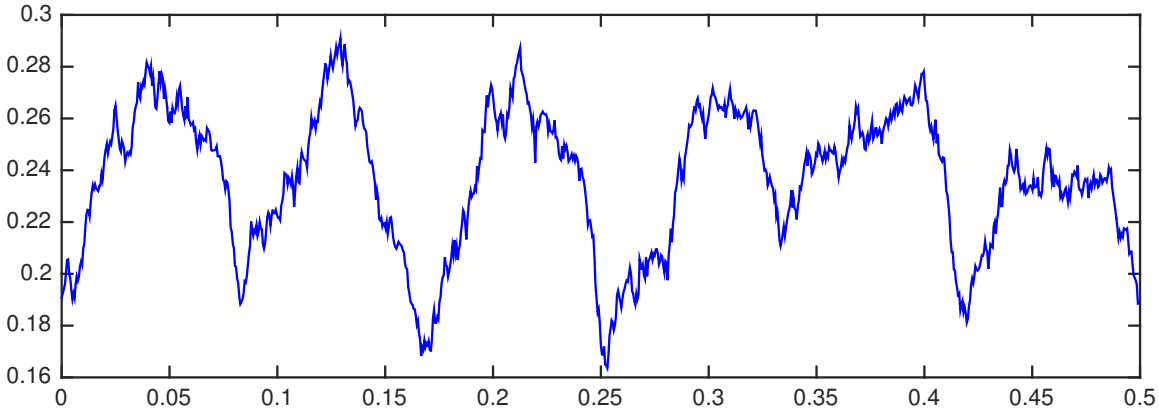

Figure 4.8: With reference to the simulated paths in Figure 4.6, we show the implied exposure coefficient β_t inferred from VXX over a 6-month period ($T = 0.5$). The x-axis marks the time in years, while the y-axis marks the value of β_t.

that

$$\alpha_t^{(V)} = r + \beta_t^{(V)}\widetilde{\kappa}\left(1 - \frac{\widetilde{\theta}}{S_t}\right),$$
$$\beta_t^{(V)} = \frac{S_t}{f_t^{T_1}}e^{-\widetilde{\kappa}(T_1-t)} - \frac{tS_te^{\widetilde{\kappa}t}}{T_1}\left(\frac{e^{-\widetilde{\kappa}T_1}}{f_t^{T_1}} - \frac{e^{-\widetilde{\kappa}T_2}}{f_t^{T_2}}\right).$$

As expected, we do not have $\beta_t^{(V)} \equiv 1$ and $\alpha_t^{(V)} \equiv 0$. Indeed both coefficients are stochastic and depend on the level of S_t.

In Figure 4.8, we plot the implied β_t over time based on the sample path of VXX in Figure 4.6. The implied β for VXX varies significantly over time, and is far from the reference value 1 (for unit exposure to VIX) all the time. On average the implied β fluctuates around 0.23 over the entire 6 month period. Recall that VXX is a long portfolio of the 1-Month and 2-Month futures, starting with a 100% allocation in the 1-Month at each maturity. Interestingly, as VXX allocates more in the 2-Month futures over time, the portfolio value reaches its maximum approximately halfway through each contract period, suggesting that concentrating on the shortest-term futures does not imply the closest tracking to the underlying index.

In Figure 4.9, we plot the stochastic α_t (based on the sample path of VXX in Figure 4.6) in units of annualized basis points for both VXX and the dynamic portfolio with $\beta = 1$. For both portfolios, α is not 0 as expected. For the dynamic portfolio with $\beta = 1$, the

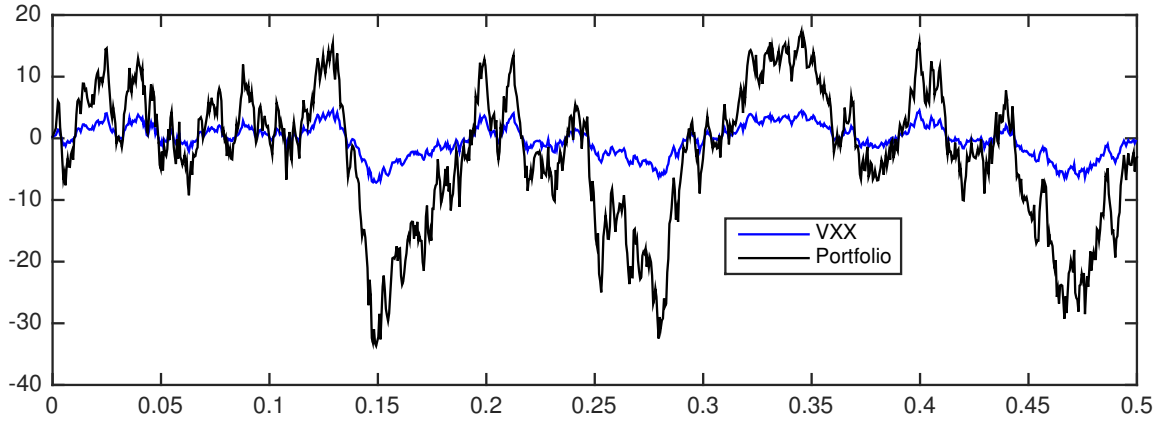

Figure 4.9: With reference to the simulated paths in Figure 4.6, we show the stochastic drift α_t for both VXX and the tracking portfolio over a 6-month period ($T = 0.5$). The x-axis marks the time in years, while the y-axis marks the value of α_t.

stochastic drift is more volatile than that for VXX, but both are relatively small compared to the returns seen in Figure 4.6(b).

We conclude this example by discussing the futures trading strategies corresponding to $\beta = 1$ (see (4.3.6)) with *either* the 1-Month futures only, *or* the 2-Month futures only. Recall that in this model only $d + 1 = 1$ derivative product is necessary to achieve unit exposure ($\beta = 1$), but the choice of derivative can lead to a very different portfolio weight over time. To see this, we plot in Figure 4.10 the sample paths of the two portfolio weights corresponding to the two futures contracts with different maturities. In general, the futures strategies tend to decrease exponentially in each maturity cycle, and become discontinuous at maturities as the portfolio rolls into the new futures contract. The 1-Month futures strategy decays roughly from 5 to 1 in each cycle. Given that futures price will converge to index price by maturity, it is intuitive that the strategy weight becomes 1 for 1-Month futures. Intuitively, futures prices are typically less volatile than the index, so leveraging (weights greater than 1) is expected and can in effect increase the portfolio's volatility to attempt to better track the index. Comparing between the two strategies, using the 2-Month futures to track VIX leads to significant leveraging.

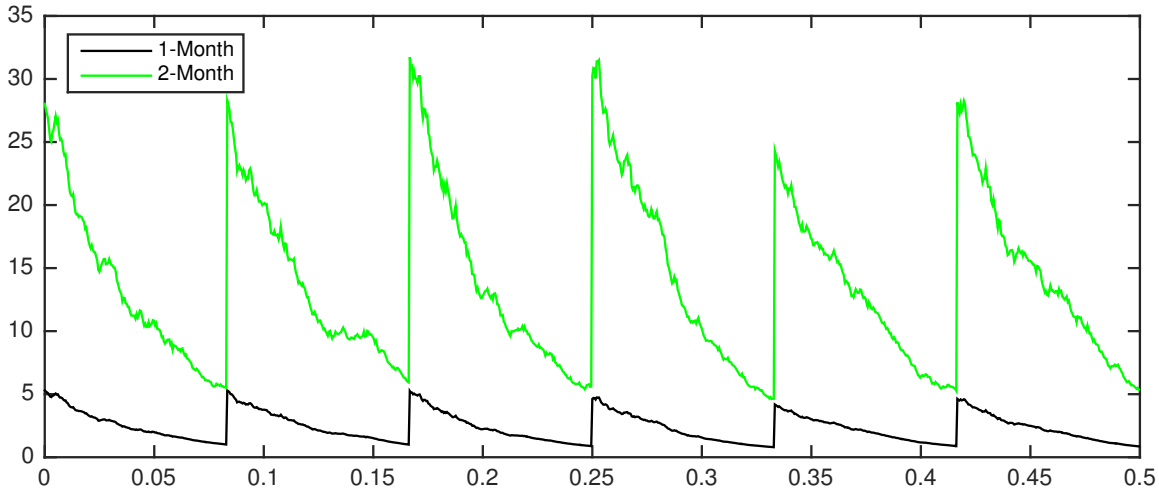

Figure 4.10: Portfolio weights of the dynamic portfolio with exposure coefficient $\beta = 1$ in Figure 4.6. The x-axis marks the time in years, while the y-axis marks the weight.

One of the advantages of futures contracts is the ease of leveraging due to margin requirements. If margin requirements are 20% of notional, then it is possible to achieve 5x leverage. Margin requirements are constantly changing for VIX futures.[9] However, 25x to 30x for the 2-Month futures is neither typical nor practical. The weights for 1-Month futures are more in line with feasible leverage that one can attain. Recall that the strategy employed by VXX is a time-deterministic one. Figure 4.10 further illustrates that stochastic portfolio weights are necessary in order to achieve unit exposure to the volatility index.

4.3.3 CSQR Model

We now investigate the tracking strategy and slippage process under an extension of the CIR Model. In this section, S will continue to be mean reverting, but the long-run mean is also stochastic. This model is referred to as the concatenated square root process (CSQR) (see

[9]See `http://cfe.cboe.com/margins/CurDoc/Default.aspx` for current margin requirements for VIX futures. Margin requirements are stated as a dollar value, rather than a percentage. That dollar value is based on one unit of VIX futures, which is 1,000 times the stated futures price. Back-of-the-envelope calculations yield historical percentages between 10% and 30%.

Mencía and Sentana (2013)):

$$dS_t = \widetilde{\gamma}(Y_t - S_t)dt + \sigma\sqrt{S_t}dB_t^{\mathbb{Q},0},$$
$$dY_t = \widetilde{\kappa}(\widetilde{\theta} - Y_t)dt + \nu\rho\sqrt{Y_t}dB_t^{\mathbb{Q},0} + \nu\sqrt{1-\rho^2}\sqrt{Y_t}dB_t^{\mathbb{Q},1}.$$

Here, $B_t^{\mathbb{Q},0}$ and $B_t^{\mathbb{Q},1}$ are independent SBMs. We assume the parameters are chosen so that the pair (S_t, Y_t) is strictly positive $\forall\, t \geq 0$.[10] Here, the index tends to revert to the stochastic level Y_t which is also mean-reverting. This accounts for the empirical observations of the path behavior of VIX, and that VIX futures calibration suggest that the long-run mean oscillates over time (see e.g. Figure 4.4).

Let the investor set the values of exposure coefficients $\beta_t \equiv \beta$ and $\eta_t \equiv \eta$, then the portfolio is subject to a stochastic drift (see Proposition 4.1.1) that is a function of S_t and Y_t:

$$\alpha_t = r - \frac{\widetilde{\gamma}(Y_t - S_t)}{S_t}\beta - \frac{\widetilde{\kappa}(\widetilde{\theta} - Y_t)}{Y_t}\eta.$$

Also, applying Proposition 4.1.2, we obtain the slippage process Z_t in the CSQR model:

$$Z_t = r - \beta\widetilde{\gamma}\left(\frac{Y_t}{S_t} - 1\right) - \eta\widetilde{\kappa}\left(\frac{\widetilde{\theta}}{Y_t} - 1\right) + \frac{1}{2}\beta(1-\beta)\frac{\sigma^2}{S_t} + \frac{1}{2}\eta(1-\eta)\frac{\nu^2}{Y_t} - \frac{\beta\eta\nu\rho\sigma}{\sqrt{S_tY_t}}.$$

As we can see, the first two terms reflect the mean-reverting properties of S_t and Y_t. On average, their effects tend to be zero, but are also proportional to the speeds of mean reversion $\widetilde{\gamma}$ and $\widetilde{\kappa}$, and exposure coefficients β and η. The next two terms account for the variances of the index and its stochastic mean, and are negative if $\beta \notin [0,1]$ and $\eta \notin [0,1]$, respectively. The final term reflects the effect of covariance between S and Y in this model. It will be negative if either (i) all three of β, η and ρ are positive, or (ii) exactly one of β, η, or ρ is positive.

Since $d = 1$, we know that $d + 1 = 2$ derivative products are required to obtain the desired exposures. Let us consider the use of futures contracts on S. The price of a futures

[10] See for example Duffie and Kan (1996) for a discussion of models of this form.

written on S with maturity T_k is given by

$$f_t^{T_k} = \widetilde{\theta} + \left(S_t - \widetilde{\theta}\right) e^{-\widetilde{\gamma}(T_k - t)} + \begin{cases} \widetilde{\gamma} e^{-\widetilde{\gamma} T_k} \left(Y_t - \widetilde{\theta}\right) e^{\widetilde{\kappa} t} (T_k - t), & \widetilde{\gamma} = \widetilde{\kappa} \\ \frac{\widetilde{\gamma}\left(Y_t - \widetilde{\theta}\right)}{\widetilde{\gamma} - \widetilde{\kappa}} \left(e^{-\widetilde{\kappa}(T_k - t)} - e^{-\widetilde{\gamma}(T_k - t)}\right), & \widetilde{\gamma} \neq \widetilde{\kappa}, \end{cases}$$

for $t \leq T_k$; see Mencía and Sentana (2013) for a derivation. Notice the first term would be the futures price if S_t were reverting to the mean $\widetilde{\theta}$ at speed $\widetilde{\gamma}$. Next we calculate the sensitivities with respect to the index and stochastic mean:

$$\frac{\partial f_t^{T_k}}{\partial S} = e^{-\widetilde{\gamma}(T_k - t)}, \quad \text{and} \quad \frac{\partial f_t^{T_k}}{\partial Y} = \begin{cases} \widetilde{\gamma} e^{\widetilde{\kappa} t - \widetilde{\gamma} T_k} (T_k - t), & \widetilde{\gamma} = \widetilde{\kappa} \\ \frac{\widetilde{\gamma}}{\widetilde{\gamma} - \widetilde{\kappa}} \left(e^{-\widetilde{\kappa}(T_k - t)} - e^{-\widetilde{\gamma}(T_k - t)}\right), & \widetilde{\gamma} \neq \widetilde{\kappa} \end{cases}.$$

Henceforth, assume the latter case that $\widetilde{\gamma} \neq \widetilde{\kappa}$.[11] In that case, the respective elasticities are given by

$$G_t^{(k)} = \frac{S_t}{f_t^{T_k}} e^{-\widetilde{\gamma}(T_k - t)}, \quad \text{and} \quad H_t^{(k)} = \frac{Y_t}{f_t^{T_k}} \frac{\widetilde{\gamma}}{\widetilde{\gamma} - \widetilde{\kappa}} \left(e^{-\widetilde{\kappa}(T_k - t)} - e^{-\widetilde{\gamma}(T_k - t)}\right). \tag{4.3.9}$$

Just as in Section 4.2.2, the second numerical superscript on $H_t^{(k)}$ has been suppressed since there is only one exogenous factor in this model.

We consider a portfolio of two futures contracts, both on S with maturities $T_2 > T_1 \geq T$. Recall that tracking does not work with two futures in the Heston Model, so one must include another type of derivative (e.g. option). Now in the CSQR model, we check if this futures portfolio works by verifying

$$G_t^{(1)} H_t^{(2)} \neq G_t^{(2)} H_t^{(1)}, \tag{4.3.10}$$

for all $t \in [0, T]$. Upon plugging in the above elasticities, we find that the condition is equivalent to $T_1 \neq T_2$ (see Appendix A.4.) Since we have assumed that $T_1 < T_2$, the

[11] Similar proofs can be found in Appendices A.2 and A.3 for $\widetilde{\gamma} = \widetilde{\kappa}$.

condition holds. Therefore, the linear system of equations

$$\begin{pmatrix} \beta \\ \eta \end{pmatrix} = \begin{pmatrix} G_t^{(1)} & G_t^{(2)} \\ H_t^{(1)} & H_t^{(2)} \end{pmatrix} \begin{pmatrix} u_t^{(1)} \\ u_t^{(2)} \end{pmatrix}, \tag{4.3.11}$$

which yields the strategy for the two futures contracts is always solvable.

Soling the system yield the portfolio weights

$$u_t^{(1)} = \frac{\beta f_t^{T_1}}{S_t} \left(\frac{e^{\widetilde{\gamma}(T_2-t)} - e^{\widetilde{\kappa}(T_2-t)}}{e^{\widetilde{\gamma}(T_2-T_1)} - e^{\widetilde{\kappa}(T_2-T_1)}} \right) - \frac{\eta f_t^{T_1}}{Y_t} \left(1 - \frac{\widetilde{\kappa}}{\widetilde{\gamma}} \right) \left(\frac{e^{\widetilde{\kappa}(T_2-t)}}{e^{\widetilde{\gamma}(T_2-T_1)} - e^{\widetilde{\kappa}(T_2-T_1)}} \right), \tag{4.3.12}$$

and

$$u_t^{(2)} = \frac{-\beta f_t^{T_2}}{S_t} \left(\frac{e^{\widetilde{\gamma}(T_1-t)} - e^{\widetilde{\kappa}(T_1-t)}}{e^{-\widetilde{\kappa}(T_2-T_1)} - e^{-\widetilde{\gamma}(T_2-T_1)}} \right) + \frac{\eta f_t^{T_2}}{Y_t} \left(1 - \frac{\widetilde{\kappa}}{\widetilde{\gamma}} \right) \left(\frac{e^{\widetilde{\kappa}(T_1-t)}}{e^{-\widetilde{\kappa}(T_2-T_1)} - e^{-\widetilde{\gamma}(T_2-T_1)}} \right). \tag{4.3.13}$$

For example, take $\beta = 1$ and $\eta = 0$. Then, only the first terms in (4.3.12) and (4.3.13) remain, and $u_t^{(1)}$ is positive but $u_t^{(2)}$ is negative. This combination of futures contracts allows for direct exposure to the volatility index, without any exposure to the stochastic mean of the volatility.

Chapter 5

Schedule Following in Algorithmic Trading

In this chapter, we consider a tracking problem that is important in algorithmic trading: schedule following. Here, we study the optimal execution of market and limit orders with permanent and temporary price impacts as well as uncertainty in the filling of limit orders. The model includes a trade speed limiter and a trader director to provide better control on the trading rates. The optimal execution problem is cast as a stochastic control problem and we solve the associated non-linear Hamilton-Jacobi-Bellman (HJB) PDE problem to determine the optimal dynamic strategy for trade execution. In Section 5.1 we set up the problem dynamics and state the optimal control problem. The problem is solved under the assumption of affine uncertainty and affine market impact in Section 5.2. Sections 5.3 and 5.4 are dedicated to describing in more detail the special cases of constant and linear uncertainty, respectively. Additionally, we adapt our model to solve the schedule-following problem that penalizes deviations from an order schedule in Section 5.5. Numerical simulations are provided to illustrate the optimal market and limit orders over time.

5.1 Optimal Order Type Selection

Throughout this paper, we take the perspective of a sell program. The mathematics for a buy program is completely analogous. We first present the formulation of our optimal execution model, then derive the optimal strategies. We will further discuss their properties in Sections 5.3 and 5.4 under constant and linear limit order uncertainty, respectively.

In the background, we fix a probability space $(\Omega, \mathcal{F}, \mathbb{P})$, and a finite trading horizon $[0, T]$. Our model involves two stochastic controls: (i) the trading rate of market orders, v_t and (ii) the trading rate of limit orders, L_t, over time $t \in [0, T]$. The trader's stock holdings, denoted by x_t at time t, is depleted by the trading rates, v_t and L_t. To capture the uncertainty of limit order fills, there is an additional diffusion term $m(L_t)dZ_t$, where m is a deterministic function of the limit order trading rate and Z is a standard Brownian motion. Precisely, the trader's position satisfies the SDE:

$$dx_t = -v_t dt + \left(-L_t dt + m(L_t) dZ_t\right). \tag{5.1.1}$$

The stock price S and transacted price $\widetilde{S}$ follow a generalized version of Almgren and Chriss (2000) dynamics:

$$\begin{aligned} dS_t &= \gamma dx_t + \mu dt + \sigma dW_t, \\ \widetilde{S}_t &= S_t + h(v_t, L_t). \end{aligned} \tag{5.1.2}$$

In other words, the price S follows an arithmetic Brownian motion with drift $\mu \in \mathbb{R}$ and volatility $\sigma > 0$, along with a linear permanent impact with coefficient $\gamma > 0$. The transacted price reflects a temporary impact, $h(v_t, L_t)$, which is a function of the current trading rates of market and limit orders. As we seek closed-form solutions, we assume that the temporary impact is affine, i.e. $h(v_t, L_t) = -\eta_0 - \eta_1 v_t - \eta_2 L_t$, with constants $\eta_0, \eta_1, \eta_2 > 0$. The two standard Brownian motions, Z and W, are correlated with an instantaneous correlation parameter $\rho \in (-1, 1)$. The trader's information flow is modeled by the filtration $\mathbb{F}$ generated by (Z, W), and all admissible strategies must be $\mathbb{F}$-adapted.

We typically expect $\rho m(L) < 0$ so long as $L \geq 0$. This parameter sign choice will give rise to an *adverse selection* effect that is often considered in algorithmic trading models. Adverse selection is an implicit cost incurred when, for example, the stock price rises just after making a sale. It would have been better for the trader to wait for the price rise before selling the stock because then she would have realized an extra profit. To see this, first consider the case with $\rho > 0$. Then, if $\Delta Z_t > 0$ is observed over some small time period Δt, we typically see $\Delta W_t > 0$, and thus $\Delta S_t > 0$, an increase in the stock price. For the model to incorporate an adverse selection effect, we want the trader to make an excess sale in limit orders. This will occur if $m(L_t) < 0$, for then $m(L_t)\Delta Z_t < 0$ and $\Delta x_t < 0$. Reversing the signs and starting with $\rho < 0$, we find that we need $m(L_t) > 0$ for $\Delta x_t < 0$. The two cases can be summarized by the restriction $\rho m(L) < 0$. In our implementation, we will choose parameters that satisfy this adverse selection criterion, though our model also works when it does not hold.

As a standard performance metric, the profit-and-loss (PNL) of any trading strategy is defined as

$$\Pi_T := x_T \left(S_T - S_0\right) + \int_0^T \left(S_0 - \widetilde{S}_u\right) dx_u \tag{5.1.3}$$

$$= x_T S_T - x_0 S_0 - \int_0^T \widetilde{S}_u dx_u. \tag{5.1.4}$$

The first two terms in (5.1.4) measure the change in fair value of the portfolio as measured by the stock price. The third term is the revenue/cost of trading: it measures at each point in time the change in position multiplied by the transacted price $\widetilde{S}_t$ at that time. In a sell program, the infinitesimal amount of shares sold (represented by $-dx_t$) tends to be positive. Thus, the integral $-\int_0^T \widetilde{S}_u dx_u$ can be interpreted as revenue of sale.

When we plug in the dynamics given by Equations (5.1.1) and (5.1.2), the PNL becomes

$$\begin{aligned}\Pi_T = &\frac{\gamma}{2}\left(x_T^2 - x_0^2\right) + \int_0^T \left[\mu x_u + \rho\sigma m(L_u) + \frac{\gamma}{2}m^2(L_u) + h(v_u, L_u)(v_u + L_u)\right] du \\ &+ \int_0^T \sigma x_u dW_u - \int_0^T h(v_u, L_u)m(L_u)dZ_u.\end{aligned} \tag{5.1.5}$$

We also incorporate three model features: (i) quadratic terminal penalty, (ii) trade director, and (iii) trade speed limiter. First, we must ensure that the position is actually liquidated. To that end, we add a quadratic penalty term $\bar{f}(x) = -\beta x^2$, so that anything but complete liquidation is undesirable. Cheng et al. (2017) use the same penalty to penalize non-liquidation. The second penalty is introduced to penalize placing buy side market orders and sell side limit orders (or vice versa) simultaneously. Such order placement would be as if the trader were buying/selling the stock to herself. This penalty is called the trade director. The goal is to encourage orders to have the same sign or equivalently, $v_t L_t \geq 0$. In combination with the non-liquidation penalty, we expect that only the choice $v_t \geq 0$, $L_t \geq 0$. We introduce the penalty integral $\int_0^T \alpha v_u L_u du$, with the Lagrange multiplier $\alpha \geq 0$.

We also add a speed limiter to prevent the trader from trading too quickly with either order type. Suppose that management has set two trading speed caps $r_1, r_2 > 0$, for market and limit orders, respectively. To encourage the trader to satisfy the constraints: $-r_1 \leq v_t \leq r_1$ and $-r_2 \leq L_t \leq r_2$, for all t, or equivalently, $v_t^2 \leq r_1^2 =: R_1$ and $L_t^2 \leq r_2^2 =: R_2$, we introduce the penalty term $\int_0^T \beta_1(R_1 - v_u^2) + \beta_2(R_2 - L_u^2)du$, with the Lagrange multipliers $\beta_1, \beta_2 \geq 0$. The use of quadratic penalties such as the ones described here is also found in other classes of trading problems, such as hedging via risk minimization with constraints (see, for example, Lee (2008)).

Incorporating these three features, and utilizing Equation (5.1.5), we now write the com-

pensated PNL as

$$\widehat{\Pi}_T = \Pi_T + \int_0^T \left[\alpha v_u L_u + \beta_1(R_1 - v_u^2) + \beta_2(R_2 - L_u^2)\right] du + \bar{f}(x_T) \tag{5.1.6}$$

$$= \frac{\gamma}{2}\left(x_T^2 - x_0^2\right) + \bar{f}(x_T) + \int_0^T \sigma x_u dW_u \tag{5.1.7}$$

$$- \int_0^T h(v_u, L_u) m(L_u) dZ_u + \int_0^T g(x_u, v_u, L_u) du, \tag{5.1.8}$$

where we have defined

$$\begin{aligned} \bar{f}(x) =& -\beta x^2, \\ g(x, v, L) =& \ \mu x + \rho\sigma m(L) + \frac{\gamma}{2} m^2(L) + h(v, L)(v + L) \\ &+ \alpha v L + \beta_1(R_1 - v^2) + \beta_2(R_2 - L^2). \end{aligned} \tag{5.1.9}$$

The trader's objective is to maximize the expectation of the compensated PNL $\widehat{\Pi}_T$ in (5.1.8) by choosing trading rates for market and limit orders. This leads to the value function

$$V(t, x) := \sup_{(v_u, L_u)_{t \le u \le T}} \mathbb{E}\left[\bar{f}(x_T) + \frac{\gamma}{2} x_T^2 + \int_t^T g(x_u, L_u, v_u) du \,\middle|\, x_t = x\right] - \frac{\gamma}{2} x^2. \tag{5.1.10}$$

We will study the nonlinear HJB PDE problem associated with the stochastic control problem (5.1.10):

$$\begin{aligned} V_t + \sup_{v, L}\left[-(v + L)V_x + \frac{1}{2} m^2(L) V_{xx} + g(x, v, L)\right] = 0, \quad (t, x) \in [0, T) \times \mathbb{R}, \\ V(T, x) = \bar{f}(x) + \frac{\gamma}{2} x^2, \quad x \in \mathbb{R}, \end{aligned} \tag{5.1.11}$$

and solve for the value function V and the corresponding optimal trading strategies.

5.2 Affine Uncertainty of Limit Orders

We present here an analytic solution to the stochastic control problem (5.1.10) when the fill uncertainty function is affine in the limit order trading rate. In subsequent sections, we will analyze the special cases with constant uncertainty and linear uncertainty, and highlight their distinct features.

Following our model formulation, we now set the fill uncertainty and temporary price impact to be the affine functions:

$$m(L) = m_0 + m_1 L, \quad \text{and} \quad h(v, L) = -\eta_0 - \eta_1 v - \eta_2 L. \tag{5.2.1}$$

In this case, the HJB PDE problem in (5.1.11) becomes

$$V_t + \mu x + \frac{m_0^2}{2}(V_{xx} + \gamma) + \rho\sigma m_0 + \beta_1 R_1 + \beta_2 R_2 + \sup_{v,L} \left\{ J(t, x, v, L) \right\} = 0, \tag{5.2.2}$$

for all $(t, x) \in [0, T) \times \mathbb{R}$, with the terminal condition $V(T, x) = \left(\frac{\gamma}{2} - \beta\right) x^2$ for all $x \in \mathbb{R}$. Note that J in (5.2.2) is defined as

$$\begin{aligned} J(t, x, v, L) :&= -(v + L)V_x + \frac{1}{2}(m_0 + m_1 L)^2 V_{xx} + g(x, v, L) \\ &\quad - \mu x - \frac{m_0^2}{2}(V_{xx} + \gamma) - \rho\sigma m_0 - \beta_1 R_1 - \beta_2 R_2 \\ &= \left(-\eta_0 - V_x + m_0 m_1 (V_{xx} + \gamma) + \rho\sigma m_1\right) L + \left(-\eta_2 - \beta_2 + \frac{m_1^2}{2}(V_{xx} + \gamma) \right) L^2 \\ &\quad \left(-\eta_0 - V_x\right) v + \left(-\eta_1 - \beta_1\right) v^2 + \left(\alpha - \eta_1 - \eta_2\right) vL \end{aligned} \tag{5.2.3}$$

where $g(x, v, L)$ is defined in (5.1.9).

Proposition 5.2.1 *Under the affine uncertainty model, if the value function $V(t, x)$ satisfies the second-order condition:*

$$m_1^2 V_{xx}(t, x) < C - \gamma m_1^2, \qquad \forall (t, x), \tag{5.2.4}$$

where

$$C := \frac{4(\eta_1\eta_2 + \beta_1\beta_2 + \eta_1\beta_2 + \eta_2\beta_1) - (\eta_1 + \eta_2 - \alpha)^2}{2(\eta_1 + \beta_1)}, \tag{5.2.5}$$

then the optimal liquidation problem has finite optimum and there exist unique globally optimal controls (v^*, L^*).

Proof. The function J in (5.2.2) is a bivariate quadratic function in v and L, so the first-order conditions for the supremum in (5.2.2) are a pair of linear equations. To facilitate the presentation, we define

$$\psi(t,x) := m_1^2(V_{xx}(t,x) + \gamma), \tag{5.2.6}$$

$$\mathbf{A} := \begin{pmatrix} -2\eta_1 - 2\beta_1 & \alpha - (\eta_1 + \eta_2) \\ \alpha - (\eta_1 + \eta_2) & \psi(t,x) - 2\eta_2 - 2\beta_2 \end{pmatrix}. \tag{5.2.7}$$

where $\mathbf{A}$ is the Hessian matrix of J w.r.t. v and L and its dependence on t and x has been suppressed. Then the first-order conditions are

$$\mathbf{A}\begin{pmatrix} v \\ L \end{pmatrix} = \begin{pmatrix} V_x + \eta_0 \\ V_x + \eta_0 - m_0 m_1 \left(V_{xx}(t,x) + \gamma\right) - \rho\sigma m_1 \end{pmatrix}.$$

Furthermore, if $\mathbf{A}$ is *negative definite* for all (t,x), then the optimal execution problem has a finite solution uniquely determined by these first-order conditions.

To check the negative definiteness of the Hessian, we calculate its eigenvalues. The characteristic equation is

$$\det(\mathbf{A} - u\mathbf{I}) = (2\eta_1 + 2\beta_1 + u)(2\eta_2 + 2\beta_2 - \psi(t,x) + u) - (\eta_1 + \eta_2 - \alpha)^2 = 0. \tag{5.2.8}$$

The solutions correspond to the two eigenvalues, $u_\pm$, given by

$$u_\pm = -\eta_1 - \eta_2 - \beta_1 - \beta_2 + \frac{\psi(t,x)}{2} \pm \sqrt{\left(\frac{\psi(t,x)}{2} + \eta_1 - \eta_2 + \beta_1 - \beta_2\right)^2 + (\eta_1 + \eta_2 - \alpha)^2}. \tag{5.2.9}$$

For $u_+ < 0$, we must have

$$\psi(t,x) < \frac{4(\eta_1\eta_2 + \beta_1\beta_2 + \eta_1\beta_2 + \eta_2\beta_1) - (\eta_1 + \eta_2 - \alpha)^2}{2(\eta_1 + \beta_1)} =: C \tag{5.2.10}$$

for all (t,x), which is equivalent to condition (5.2.4). Next, since $u_- \leq u_+$, $u_+ < 0$ implies $u_- < 0$. As a result, if the controls v and L that solve the first-order conditions yield a solution V to the HJB equation such that (5.2.10) holds (or equivalently (5.2.4) after rearrangement), rearrangement, then the optimal liquidation problem has a finite optimum. Moreover, the first-order conditions have a unique solution. Therefore, there exist unique globally optimal controls. ■

Remark 5.2.1 *We will consider in Section 5.3 the special case with constant uncertainty ($m_1 = 0$). Then, condition* (5.2.4) *in Proposition 5.2.1 no longer depends on (t,x) and can be simplified as $C > 0$. In Section 5.3.1 we discuss the practical consequences of this condition. As we will derive the value function V explicitly, we can directly verify condition* (5.2.4).

Given the above proposition, we know there exist unique globally optimal controls under the condition (5.2.4). We proceed now to find those controls. For simplicity, we denote the determinant of A by $\Delta(t,x)$. This is given by:

$$\Delta(t,x) = (2\eta_1 + 2\beta_1)(2\eta_2 + 2\beta_2 - \psi(t,x)) - (\eta_1 + \eta_2 - \alpha)^2. \tag{5.2.11}$$

With this notation, the solutions to the first-order conditions are

$$\begin{aligned} v_t^* &= \frac{(m_1^2(V_{xx}+\gamma)+\eta_1-\eta_2-2\beta_2-\alpha)(V_x+\eta_0)-(\eta_1+\eta_2-\alpha)(m_0m_1(V_{xx}+\gamma)+\rho\sigma m_1)}{\Delta}, \\ L_t^* &= \frac{(\eta_2-\eta_1-\alpha-2\beta_1)(V_x+\eta_0)+2(\eta_1+\beta_1)(m_0m_1(V_{xx}+\gamma)+\rho\sigma m_1)}{\Delta}. \end{aligned} \tag{5.2.12}$$

Substituting (v^*, L^*) into the HJB equation, we arrive at the following nonlinear PDE:

$$\begin{aligned} 0 = V_t + \mu x + \frac{m_0^2}{2}(V_{xx}+\gamma) + \rho\sigma m_0 + \beta_1 R_1 + \beta_2 R_2 + \frac{(V_x+\eta_0)^2}{4(\eta_1+\beta_1)} \\ + \frac{2(\alpha+\beta_1+\beta_2)-C}{2\Delta}\left[V_x+\eta_0+\frac{(\eta_2-\eta_1-\alpha-2\beta_1)(m_0m_1(V_{xx}+\gamma)+\rho\sigma m_1)}{2(\alpha+\beta_1+\beta_2)-C}\right]^2, \end{aligned} \tag{5.2.13}$$

subject to the terminal condition $V(t,x) = \left(\frac{\gamma}{2}-\beta\right)x^2$.

The quadratic terminal condition suggests the ansatz $V(t,x) = a(t)x^2 + b(t)x + c(t)$. This ansatz will solve Equation (5.2.13) as long as the coefficient functions solve the following system of first-order ODEs:

$$\begin{aligned} 0 &= a'(t) + \frac{2(\alpha+\beta_1+\beta_2)-m_1^2(2a(t)+\gamma)}{(\eta_1+\beta_1)(C-m_1^2(2a(t)+\gamma))}\,a^2(t), && a(T) = \frac{\gamma}{2}-\beta, \\ 0 &= b'(t) + \mu + \frac{2(\alpha+\beta_1+\beta_2)-m_1^2(2a(t)+\gamma)}{(\eta_1+\beta_1)(C-m_1^2(2a(t)+\gamma))}a(t)(b(t)+\eta_0), \\ &\quad + \frac{(\eta_2-\eta_1-\alpha-2\beta_1)(m_0m_1(2a(t)+\gamma)+\rho\sigma m_0)}{(\eta_1+\beta_1)(C-m_1^2(2a(t)+\gamma))}a(t), && b(T) = 0, \\ 0 &= c'(t) + \frac{m_0^2}{2}(2a(t)+\gamma) + \rho\sigma m_0 + \beta_1 R_1 + \beta_2 R_2 \\ &\quad + \frac{2(\alpha+\beta_1+\beta_2)-m_1^2(2a(t)+\gamma)}{4(\eta_1+\beta_1)(C-m_1^2(2a(t)+\gamma))}(b(t)+\eta_0)^2 \\ &\quad + \frac{(\eta_2-\eta_1-\alpha-2\beta_1)(m_0m_1(2a(t)+\gamma)+\rho\sigma m_0)}{2(\eta_1+\beta_1)(C-m_1^2(2a(t)+\gamma))}(b(t)+\eta_0) \\ &\quad + \frac{(\eta_2-\eta_1-\alpha-2\beta_1)^2(m_0m_1(2a(t)+\gamma)+\rho\sigma m_0)^2}{8(\eta_1+\beta_1)(C-m_1^2(2a(t)+\gamma))(2(\alpha+\beta_1+\beta_2)-C)}, && c(T) = 0. \end{aligned} \tag{5.2.14}$$

These ODEs can be solved numerically successively. An analytic strategy would be to first solve for $a(t)$ by separation of variables. Then we can plug $a(t)$ into the ODE for $b(t)$. The resulting first-order linear inhomogeneous ODE is readily solved. In turn, given $a(t)$ and

$b(t)$, the third ODE is separable and solved directly by integration. In the next sections, we will solve these equations analytically or numerically to present the solutions and associated trading strategies.

Given that $V(t,x) = a(t)x^2 + b(t)x + c(t)$, we can now simplify the second-order condition (5.2.4) and express it in terms of $a(t)$ and model parameters:

$$2m_1^2 a(t) < C - \gamma m_1^2, \qquad \forall (t,x). \tag{5.2.15}$$

At this point, a satisfies an implicit equation, so it is not possible to simplify the condition further. Nevertheless, under constant uncertainty, it will simplify significantly as $m_1 = 0$. The linear uncertainty model will also allow for an analytical solution for $a(t)$.

5.2.1 Numerical Illustration

Before displaying the numerical implementation of our model, we discuss parameter choices. For this paper, we are thinking about trades that will be executed within a few hours at very high speeds. Therefore, it makes sense to consider *seconds* as the time interval and we use $T = 3,600$ seconds in all simulations. For the other parameters, we assume 6.5 trading hours per day and 252 trading days per year and select parameters of the same magnitude that Almgren and Chriss (2000) use:

$$\begin{aligned}
&S_0 = 40\,\$/\text{share}, && x_0 = 10,000\,\text{share},\\
&\sigma = 0.005\,(\$/\text{share})/\text{sec.}^{0.5}, && \mu = 10^{-6}\,(\$/\text{share})/\text{sec.},\\
&\gamma = 2.5 \cdot 10^{-7}\,\$/\text{share}^2, && \eta_0 = 0.05\,\$/\text{share},\\
&\eta_1 = 0.1\,(\$/\text{share})/(\text{share/sec.}), && \eta_2 = 0.08\,(\$/\text{share})/(\text{share/sec.}).
\end{aligned}$$

Note that converting with 6.5 trading hours per day and 252 trading days per year, we find that this value of σ and initial stock price correspond to approximately 30% annual volatility.

The value of μ corresponds to approximately 15% annual growth.

A small correlation value, $\rho = -0.2$, along with positive values of m_0 and m_1, are selected to include the adverse selection effect. The uncertainty parameters are chosen as $m_0 = p_0 x_0 T^{-0.5}$, and $m_1 = p_1\sqrt{T}$ for some (unitless) constants p_0 and p_1. If we want to compare the constant and linear uncertainty models then $p_0 = p_1$ correspond to similar coefficients on the Brownian motion driving x_t. This is because m_1 will multiply L_t, which will roughly be of order x_0/T. Under constant or linear uncertainty we set $p_0 = p_1 = 0.1$, whereas under affine uncertainty we choose $p_0 = p_1 = 0.05$ to split the uncertainty between the two components.

The terminal liquidation penalty will be $\beta = 10^{-3}\,\$/\text{share}^2$. For the speed limiter we choose $\beta_1 = 5\cdot 10^{-4}\,\$/(\text{share/sec.})^2$, and $\beta_2 = 10^{-4}\,\$/(\text{share/sec.})^2$. These are small penalties so they will not over-reduce the trade speed and they are of the same order as the terminal liquidation penalty. Finally, the trade director penalty is chosen as $\alpha = 0.15$. In a subsequent section, we will find an allowable interval for α. For the above parameter values, 0.15 is in the middle of the interval, just to the left of the center so it does not over-encourage high trade speeds. Throughout our numerical simulations, these will be the baseline parameters. We highlight the effects of each parameter by changing them from these baseline values in our numerical examples.

In Figure 5.1, we plot the trading rates for models with constant uncertainty, linear uncertainty, and zero uncertainty in the limit order fills. To ensure a fair comparison, the Brownian motions generating the asset dynamics and the uncertainty in position are the same across all simulations. Only the functional forms of the trading rates change. Note that both rates are positive for all three models. Furthermore, the strategies are primarily dominated by limit orders. This is preferred in practice because limit orders tend to be lower impact and lower cost. Indeed, that is the selected parameter choice. For the most part, over the life of the 1 hour sell program, the trading rates are almost constant when there is no uncertainty, and remain quite stable in the uncertainty cases. As we approach the execution

horizon the rates become more unstable: the algorithm reacts to small moves to capitalize on low cost opportunities to liquidate the asset.

Nevertheless, over the life of a trade, the linear uncertainty trading rates are typically more stable and lower than the constant uncertainty trading rates. To see this, notice that the linear uncertainty can be avoided by choosing $L_t = 0$, but this is not possible in the constant uncertainty case. In this sense, there is less uncertainty for a linear uncertainty model versus a constant uncertainty model. This helps explain the ordering of the trading rates. As the uncertainty diminishes to no uncertainty, the future is more predictable, so the trader does not need to resort to overtrading. Finally, note that the trading rates under linear and constant uncertainties tend to spike up significantly towards the end. The reason is that the non-liquidation penalty dominates all other costs, and thus, trading is sped up to achieve full liquidation. Again, even in this highly volatile period, linear uncertainty results in lower trading rates than constant uncertainty. Interestingly, it is observed that the market order rate exceeds the limit order rate for the first time near the end of the trading horizon under linear uncertainty. The same does not occur under constant uncertainty. This is because under linear uncertainty limit order fill uncertainty can be eliminated by avoiding placing such orders, and the trader who wants to achieve full liquidation turns to market orders, which do not have fill uncertainty.

Our method encourages non-negativity of trading rates, and the trader tends to maintain $v_t > 0$ and $L_t > 0$ for the majority of the sell-program. However, this need not be the case in general and trading rates have the potential to be negative. Later, in Section 5.3.2 we will show that non-negative trading rates can be guaranteed in special cases.

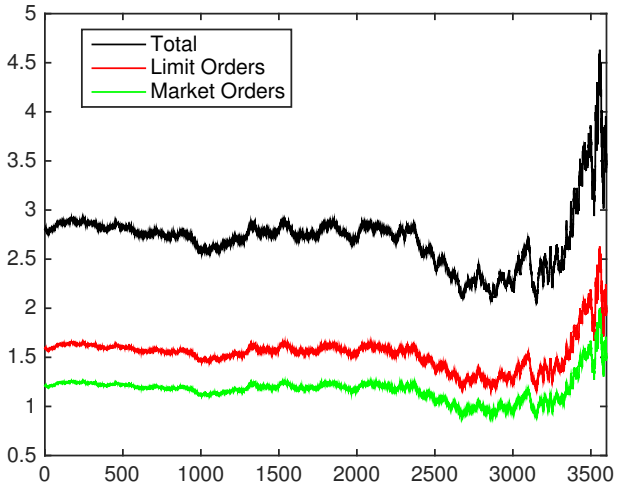

(a) (a) Constant Uncertainty

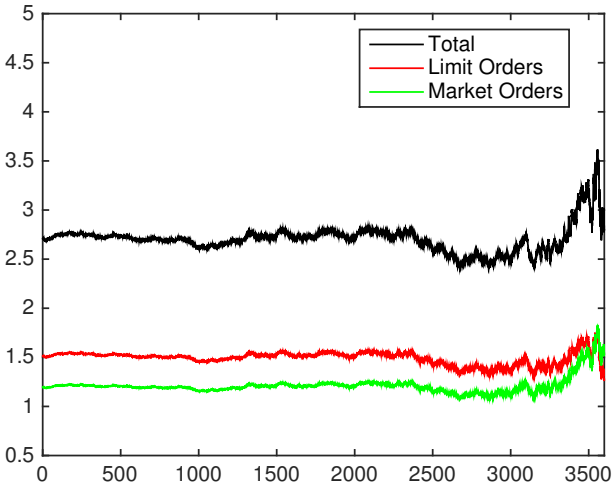

(b) (a) Linear Uncertainty

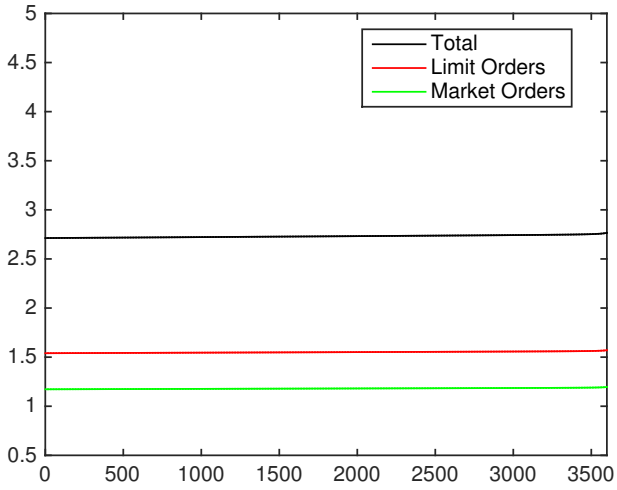

(c) (a) No Uncertainty

Figure 5.1: Sample paths of the optimal trading rates under (a) constant uncertainty ($m_0 = 16.\bar{6}$), (b) linear uncertainty ($m_1 = 6$), and (c) no uncertainty. Final positions are 217.25, 203.39, and 168.75 shares, respectively. The parameters are $x_0 = 10,000$, $T = 3,600$, $\beta = 10^{-3}$, $\eta_0 = 0.05$, $\gamma = 2.5 \cdot 10^{-7}$, $\alpha = 0.15$, $\beta_1 = 5 \cdot 10^{-4}$, $\beta_2 = 10^{-4}$, $\eta_1 = 0.1$, $\eta_2 = 0.08$, $\rho = -0.2$, $\mu = 10^{-6}$, and $\sigma = 0.005$. The x-axis marks the time in seconds, while the y-axis marks the trading rate in shares/sec.

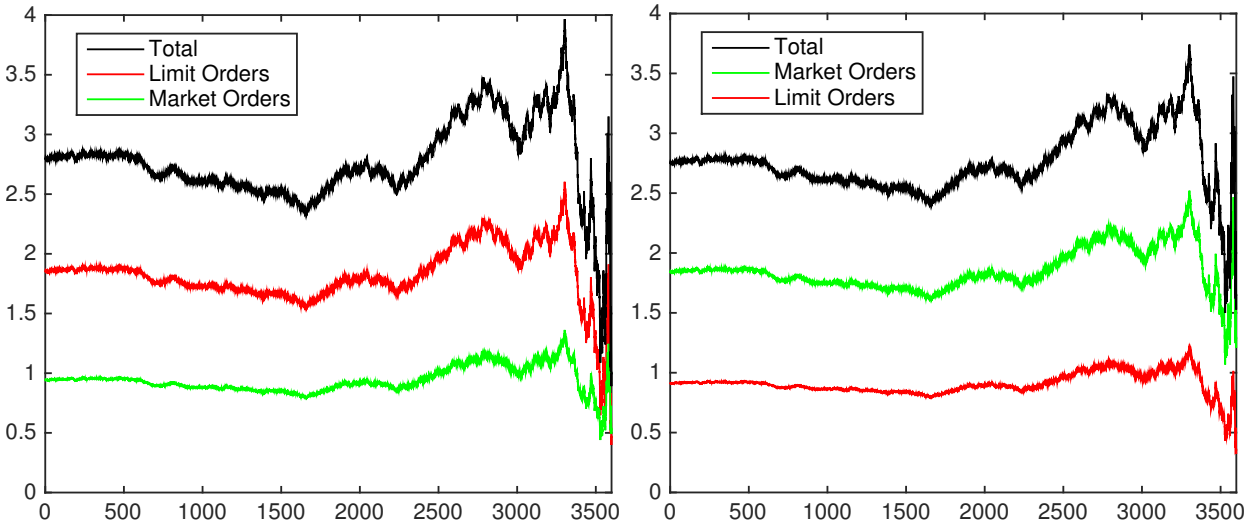

Figure 5.2: The optimal trading rates under one simulation with the following parameters: $x_0 = 10,000$, $T = 3,600$, $\beta = 10^{-3}$, $\eta_0 = 0.05$, $\gamma = 2.5 \cdot 10^{-7}$, $\alpha = 0.15$, $\beta_1 = 5 \cdot 10^{-4}$, $\beta_2 = 10^{-4}$, $\rho = -0.2$, $\mu = 10^{-6}$, $\sigma = 0.005$, $m_0 = 8.\overline{3}$ and $m_1 = 3$. On the left, $\eta_1 = 0.1$, and $\eta_2 = 0.05$, while on the right $\eta_1 = 0.05$, and $\eta_2 = 0.1$. Final positions are 68.5384, and 80.2371 shares, respectively. The x-axis marks the time in seconds, while the y-axis marks the trading rate in shares/sec.

Next, we look at the effect of market impact in Figure 5.2. We display the simulated trading rates based on different values of market impact coefficients (η_1, η_2). On the left panel, market orders have higher temporary market impact ($\eta_1 = 0.1$, and $\eta_2 = 0.05$), and on the right, limit orders have higher temporary market impact ($\eta_1 = 0.05$, and $\eta_2 = 0.1$). As seen in both scenarios, the trading rate is higher for the order type with the lower market impact cost. In practice, market orders are expected to have a higher market impact so $\eta_1 > \eta_2$ is the more realistic setting.

The sample path for stock holdings over time is shown in Figure 5.3. Our trading strategy appears to follow a time-weighted average price (TWAP) strategy. This is evident in the linear and decreasing path of holdings over time. A TWAP strategy seeks to trade constantly through time so that the average realized price is the time-weighted price over the execution period. A linear path of holdings indicates that the total trading rate is approximately constant. In contrast to TWAP, the optimal strategy appears to have a non-zero terminal target for x_T. A higher β leads the trader to sell more rapidly, and the position ends much

closer to zero. Furthermore, the position is generally decreasing, but we remark that even if $v_t > 0$, and $L_t > 0$, x_t may increase temporarily due to the Brownian motion movement. s

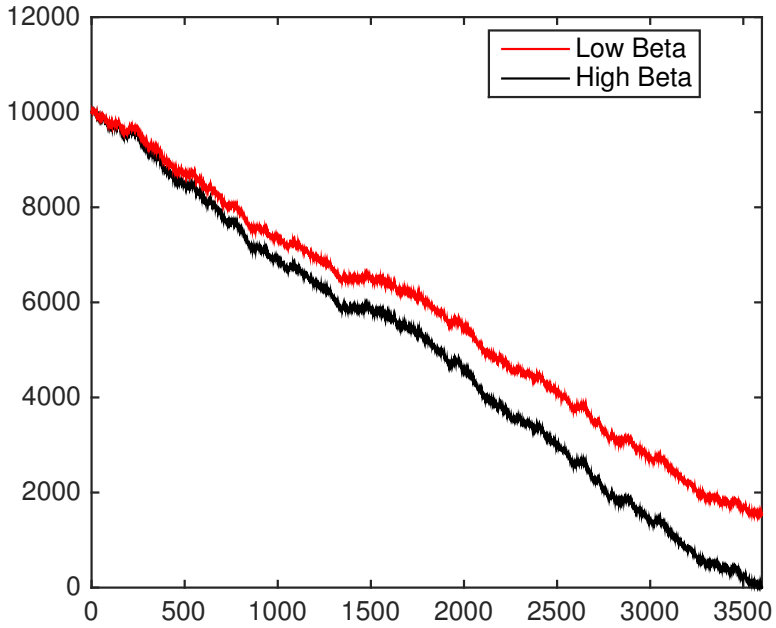

Figure 5.3: Sample path of stock holdings with different non-liquidation penalty. The parameters are: $x_0 = 10,000$, $T = 3,600$, $\eta_0 = 0.05$, $\gamma = 2.5 \cdot 10^{-7}$, $\alpha = 0.15$, $\beta_1 = 5 \cdot 10^{-4}$, $\beta_2 = 10^{-4}$, $\rho = -0.2$, $\mu = 10^{-6}$, $\sigma = 0.005$, $\eta_1 = 0.1$, $\eta_2 = 0.08$, $m_0 = 8.\bar{3}$ and $m_1 = 3$. The low value of β is 10^{-4} and the high value is 0.1. Final positions are 1546.0197 and 5.3967, respectively. The x-axis marks the time in seconds, while the y-axis marks the position size in shares.

5.3 Constant Uncertainty of Limit Orders

In this section, we discuss a number of properties of our model under constant uncertainty of limit orders fills. Recall that constant uncertainty means the total position, x_t is subject to uncertainty and it is not simply due to trading in limit orders. Since the risk in stock holdings cannot be avoided, the tradeoff in choosing market and limit orders is between explicit market impact costs and various implicit costs. The latter costs comprise of the trading penalties set by the trade director and speed limiter discussed in Section 5.1. Another way to view this section is that v_t could be a trading rate in one exchange, while L_t is a trading rate in another exchange. The two venues have different costs of trading in terms of market impact, and the total position is subject to risk, measured by constant uncertainty.

5.3.1 Trade Direction-Speed Trade-off

First, we must check the second-order condition in (5.2.4). Since we have $m_1 = 0$, so the inequality simplifies to $C > 0$, or equivalently

$$(\eta_1 + \eta_2 - \alpha)^2 - 4(\eta_1\eta_2 + \beta_1\beta_2 + \eta_1\beta_2 + \eta_2\beta_1) < 0. \tag{5.3.1}$$

Since η_1, and η_2 are exogenous parameters to be inferred from market data, condition (5.3.1) becomes a restriction on the Lagrange multipliers, α, β_1 and β_2. Suppose that we fix β_1 and β_2. Then the left-hand side of (5.3.1) is a convex quadratic function of α. Thus, there are 2 roots, and if α is between them, the optimal control problem has a finite solution given uniquely by the first-order conditions. This results in the admissible range for α:

$$\alpha \in \left(\eta_1 + \eta_2 - 2\sqrt{\eta_1\eta_2 + \beta_1\beta_2 + \eta_1\beta_2 + \eta_2\beta_1}, \eta_1 + \eta_2 + 2\sqrt{\eta_1\eta_2 + \beta_1\beta_2 + \eta_1\beta_2 + \eta_2\beta_1}\right). \tag{5.3.2}$$

This leads to our first trade-off. The trader director's Lagrange multiplier, α, ensures our order types go in the same direction. On the other hand, the Lagrange multipliers, β_1 and β_2, tend to reduce the values of v_t and L_t since high values are less preferable. However, increasing β_i widens the allowable interval for α. In particular, when $\beta_i = 0$, the interval is $\left(\eta_1 + \eta_2 - 2\sqrt{\eta_1\eta_2}, \eta_1 + \eta_2 + 2\sqrt{\eta_1\eta_2}\right)$. As the arithmetic mean of a set of numbers is greater than its geometric mean, the left endpoint is positive, which renders $\alpha = 0$ an invalid choice. However, if β_i is sufficiently large, then the interval may include $\alpha = 0$. This discussion reveals the interesting trade-off between over-reducing trade speed and correctly setting trade direction in choosing the endogenous parameters, α, β_1 and β_2. In summary, the trade director cannot be too strong or too weak unless the speed limiters are sufficiently severe.

5.3.2 Optimal Strategies

We now consider the associated trading strategies. First, we must solve the ODE system:

$$\begin{aligned}
0 &= a'(t) + \frac{2(\alpha+\beta_1+\beta_2)}{(\eta_1+\beta_1)C}a^2(t),\\
0 &= b'(t) + \mu + \frac{2(\alpha+\beta_1+\beta_2)}{(\eta_1+\beta_1)C}a(t)(b(t)+\eta_0) + \frac{(\eta_2-\eta_1-\alpha-2\beta_1)\rho\sigma m_0}{(\eta_1+\beta_1)C}a(t),\\
0 &= c'(t) + \frac{m_0^2}{2}(2a(t)+\gamma) + \rho\sigma m_0 + \beta_1 R_1 + \beta_2 R_2 + \frac{(\alpha+\beta_1+\beta_2)}{2(\eta_1+\beta_1)C}(b(t)+\eta_0)^2\\
&\quad + \frac{(\eta_2-\eta_1-\alpha-2\beta_1)\rho\sigma m_0}{2(\eta_1+\beta_1)C}(b(t)+\eta_0) + \frac{(\eta_2-\eta_1-\alpha-2\beta_1)^2\rho^2\sigma^2 m_0^2}{8(\eta_1+\beta_1)C(2(\alpha+\beta_1+\beta_2)-C)},
\end{aligned} \tag{5.3.3}$$

with terminal conditions $a(T) = \frac{\gamma}{2} - \beta$, $b(T) = c(T) = 0$. By separation of variables, we obtain the explicit solution for $a(t)$:

$$a(t) = -\frac{(\eta_1+\beta_1)(2\beta-\gamma)C}{2(\alpha+\beta_1+\beta_2)(2\beta-\gamma)(T-t)+2(\eta_1+\beta_1)C}.$$

The function $a(t)$ is well defined everywhere except for

$$t = T + \frac{(\eta_1+\beta_1)C}{(\alpha+\beta_1+\beta_2)(2\beta-\gamma)} =: T_{crit}. \tag{5.3.4}$$

Suppose that we choose β to be large in order to penalize non-liquidation, and specifically let us consider $\beta > \frac{\gamma}{2}$. Then, the second term in (5.3.4) is positive, and T_{crit} is never reached as it is beyond the execution horizon, T, of the sell program. With this definition, $a(t)$ simplifies to

$$a(t) = -\frac{(\eta_1+\beta_1)C}{2(\alpha+\beta_1+\beta_2)(T_{crit}-t)}.$$

Since, $t \in [0,T] \subsetneq [0,T_{crit}]$, we conclude $a(t) < 0$ for $t \in [0,T]$, which implies that $V_{xx}(t,x) < 0$ for all $(t,x) \in [0,T]\times\mathbb{R}$.

To solve for $b(t)$, we divide the second ODE by $a(t)$, and rearrange to get

$$\frac{b'(t)}{a(t)} + \frac{2(\alpha+\beta_1+\beta_2)}{(\eta_1+\beta_1)C}(b(t)+\eta_0) = -\frac{\mu}{a(t)} - \frac{(\eta_2-\eta_1-\alpha-2\beta_1)\rho\sigma m_0}{(\eta_1+\beta_1)C}. \tag{5.3.5}$$

By using the product rule followed by the ODE for $a(t)$, we have the following identity:

$$\frac{d}{dt}\left[\frac{b(t)+\eta_0}{a(t)}\right] = \frac{b'(t)}{a(t)} - \frac{(b(t)+\eta_0)\,a'(t)}{a^2(t)} = \frac{b'(t)}{a(t)} + \frac{2(\alpha+\beta_1+\beta_2)}{(\eta_1+\beta_1)C}(b(t)+\eta_0). \tag{5.3.6}$$

Define

$$b_0(t) := \frac{(\alpha+\beta_1+\beta_2)\mu}{(\eta_1+\beta_1)C}\left[(T_{crit}-t)^2 - (T_{crit}-T)^2\right] - \frac{(\eta_2-\eta_1-\alpha-2\beta_1)\rho\sigma m_0(T-t)}{(\eta_1+\beta_1)C}$$

to be the integral of the right-hand side function in (5.3.5) from t to T. Then, $b(t)$ is explicitly solved as follows:

$$\begin{aligned}\frac{d}{dt}\left[\frac{b(t)+\eta_0}{a(t)}\right] &= -\frac{\mu}{a(t)} - \frac{(\eta_2-\eta_1-\alpha-2\beta_1)\rho\sigma m_0}{(\eta_1+\beta_1)C} \\ \implies\quad b(t) &= -\eta_0 - a(t)\left[\frac{2\eta_0}{2\beta-\gamma} + b_0(t)\right].\end{aligned}$$

Finally, $c(t)$ can be computed via direct integration. As the integral is rather complicated and we will not need its closed-form expression, we omit it. Direct computation shows that the optimal trading rates are

$$v_t^* = \frac{(\eta_1-\eta_2-2\beta_2-\alpha)(2a(t)x_t + b(t)+\eta_0)}{2(\eta_1+\beta_1)C}, \tag{5.3.7}$$

$$L_t^* = \frac{(\eta_2-\eta_1-\alpha-2\beta_1)(2a(t)x_t + b(t)+\eta_0)}{2(\eta_1+\beta_1)C}. \tag{5.3.8}$$

Notice that the optimal trading strategies are both affine in x_t at any time t. We will study the sign of the trading rates in the next section.

5.3.3 Buy-Sell Boundary

In this section, we describe the properties that guarantee non-negativity of the trading rates for constant uncertainty. Naturally, the optimal trading rates should be non-negative because this means trading strategies do not go against the overall sell program. At the very least,

if one order rate is non-positive, the other should be non-positive to avoid simultaneous buy and sell orders.

For simplicity, let us assume $\eta_1 = \eta_2 \equiv \eta$.[1] Then the optimal trading rates are

$$v_t^* = \frac{(-2\beta_2 - \alpha)\,(2a(t)x_t + b(t) + \eta_0)}{2(\eta + \beta_1)C}, \tag{5.3.9}$$

$$L_t^* = \frac{(-2\beta_1 - \alpha)\,(2a(t)x_t + b(t) + \eta_0)}{2(\eta + \beta_1)C}. \tag{5.3.10}$$

It follows that $v_t^*, L_t^* > 0$ if and only if $2a(t)x_t + b(t) + \eta_0 < 0$, or equivalently

$$2a(t)x_t - a(t)\left[\frac{2\eta_0}{2\beta - \gamma} + b_0(t)\right] < 0.$$

Since $a(t) < 0$ for all t, this gives the lower bound as a time deterministic function, above which the optimal strategy derived in (5.3.9) and (5.3.10) simultaneously places sell orders, and below which the optimal order strategy simultaneously places buy orders. Explicitly, the condition is

$$x_t > \frac{(T_{crit} - t)^2(\alpha + \beta_1 + \beta_2)\mu}{2(\eta + \beta_1)C} - \frac{(T_{crit} - T)^2(\alpha + \beta_1 + \beta_2)\mu}{2(\eta + \beta_1)C} + \frac{(\alpha + 2\beta_1)\rho\sigma m_0(T - t)}{2(\eta + \beta_1)C} + \frac{\eta_0}{2\beta - \gamma}.$$

We call this lower boundary on the right-hand side the *buy-sell boundary*, and denote it by $P(t)$.

Example 5.3.1 *Before discussing the general properties of the buy-sell boundary, we will consider a special case. Often in practice, μ is assumed to be 0 as it is unknown. Furthermore, setting $\eta_0 = 0$, the buy-sell boundary becomes*

$$P(t) = \frac{(\alpha + 2\beta_1)\rho\sigma m_0(T - t)}{2(\eta + \beta_1)C}, \quad t \in [0, T].$$

[1] The results in this section still hold if $\eta_1 - \eta_2 < 2\beta_2 + \alpha$ and $\eta_2 - \eta_1 < 2\beta_1 + \alpha$. So even if $\eta_1 \neq \eta_2$, then one of these conditions certainly holds (because $\beta_1, \beta_2, \alpha > 0$ and we either have $\eta_1 < \eta_2$ or $\eta_2 < \eta_1$.) and the other holds if $|\eta_1 - \eta_2|$ is small relative to the Lagrange multipliers.

With the adverse selection condition $\rho m_0 < 0$, $P(t)$ is negative $\forall\, t \in [0, T)$ and increases to the value 0 at $t = T$. Thus, the algorithm continues to sell even if the position becomes short and will only buy if the position becomes substantially negative.

The boundary is a quadratic[2] function of time and is convex (resp. concave) if $\mu > 0$ (resp. $\mu < 0$). The intuition is that when the position size is sufficiently low, the trader need not worry about non-liquidation as she has plenty of time to fully liquidate.

To understand its shape properties further, we compute the first derivative of P:

$$P'(t) = -\frac{(T_{crit} - t)(\alpha + \beta_1 + \beta_2)\mu}{(\eta + \beta_1)C} - \frac{(\alpha + 2\beta_1)\rho\sigma m_0}{2(\eta + \beta_1)C}.$$

Generally, we expect $P(t)$ to be a non-increasing function of time. To understand when this is the case, let us fix ideas and assume $\mu > 0$. Then, $P(t)$ is non-increasing for

$$t \leq T_{crit} + \frac{(\alpha + 2\beta_1)\rho\sigma m_0}{2(\alpha + \beta_1 + \beta_2)\mu} \tag{5.3.11}$$

$$= T + \frac{(\alpha + 2\beta_1)\rho\sigma m_0(2\beta - \gamma) + 2(\eta + \beta_1)C\mu}{2\mu(\alpha + \beta_1 + \beta_2)(2\beta - \gamma)}. \tag{5.3.12}$$

If there is no adverse selection effect, then $\rho m_0 \geq 0$, and the second term is positive, so P is non-increasing for all $t \in [0, T]$. However, if there is adverse selection, then $\rho m_0 < 0$, and it is possible that the second term is negative. However as long as

$$|\rho| \leq \left| \frac{2(\eta + \beta_1)C\mu}{(\alpha + 2\beta_1)\sigma(2\beta - \gamma)m_0} \right|,$$

then the second term is non-negative and $P(t)$ is non-increasing for all t. In contrast, to

[2]The boundary is quadratic as long as $\mu \neq 0$. Otherwise, $P(t)$ is linear increasing (resp. decreasing) if $\rho m_0 < 0$ (resp. > 0). For constant uncertainty, $\rho m_0 < 0$ gives us the desired adverse selection effect as discussed. See Example 5.3.1 for more details.

require P to be non-decreasing for all t means reversing the inequality (5.3.11), that is,

$$t \geq T_{crit} + \frac{(\alpha + 2\beta_1)\rho\sigma m_0}{2(\alpha + \beta_1 + \beta_1)\mu} \tag{5.3.13}$$

$$= T + \frac{(\alpha + 2\beta_1)\rho\sigma m_0(2\beta - \gamma) + 2(\eta + \beta_1)C\mu}{2\mu(\alpha + \beta_1 + \beta_2)(2\beta - \gamma)}. \tag{5.3.14}$$

In order to ensure that $P(t)$ be non-decreasing for all t, we bound the right-hand side of (5.3.14) from above by 0 and rearrange the inequality to obtain

$$|\rho| \geq \left| \frac{2(\eta + \beta_1)C\mu + 2T\mu(\alpha + \beta_1 + \beta_2)(2\beta - \gamma)}{(\alpha + 2\beta_1)\sigma(2\beta - \gamma)m_0} \right|.$$

In Figure 5.4, we display the buy-sell boundary for different parameter values. As β governs aversion to non-liquidation, we analyze the effect of increasing β on the boundary. In the left panel, we find that the choice of $\rho = -0.2$ from before leads to a generally increasing P. As the more intuitive case was a generally decreasing boundary, we also plot this pair of boundaries for ρ close to zero.[3]

We expect that a larger β will induce the trader to place sell orders more often than with a smaller β. Placing buy orders takes us further from liquidation so the boundary is expected to shift downward. Indeed this can be seen in both panels of Figure 5.4. As the whole buy-sell boundary shifts downward, there will of course be a decrease in the terminal value $P(T)$, which can be viewed as the *target* the algorithm has for stock holdings at time T. In fact, we have

$$P(T) = \frac{\eta_0}{2\beta - \gamma}. \tag{5.3.15}$$

We can see directly that if the non-liquidation penalty coefficient β increases, the target $P(T)$ approaches 0. This is consistent with our discussion following Figure 5.3.

[3]To have the adverse selection effect, we need ρ to be smaller in absolute value.

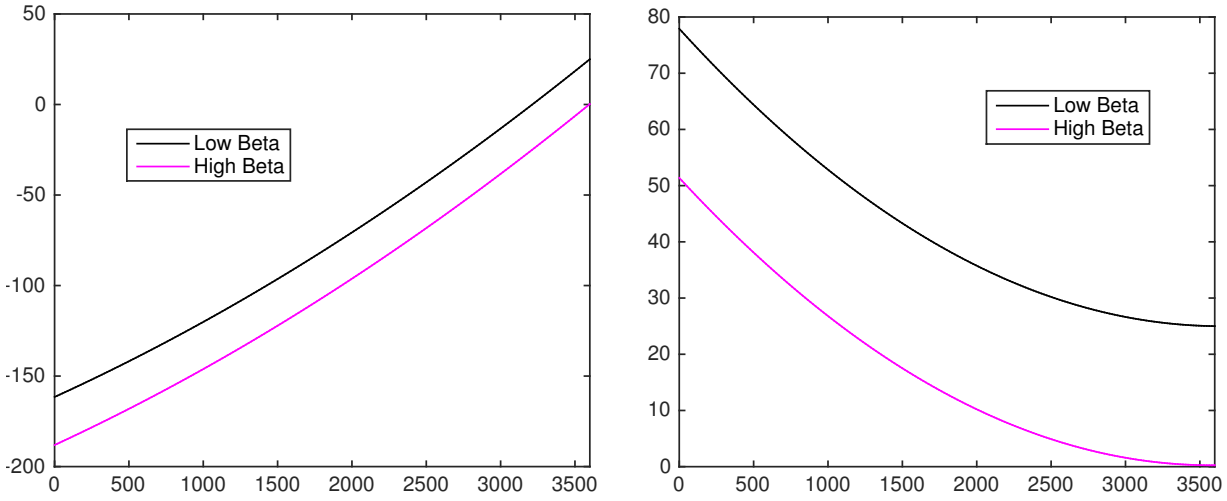

Figure 5.4: Buy-sell boundaries over time when $T = 3,600$, $\beta_1 = 5 \cdot 10^{-4}$ $\beta_2 = 10^{-4}$, $\eta_0 = 0.05$, $\gamma = 2.5 \cdot 10^{-7}$, $\eta_1 = \eta_2 = 0.1$, $\mu = 10^{-6}$, $\sigma = 5 \cdot 10^{-3}$ and $m_0 = 16.\bar{6}$. On the left the boundary is increasing ($\rho = -0.2$), while on the right, it is decreasing ($\rho = -0.0005$). We vary β in each figure. The low β is equal to 10^{-3} while the high β is 0.1. The x-axis marks the time in seconds, while the y-axis marks the position size in shares.

5.4 Linear Uncertainty of Limit Orders

In this section, we consider the case of linear uncertainty of limit orders. This amounts to taking $m_0 = 0$ in the affine uncertainty model. We discuss a number of properties of the solution and optimal strategies.

5.4.1 Liquidation Penalty and Trading Horizon Trade-off

We begin by writing down the condition for optimality as well as the ODEs for a, b and c that characterize the solution to the optimal execution problem. Recall the second-order condition: $V_{xx}(t,x) < \frac{C}{m_1^2} - \gamma$. From the quadratic ansatz, V_{xx} is independent of x, so the condition depends only on time. Thus, we find that upon solving the ODE for $a(t)$ numerically or otherwise, we must check that

$$\sup_{0 \le t \le T} a(t) < \frac{C}{2m_1^2} - \frac{\gamma}{2},$$

for the particular set of problem parameters.

To that end, let us look at the ODEs for a, b and c. In this case, they solve the system:

$$\begin{aligned}
0 &= a'(t) + \frac{2(\alpha+\beta_1+\beta_2) - m_1^2(2a(t)+\gamma)}{(\eta_1+\beta_1)(C - m_1^2(2a(t)+\gamma))}a^2(t), \\
0 &= b'(t) + \mu + \frac{2(\alpha+\beta_1+\beta_2) - m_1^2(2a(t)+\gamma)}{(\eta_1+\beta_1)(C - m_1^2(2a(t)+\gamma))}a(t)(b(t)+\eta_0) \\
0 &= c'(t) + \beta_1 R_1 + \beta_2 R_2 + \frac{2(\alpha+\beta_1+\beta_2) - m_1^2(2a(t)+\gamma)}{4(\eta_1+\beta_1)(C - m_1^2(2a(t)+\gamma))}(b(t)+\eta_0)^2.
\end{aligned} \tag{5.4.1}$$

An implicit equation is available for $a(t)$. However, it is much more enlightening to have an explicit solution. One condition that allows for an explicit solution is

$$2(\alpha+\beta_1+\beta_2) = C. \tag{5.4.2}$$

Although this may seem arbitrary, there are 3 exogenous Lagrange multipliers we can choose freely so it is not too hard to impose this condition. With this restriction, we simplify the equation for $a(t)$ to

$$0 = a'(t) + \frac{a^2(t)}{\eta_1+\beta_1}, \tag{5.4.3}$$

with the terminal condition $a(T) = \frac{\gamma}{2} - \beta$. This leads to the explicit solution

$$a(t) = -\frac{(\eta_1+\beta_1)(2\beta-\gamma)}{2(\eta_1+\beta_1) + (T-t)(2\beta-\gamma)}. \tag{5.4.4}$$

Next, we solve for $b(t)$. Divide equation for $b(t)$ by $a(t)$ (again valid since $a(t) < 0 \,\forall\, t$) and rearrange, we have

$$-\frac{\mu}{a(t)} = \frac{b'(t)}{a(t)} + \frac{b(t)+\eta_0}{\eta_1+\beta_1}. \tag{5.4.5}$$

Plugging in the expression of $a(t)$ from (5.4.4) and recalling (5.3.6), we arrive at

$$\begin{aligned}
\frac{d}{dt}\left[\frac{b(t)+\eta_0}{a(t)}\right] &= \frac{2\mu}{2\beta-\gamma} + \frac{\mu(T-t)}{\eta_1+\beta_1} \\
\implies b(t) &= -\eta_0 - a(t)\left[\frac{2\eta_0}{2\beta-\gamma} + \frac{2\mu(T-t)}{2\beta-\gamma} + \frac{\mu(T-t)^2}{2(\eta_1+\beta_1)}\right].
\end{aligned} \tag{5.4.6}$$

With this, $c(t)$ can be computed by direct integration of the associated ODE. The solution is not useful in our analysis however.

Using (5.4.4), we can express condition (5.2.4) that ensures the finiteness of the value function as

$$-\frac{(\eta_1+\beta_1)(2\beta-\gamma)}{2(\eta_1+\beta_1)+T(2\beta-\gamma)} < \frac{C-\gamma m_1^2}{2m_1^2}. \tag{5.4.7}$$

Again, we assume $2\beta > \gamma$. If $C \geq \gamma m_1^2$, the left-hand side of (5.4.7) is negative, while the right-hand side is non-negative so the condition holds. If on the other hand, $C < \gamma m_1^2$, we must have

$$T < \frac{4m_1^2(\eta_1+\beta_1)(\beta-\gamma)+2(\eta_1+\beta_1)C}{(\gamma m_1^2-C)(2\beta-\gamma)} := T_{max}. \tag{5.4.8}$$

In other words, we have translated condition (5.2.4) into an upper bound on the horizon T. This means that there is a finite maximum trading horizon in order for the value function to be finite.

Given a fixed $T > 0$, we can turn condition (5.4.8) to a lower bound on β, that is,

$$\beta > \gamma - \frac{C}{2m_1^2} > \frac{\gamma}{2}. \tag{5.4.9}$$

In fact, condition (5.4.9) is more stringent than the original condition: $\beta > \gamma/2$.

Also, the maximum horizon T_{max} is increasing in β, namely,

$$\frac{\partial T_{max}}{\partial \beta} = \frac{\partial}{\partial \beta}\left[\frac{4m_1^2(\eta_1+\beta_1)(\beta-\gamma)+2(\eta_1+\beta_1)C}{(\gamma m_1^2-C)(2\beta-\gamma)}\right] = \frac{4(\eta_1+\beta_1)}{(2\beta-\gamma)^2} > 0.$$

This reveals that a higher non-liquidation penalty coefficient β permits a longer admissible trading horizon $T_{\max}$ because the trader is sufficiently motivated to achieve full liquidation, rather than trading for profits. Nevertheless, there is a finite limit for the maximum horizon. Indeed, as $\beta \to \infty$, $T_{max} \to 2m_1^2(\eta_1+\beta_1)/(\gamma m_1^2 - C)$.

Let us consider the trade-off differently by imposing a condition on β. Starting from

Equation (5.4.7), we obtain

$$-\left[\eta_1+\beta_1+\frac{C-\gamma m_1^2}{2m_1^2}T\right]\left(\beta-\frac{\gamma}{2}\right)<\frac{C-\gamma m_1^2}{2m_1^2}(\eta_1+\beta_1).$$

The coefficient of $\beta-\frac{\gamma}{2}$ must be positive. If it were non-positive then the fact that both $\eta_1>0$ and $\beta_1>0$ implies $C<\gamma m_1^2$ (it must be strict for otherwise, the coefficient would be positive) and so the right-hand side of the inequality is negative. However, the left-hand side would then be non-negative after accounting for the negative sign, so the condition cannot hold if this coefficient is non-positive. It follows that we can rewrite condition (5.4.7) as

$$\beta>\frac{\gamma}{2}-\frac{(C-\gamma m_1^2)(\eta_1+\beta_1)}{2m_1^2(\eta_1+\beta_1)+(C-\gamma m_1^2)T}.$$

Our discussion above demonstrates that the denominator of the second term is positive does not necessarily require $C\geq\gamma m_1^2$ (the difference can be negative, just not *too* negative), so this is not a trivial condition.[4] Putting this together with the previous restriction on β, we have

$$\beta>\frac{\gamma}{2}+\left[\frac{(\gamma m_1^2-C)(\eta_1+\beta_1)}{2m_1^2(\eta_1+\beta_1)+(C-\gamma m_1^2)T}\right]^+.$$

From this condition, we see that the trader must be imposed with a sufficiently high non-liquidation penalty. If not, she will spend time profiting from other opportunities over the trading horizon and by time $t=T$, she need not liquidate the asset fully. In particular, she will follow a strategy that exploits profits in the model far in excess of her costs for non-liquidation. Mathematically, this condition on β guarantees the finiteness of the value function for the optimal liquidation problem.

[4] In other words, if $C\geq\gamma m_1^2$, then (accounting for the negative sign), the lower bound is strictly less than $\frac{\gamma}{2}$. We already require that $\beta>\frac{\gamma}{2}$, so in this case the extra condition is trivial.

5.4.2 Infinite Uncertainty Limit

In the case of linear uncertainty, it is possible to set $L_t = 0$ and ignore the limit order fill uncertainty. Conversely, a large linear uncertainty should promote little to no limit orders. Intuitively, if limit orders have infinite uncertainty to fill, then we expect that they will not be utilized. To demonstrate this, we begin by taking the limit as $m_1 \to \infty$ in Equation (5.2.14) with $m_0 = 0$.[5] For simplicity, we also take $\mu = 0$. The limiting ODE system becomes

$$\begin{aligned} 0 &= a'(t) + \frac{a^2(t)}{\eta_1 + \beta_1}, \\ 0 &= b'(t) + \frac{a(t)(b(t) + \eta_0)}{\eta_1 + \beta_1}, \\ 0 &= c'(t) + \beta_1 R_1 + \beta_2 R_2 + \frac{(b(t) + \eta_0)^2}{4(\eta_1 + \beta_1)}, \end{aligned} \tag{5.4.10}$$

with the terminal conditions $a(T) = \frac{\gamma}{2} - \beta$, $b(T) = 0$, $c(T) = 0$.[6] We have previously solved the ODE for $a(t)$ in Section 5.4.1. Therefore, the optimality condition regarding the supremum of $a(t)$ is the same and since $m_1 \to \infty$, we can never have $C \geq \gamma m_1^2$. Thus, there is a condition on T that it must be less than T_{max}, when $m_1 \to \infty$. This limit indicates

$$T < \frac{4(\eta_1 + \beta_1)(\beta - \gamma)}{\gamma(2\beta - \gamma)}. \tag{5.4.11}$$

We can put this in terms of a lower bound on the non-liquidation penalty:

$$\beta > \frac{\gamma}{2} + \left[\frac{\gamma(\eta_1 + \beta_1)}{2(\eta_1 + \beta_1) - \gamma T}\right]^+.$$

[5] The ODE is different for c if $m_0 \neq 0$, but everything else that follows in this section still holds for a and b.

[6] As the solution to an ODE is effectively an integral, we are interchanging limit and integral and must justify the switch. The implicit solution to the ODE for $a(t)$ is $-K_1 \ln|z_1 - a(T)| + K_1 \ln|z_1 - a(t)| + K_2 \ln|a(T)| - K_2 \ln|a(t)| - \frac{K_3}{a(T)} + \frac{K_3}{a(t)} = -z_3(T-t)$, where $K_1 = K_2 = \frac{z_2 - z_1}{z_1^2}$, $K_3 = \frac{z_2}{z_1}$, $z_1 = \frac{2(\alpha + \beta_1 + \beta_2) - \gamma m_1^2}{2m_1^2}$, $z_2 = \frac{C - \gamma m_1^2}{2m_1^2}$, and $z_3 = \frac{1}{\eta_1 + \beta_1}$. The limiting solution as $m_1 \to \infty$ is exactly the solution to the above ODE for a. The closed form solution for b is $b(t) = -\eta_0 + a(t)\left[\int_t^T \frac{\mu}{a(s)} ds - \frac{2\eta_0}{2\beta - \gamma}\right]$. If $\mu = 0$, then we can take the limit and get the solution for $b(t)$ from the last section when $\mu = 0$ and $m_1 \to \infty$.

Assuming the optimality condition holds, then the solution we have generated from the first order conditions is the unique optimizer for the stochastic control problem. Note that implicitly, β must be greater than γ now for the right-hand side bound to even be positive.

Next we consider the trading rates. Looking at Equation (5.2.12), we let $m_1 \to \infty$. When we do that, $L_t^* \to 0$, while

$$v_t^* \to -\frac{1}{2}\left(\frac{V_x + \eta_0}{\eta_1 + \beta_1}\right) = \left(x_t - \frac{\eta_0}{\eta_1 + \beta_1}\right) \frac{2\beta - \gamma}{2\left(\eta_1 + \beta_1\right) + \left(T - t\right)\left(2\beta - \gamma\right)}. \tag{5.4.12}$$

So in the infinite uncertainty case, the strategy is to place *only* market orders.[7] Interestingly, the infinite uncertainty limit is exactly that of Cheng et al. (2017) in the constant uncertainty case (recall before that this did not depend on m_0.) When $\eta_0 = 0$ and $\beta_1 = 0$, we get the optimal trading rate derived in the appendix of that paper.

5.5 Schedule Following

In this section, we incorporate a parent order schedule into the order placement problem. The trader has both market and limit orders at her disposal and is now given a time-deterministic schedule function, $Q(t)$ defined over the trading horizon $[0, T]$. We assume that $Q(t)$ is a non-negative, non-increasing, bounded continuous function of time, with an initial value $Q(0) = x_0$. The trader seeks to track $Q(t)$ as closely as possible. Specifically, we would like to keep the stochastic number of shares that we hold at time t, x_t close to $Q(t)$ for all times $t \in [0, T]$ and not only at the terminal time T. To avoid having conflicting goals, we set $Q(T) = 0$ to have a schedule for full liquidation.

In order to keep x_t close to $Q(t)$, we consider a penalty of the form $\int_0^T \lambda\left(u, x_u - Q(u)\right) du$, where $\lambda(t, y)$ is a function with global maximum of 0 at $y = 0$, $\forall\, t \in [0, T]$. Since $\lambda(t, y)$ has a global max of 0 at 0, the optimizer should choose order types in such a way as to keep $x_t - Q(t)$ close to or equal to 0. Furthermore, the penalty term accumulates deviations

[7] It is worth noting that the trading rate is non-negative as long as $x_t > \frac{\eta_0}{\eta_1 + \beta_1}$.

at all times $t \in [0,T]$ and may even place more emphasis on certain times due to its time argument. For example, $\lambda(t,y)$ could be increasing in t for all y then deviations early on are allowed, but as we approach the terminal time, the scheduler shall be forced to push x_t closer to $Q(t)$. Henceforth, we let $\lambda(t,y) = -w(t)y^2$ so that deviations from above/below are penalized equally, and in just the same manner as the terminal penalty. We assume that $w(t)$ is a non-negative and continous function of time. Moreover, we assume that $w(t)$ is bounded over the interval $[0,T]$.

Now we will maximize the sum of expected compensated PNL as defined previously together with expected accumulated deviations. The value function is

$$V(t,x) := \sup_{(v_t,L_t)_{0\le t\le T}} \mathbb{E}\left[\bar{f}(x) + \frac{\gamma}{2}x_T^2 + \int_t^T \left[g(x_u,L_u,v_u) + \lambda(u,x_u - Q(u))\right] du \middle| x_t = x\right] - \frac{\gamma}{2}x^2. \tag{5.5.1}$$

We then conclude that V satisfies the following nonlinear HJB PDE problem:

$$V_t + \sup_{v,L}\left[-(v+L)V_x + \frac{1}{2}m^2(L)V_{xx} + g(x,v,L)\right] + \lambda(t,x-Q(t)) = 0, \quad (t,x) \in [0,T)\times\mathbb{R},$$
$$V(T,x) = \bar{f}(x) + \frac{\gamma}{2}x^2, \quad x \in \mathbb{R}. \tag{5.5.2}$$

Like in previous sections, one can perform the same optimization to derive the optimal trading rates v^* and L^*, and the value function will be of the same quadratic form: $V(t,x) = a(t)x^2 + b(t)x + c(t)$. However, the inhomogeneous term $\lambda(t,x-Q(t))$ will affect the solutions

of resulting ODEs. Specifically, we have the ODE system:

$$
\begin{aligned}
0 &= a'(t) + \frac{2(\alpha+\beta_1+\beta_2) - m_1^2(2a(t)+\gamma)}{(\eta_1+\beta_1)(C - m_1^2(2a(t)+\gamma))}a^2(t) - w(t), \\
0 &= b'(t) + \mu + \frac{2(\alpha+\beta_1+\beta_2) - m_1^2(2a(t)+\gamma)}{(\eta_1+\beta_1)(C - m_1^2(2a(t)+\gamma))}a(t)(b(t)+\eta_0) \\
&\quad + \frac{(\eta_2-\eta_1-\alpha-2\beta_1)(m_0m_1(2a(t)+\gamma)+\rho\sigma m_0)}{(\eta_1+\beta_1)(C - m_1^2(2a(t)+\gamma))}a(t) + 2w(t)Q(t), \\
0 &= c'(t) + \frac{m_0^2}{2}(2a(t)+\gamma) + \rho\sigma m_0 + \beta_1 R_1 + \beta_2 R_2 + \frac{2(\alpha+\beta_1+\beta_2) - m_1^2(2a(t)+\gamma)}{4(\eta_1+\beta_1)(C - m_1^2(2a(t)+\gamma))}(b(t)+\eta_0)^2 \\
&\quad + \frac{(\eta_2-\eta_1-\alpha-2\beta_1)(m_0m_1(2a(t)+\gamma)+\rho\sigma m_0)}{2(\eta_1+\beta_1)(C - m_1^2(2a(t)+\gamma))}(b(t)+\eta_0) \\
&\quad + \frac{(\eta_2-\eta_1-\alpha-2\beta_1)^2(m_0m_1(2a(t)+\gamma)+\rho\sigma m_0)^2}{8(\eta_1+\beta_1)(C - m_1^2(2a(t)+\gamma))(2(\alpha+\beta_1+\beta_2) - C)} - w(t)Q(t)^2
\end{aligned}
\tag{5.5.3}
$$

with terminal conditions $a(T) = \frac{\gamma}{2} - \beta$, $b(T) = c(T) = 0$.

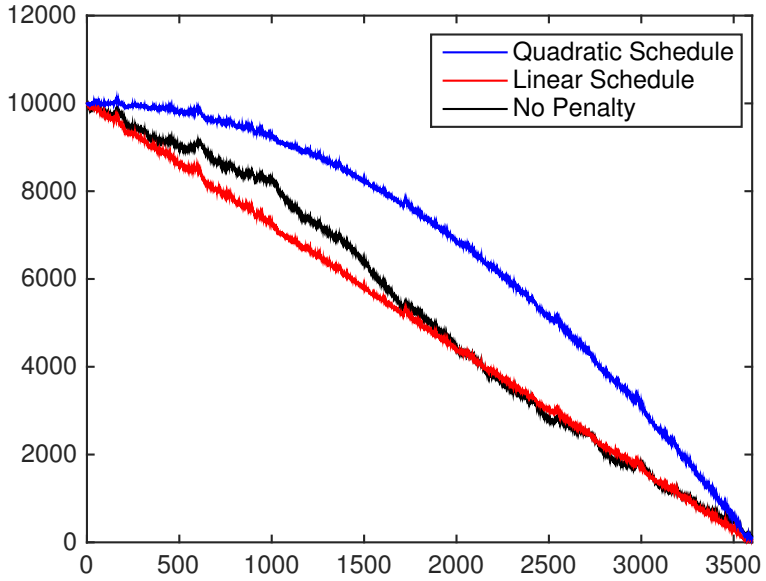

Figure 5.5: The improvement to schedule following with a small, time-uniform penalty $w(t) = 10^{-4}\,\forall\, t$. Other parameters are $x_0 = 10,000$, $T = 3,600$, $\beta_1 = 5 \cdot 10^{-4}$, $\beta_2 = 10^{-4}$, $\eta_0 = 0.05$, $\gamma = 2.5 \cdot 10^{-7}$, $\eta_1 = 0.1$, $\eta_2 = 0.08$, $\mu = 10^{-6}$, $\sigma = 0.005$, $\rho = -0.2$, $m_0 = 8.\bar{3}$, and $m_1 = 3$. Superimposed are an unpenalized time series (blue), a time series targeting TWAP (red) and a time series targeting $Q(t) = x_0\left[1 - \left(\frac{t}{T}\right)^2\right]$. The x-axis marks the time in seconds, while the y-axis marks the position size in shares.

In practice, traders may be given guidance to follow the time-deterministic schedule, such as the one in Almgren and Chriss (2000). Our model allows a trader to quantitatively

evaluate the cost of deviating from schedule. Here, we illustrate the allocation of market and limit orders over time accounting for the penalty of schedule deviation. Figure 5.5 displays the trader's stock holdings over time in three settings: (i) a quadratic schedule defined by $Q(t) = x_0 \left[1 - \left(\frac{t}{T}\right)^2\right]$, and (ii) a linear schedule $Q(t) = x_0 \left(1 - \frac{t}{T}\right)$, and (iii) no schedule (wherein we set $w(t) \equiv 0$). As we can see, the trader's position persistently tracks the schedule over the trading horizon, even with a small constant penalization coefficient $w(t) = 10^{-4}$. Compared to the linear schedule, the quadratic schedule is useful for an institution that seeks to start out trading slowly and eventually speed up at the end of the sell program. We see that our model is capable of handling complicated non-linear schedules for stock holdings over time.

We examine the effects on trading rates in Figure 5.6. On the left panel, there is no penalty for deviating from the linear schedule, while on the right we give a small penalty for deviating. We find that the penalized allocator trades much more quickly and reacts more quickly to price movements. Indeed, the non-penalized trading rates are very stable until the very end of the sell program and the penalized trading rates change rapidly over time. In contrast, the total trading rate in the non-penalized case (right panel) is fluctuating in a relatively small range. In the penalized case, more market orders are used over time, but the opposite is true when the penalty is removed.

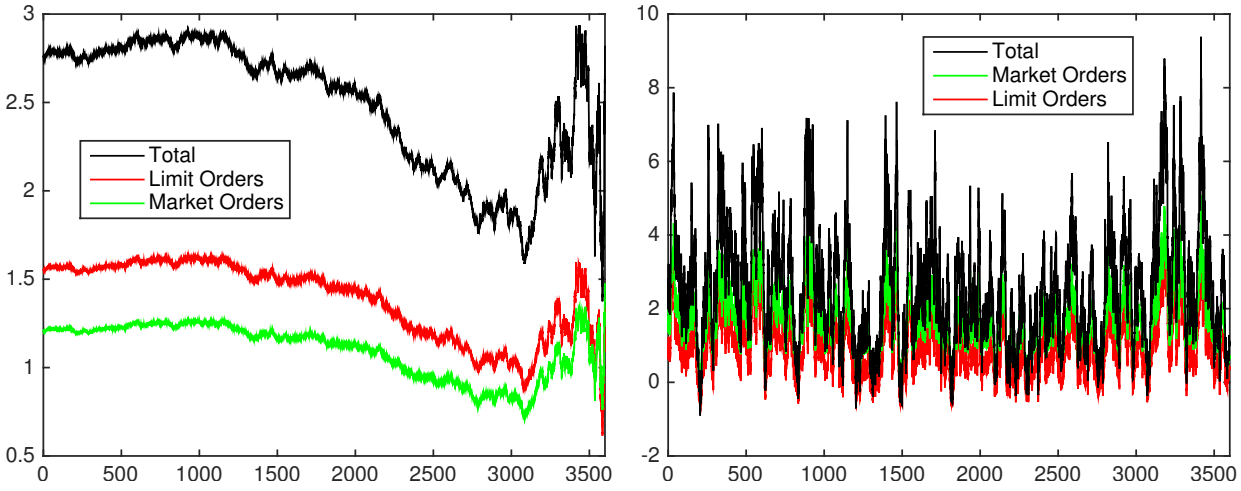

Figure 5.6: Comparison of trading rates with (left) and without penalty (right). In the penalized case, we penalize deviations from a linear schedule with constant weight $w(t) = 10^{-4}$. Other parameters are $x_0 = 10,000$, $T = 3,600$, $\beta_1 = 5 \cdot 10^{-4}$, $\beta_2 = 10^{-4}$, $\eta_0 = 0.05$, $\gamma = 2.5 \cdot 10^{-7}$, $\eta_1 = 0.1$, $\eta_2 = 0.08$, $\mu = 10^{-6}$, $\sigma = 0.005$, $\rho = -0.2$, $m_0 = 8.\bar{3}$, and $m_1 = 3$. Final positions are 190.4408 and 94.4218, respectively. The x-axis marks the time in seconds, while the y-axis marks the trading rate in shares/sec.

Bibliography

Ahn, D. and Gao, B. (1999). A parametric nonlinear model of term structure dynamics. *The Review of Financial Studies*, 12(4):721–762.

Alexander, C. and Barbosa, A. (2008). Hedging index exchange traded funds. *Journal of Banking and Finance*, 32(2):326–337.

Alexander, C. and Korovilas, D. (2013). Volatility exchange-traded notes: Curse or cure? *The Journal of Alternative Investments*, 16(2):52–70.

Almgren, R. and Chriss, N. (2000). Optimal execution of portfolio transactions. *Journal of Risk*, 3:5–39.

Avellaneda, M. and Stoikov, S. (2008). High-frequency trading in a limit order book. *Quantitative Finance*, 8(3):217–224.

Avellaneda, M. and Zhang, S. (2010). Path-dependence of leveraged ETF returns. *SIAM Journal of Financial Mathematics*, 1(2):586–603.

Bamberg, G. and Wagner, N. (2000). Equity index replication with standard and robust regression estimators. *OR Spektrum*, 22(4):525–543.

Baur, D. G. (2012). Asymmetric volatility in the gold market. *The Journal of Alternative Investments*, 14(4):26–38.

Baur, D. G. (2013). Exchange-traded funds on gold - a free lunch? *FIRN Research Paper*.

Baur, D. G. and McDermott, T. K. (2010). Is gold a safe haven? International evidence. *Journal of Banking and Finance*, 34(8):18861898.

Bertsimas, D. and Lo, A. (1998). Optimal control of execution costs. *Journal of Financial Markets*, 1(1):1–50.

Black, F. (1976). Studies of stock price volatility changes. In *Proceedings of the 1976 Meetings of the American Statistical Association, Business and Economics Statistics Section*, pages 177–181.

Black, F. and Scholes, M. (1973). The pricing of options and corporate liabilities. *The Journel of Political Economy*, 81(3):637–654.

Bulthuis, B., Concha, J., Leung, T., and Ward, B. (2017a). Fast and precautious: Order controls for trade execution. *Risk Magazine*, pages 84–89.

Bulthuis, B., Concha, J., Leung, T., and Ward, B. (2017b). Optimal execution of limit and market orders with trade director, speed limiter, and fill uncertainty. *Journal of Financial Engineering*.

Cartea, A. and Jaimungal, S. (2015). Optimal execution with limit and market orders. *Quantitative Finance*, 15(8):1279–1291.

Cartea, A. and Jaimungal, S. (2016). A closed-form execution strategy to target volume weighted average price. *SIAM Journal of Financial Mathematics*, 7(1):760–785.

Cartea, A., Jaimungal, S., and Penalva, J. (2015). *Algorithmic and High-Frequency Trading*. Cambridge University Press, 1st edition.

Cheng, M. and Madhavan, A. (2009). The dynamics of leveraged and inverse exchange-traded funds. *Journal of Investment Management*, 7(4):43–62.

Cheng, X., Di Giacinto, M., and Wang, T. (2017). Optimal execution with uncertain order fills in Almgren-Chriss framework. *Quantitative Finance*, 17(1):55–69.

Cox, J. C., Ingersoll, J. E., and Ross, S. A. (1985). A theory of the term structure of interest rates. *Econometrica*, 53(2):385–408.

Deng, G., McCann, C., and Wang, O. (2012). Are VIX futures ETPs effective hedges? *The Journal of Index Investing*, 3(3):35–48.

Duffie, D. and Kan, R. (1996). A yield-factor model of interest rates. *Mathematical Finance*, 6(4):379–406.

Dunis, C. L., Laws, J., Middleton, P. W., and Karathanasopoulos, A. (2013). Nonlinear forecasting of the gold miner spread: An application of correlation filters. *Intelligent Systems in Accounting, Finance and Management*, 20(4):207–231.

Edirisinghe, N. C. P. (2013). Index-tracking optimal portfolio selection. *Quantitative Finance Letters*, 1(1):16–20.

Feller, W. (1951). Two singular diffusion problems. *The Annals of Mathematics*, 54(1):173–182.

Ghosh, D., Levin, E. J., MacMillan, P., and Wright, R. E. (2004). Gold as an inflation hedge? *Studies in Economics and Finance*, 22(1):1–25.

Grübichler, A. and Longstaff, F. (1996). Valuing futures and options on volatility. *Journal of Banking and Finance*, 20(6):985–1001.

Guedj, I., Li, G., and McCann, C. (2011). Futures-based commodities ETFs. *The Journal of Index Investing*, 2(1):14–24.

Guilbaud, F. and Pham, H. (2013). Optimal high-frequency trading with limit and market orders. *Quantitative Finance*, 13(1):79–94.

Guo, K. and Leung, T. (2015). Understanding the tracking errors of commodity leveraged ETFs. In Ludkovski, M., Sircar, R., and Aid, R., editors, *Commodities, Energy, and Environmental Finance, Fields Institute Communications*, pages 39–63. Springer.

Guo, K. and Leung, T. (2017). Understanding the non-converge of agricultural futures via stochastic storage costs and timing options. *Journal of Commodity Markets*.

Heston, S. L. (1993). A closed-form solution for options with stochastic volatility with applications to bond and currency options. *Review of Financial Studies*, 6(2):327–343.

Holzhauer, H., Lu, X., McLeod, R. W., and Mehran, J. (2013). Bad news bears: Effects of expected market volatility on daily tracking error leveraged bull and bear ETFs. *Managerial Finance*, 39(12):1169–1187.

Husson, T. and McCann, C. (2011). The VXX ETN and volatility exposure. *PIABA Bar Journal*, 18(2):235–252.

Ivanov, S. (2013). The influence of ETFs on the price discovery of gold, silver and oil. *Journal of Economics and Finance*, 37(3):453–462.

Jarrow, R. (2010). Understanding the risks of leveraged ETFs. *Finance Research Letters*, 7(3):135–139.

Kladivko, K. (2007). Maximum likelihood estimation of the Cox-Ingersoll-Ross process: the MATLAB implementation. Technical Computing Prague.

Lee, K. (2008). Risk minimization under budget constraints. *The Journal of Risk Finance*, 9(1):71–80.

Lehalle, C. and Laruelle, S. (2013). *Market Microstructure in Practice*. World Scientific Publishing Company, 1st edition.

Leung, T., Li, J., Li, X., and Wang, Z. (2016a). Speculative futures trading under mean reversion. *Asia-Pacific Financial Markets*, 23(4):281304.

Leung, T. and Li, X. (2015). Optimal mean reversion trading with transaction costs and stop-loss exit. *International Journal of Theoretical and Applied Finance*, 18(3):1550020.

Leung, T. and Li, X. (2016). *Optimal Mean Reversion Trading: Mathematical Analysis and Practical Applications*. World Scientific, Singapore.

Leung, T., Lorig, M., and Pascucci, A. (2016b). Leveraged ETF implied volatilities from ETF dynamics. *Mathematical Finance*.

Leung, T. and Park, H. (2016). Long-term growth rate of expected utility for leveraged ETFs: Martingale extraction approach. *Working Paper*. Available at `https://ssrn.com/abstract=2879976`.

Leung, T. and Santoli, M. (2016). *Leveraged Exchange-Traded Funds: Price Dynamics and Options Valuation*. Springer Briefs in Quantitative Finance, Springer.

Leung, T. and Sircar, R. (2015). Implied volatility of leveraged ETF options. *Applied Mathematical Finance*, 22(2):162–188.

Leung, T. and Ward, B. (2015). The golden target: Analyzing the tracking performance of leveraged gold ETFs. *Studies in Economics and Finance*, 32(3):278–297.

Leung, T. and Ward, B. (2017). Dynamic index tracking and risk exposure control using derivatives. *Working Paper*. Available at `https://ssrn.com/abstract=2976500`.

Li, J. (2016). Trading VIX futures under mean reversion with regime switching. *Journal of Financial Engineering*, 03(03):1650021.

Mencía, J. and Sentana, E. (2013). Valuation of VIX derivatives. *Journal of Financial Economics*, 108(2):367–391.

Murphy, R. and Wright, C. (2010). An empirical investigation of the performance of commodity-based leveraged ETFs. *The Journal of Index Investing*, 1(3):14–23.

Naylor, M., Wongchoti, U., and Gianotti, C. (2011). Abnormal returns in gold and silver exchange traded funds. *The Journal of Index Investing*, 2(2):96–103.

Pavlova, I. and Daigler, R. T. (2008). The nonconvergence of vix futures at expiration. *Review of Futures Markets*, 17(2):201–223.

Primbs, J. and Sung, C. (2008). A stochastic receding horizon control approach to constrained index tracking. *Asia-Pacific Financial Markets*, 15(1):3–24.

Rompotis, G. G. (2011). Predictable patterns in ETFs' return and tracking error. *Studies in Economics and Finance*, 28(1):14–35.

Smales, L. A. (2015). Asymmetric volatility response to news sentiment in gold futures. *Journal of International Financial Markets, Institutions & Money*, 34:161–172.

Triantafyllopoulos, K. and Montana, G. (2011). Dynamic modeling of mean-reverting spreads for statistical arbitrage. *Computational Management Science*, 8(1):23–49.

Uhlenbeck, G. E. and Ornstein, L. S. (1930). On the theory of the brownian motion. *Physical Review*, 36(5):823–841.

Whaley, R. E. (2013). Trading volatility: At what cost? *The Journal of Portfolio Management*, 40(1):95–108.

Yao, D., Zhang, S., and Zhou, X. (2006). Tracking a financial benchmark using a few assets. *Operations Research*, 54(2):232–246.

Appendix

In this Appendix, we provide a few proofs and derivations of the various formulas stated in Chapter 4.

A.1 Derivation of SDE (4.1.5)

By Ito's formula, the option price satisfies the SDE

$$dc_t^{(k)} = \frac{\partial c^{(k)}}{\partial t}dt + dM_t^\intercal \nabla c^{(k)} + \frac{1}{2} dM_t^\intercal \nabla^2 c^{(k)} dM_t. \tag{A.1.1}$$

Here, the gradient and Hessian are taken with respect to all market variables, $(S, Y^{(1)}, ..., Y^{(d)})$. We rewrite the last term in (A.1.1) as follows:

$$\begin{aligned} dM_t^\intercal \nabla^2 c^{(k)} dM_t &= (\widetilde{\gamma}_t dt + \Sigma_t dB_t^{\mathbb{Q}})^\intercal \nabla^2 c^{(k)} (\widetilde{\gamma}_t dt + \Sigma_t dB_t^{\mathbb{Q}}) \\ &= \left(dB_t^{\mathbb{Q}}\right)^\intercal \Sigma_t^\intercal \nabla^2 c^{(k)} \Sigma_t dB_t^{\mathbb{Q}} \\ &= \mathrm{Tr}\left[\left(dB_t^{\mathbb{Q}}\right)^\intercal \Sigma_t^\intercal \nabla^2 c^{(k)} \Sigma_t dB_t^{\mathbb{Q}}\right], \end{aligned} \tag{A.1.2}$$

where we have used the property that a scalar is equal to its own trace. Using that along with the cyclic property of the trace, we have

$$\begin{aligned} dM_t^\intercal \nabla^2 c^{(k)} dM_t &= \mathrm{Tr}\left[\Sigma_t^\intercal \nabla^2 c^{(k)} \Sigma_t dB_t^{\mathbb{Q}} \left(dB_t^{\mathbb{Q}}\right)^\intercal\right] \\ &= \mathrm{Tr}\left[\Sigma_t^\intercal \nabla^2 c^{(k)} \Sigma_t \mathbf{I} dt\right] = \mathrm{Tr}\left[\Sigma_t^\intercal \nabla^2 c^{(k)} \Sigma_t\right] dt. \end{aligned} \tag{A.1.3}$$

Substituting (A.1.3) into (A.1.1), we obtain

$$dc_t^{(k)} = \left(\frac{\partial c^{(k)}}{\partial t} + \frac{1}{2}\,\mathrm{Tr}\left[\Sigma_t^\intercal \nabla^2 c^{(k)} \Sigma_t\right]\right) dt + \frac{\partial c^{(k)}}{\partial S} dS_t + \frac{\partial c^{(k)}}{\partial Y^{(1)}} dY_t^{(1)} + ... + \frac{\partial c^{(k)}}{\partial Y^{(d)}} dY_t^{(d)}. \tag{A.1.4}$$

On the other hand, the Feynman-Kac formula tells us that the derivative price satisfies

$$\frac{\partial c^{(k)}}{\partial t} + \widetilde{\gamma}_t^{(0)} \frac{\partial c^{(k)}}{\partial S} + \widetilde{\gamma}_t^{(1)} \frac{\partial c^{(k)}}{\partial Y^{(1)}} + ... + \widetilde{\gamma}_t^{(d)} \frac{\partial c^{(k)}}{\partial Y^{(d)}} + \frac{1}{2}\,\mathrm{Tr}\left[\Sigma_t^\intercal \nabla^2 c^{(k)} \Sigma_t\right] = r c^{(k)}, \tag{A.1.5}$$

with the terminal condition: $c^{(k)}(T_k, s, y^{(1)}, ..., y^{(d)}) = h^{(k)}(s, y_1, ..., y_d)$ for all vectors $(s, y_1, ..., y_d)$ with strictly positive components. Using (A.1.4), we have

$$\begin{aligned} dc_t^{(k)} = &\left(r c_t^{(k)} - \widetilde{\gamma}_t^{(0)} \frac{\partial c^{(k)}}{\partial S} - \widetilde{\gamma}_t^{(1)} \frac{\partial c^{(k)}}{\partial Y^{(1)}} - ... - \widetilde{\gamma}_t^{(d)} \frac{\partial c^{(k)}}{\partial Y^{(d)}}\right) dt \\ &+ \frac{\partial c^{(k)}}{\partial S} dS_t + \frac{\partial c^{(k)}}{\partial Y^{(1)}} dY_t^{(1)} + ... + \frac{\partial c^{(k)}}{\partial Y^{(d)}} dY_t^{(d)}. \end{aligned}$$

Dividing both sides by $c_t^{(k)}$ and using the definitions listed in (4.1.6), we obtain SDE (4.1.5).

A.2 Validation of (4.3.10) when Mean-Reversion Speeds are Equal

We now demonstrate that, in the special case of $\widetilde{\kappa} = \widetilde{\gamma}$ under the CSQR model, tracking strategies exist using two futures on S of different maturities. The elasticity with respect to the index is the same as in (4.3.9); however, the elasticity with respect to the stochastic

mean is

$$H_t^{(k)} = \frac{Y_t}{f_t^{T_k}} \frac{\partial f_t^{T_k}}{\partial Y} = \frac{Y_t}{f_t^{T_k}} \widetilde{\gamma} e^{\widetilde{\kappa} t - \widetilde{\gamma} T_k} (T_k - t). \tag{A.2.1}$$

Substituting (A.2.1) into (4.3.10), we have

$$\begin{aligned} &\frac{S_t}{f_t^{T_1}} e^{-\widetilde{\gamma}(T_1 - t)} \frac{Y_t}{f_t^{T_2}} \widetilde{\gamma} e^{\widetilde{\kappa} t - \widetilde{\gamma} T_2} (T_2 - t) \neq \frac{S_t}{f_t^{T_2}} e^{-\widetilde{\gamma}(T_2 - t)} \frac{Y_t}{f_t^{T_1}} \widetilde{\gamma} e^{\widetilde{\kappa} t - \widetilde{\gamma} T_1} (T_1 - t) \\ \iff & e^{-\widetilde{\gamma}(T_1 - t)} e^{\widetilde{\kappa} t - \widetilde{\gamma} T_2} (T_2 - t) \neq e^{-\widetilde{\gamma}(T_2 - t)} e^{\widetilde{\kappa} t - \widetilde{\gamma} T_1} (T_1 - t) \iff T_1 \neq T_2. \end{aligned}$$

Under the assumption that $T_1 < T_2$, the resulting system is solvable and yields strategies that achieve the given exposures.

A.3 Solution to (4.3.11) when Mean-Reversion Speeds are Equal

With the elasticity with respect to the stochastic mean given by (A.2.1) and $\widetilde{\kappa} = \widetilde{\gamma}$ under the CSQR model, the portfolio weights that solve system (4.3.11) are

$$u_t^{(1)} = \frac{\beta f_t^{T_1}}{S_t} \left(\frac{e^{\widetilde{\gamma}(T_1 - t)} (T_2 - t)}{T_2 - T_1} \right) - \frac{\eta f_t^{T_1}}{Y_t} \left(\frac{e^{\widetilde{\gamma}(T_1 - t)}}{\widetilde{\gamma}(T_2 - T_1)} \right),$$

and

$$u_t^{(2)} = \frac{-\beta f_t^{T_2}}{S_t} \left(\frac{e^{\widetilde{\gamma}(T_2 - t)} (T_1 - t)}{T_2 - T_1} \right) + \frac{\eta f_t^{T_2}}{Y_t} \left(\frac{e^{\widetilde{\gamma}(T_2 - t)}}{\widetilde{\gamma}(T_2 - T_1)} \right).$$

In particular, take $\beta = 1$ and $\eta = 0$. Then, the portfolio weights simplify to

$$u_t^{(1)} = \frac{f_t^{T_1}}{S_t} \left(\frac{e^{\widetilde{\gamma}(T_1 - t)} (T_2 - t)}{T_2 - T_1} \right), \quad \text{and} \quad u_t^{(2)} = \frac{-f_t^{T_2}}{S_t} \left(\frac{e^{\widetilde{\gamma}(T_2 - t)} (T_1 - t)}{T_2 - T_1} \right).$$

By inspection, $u_t^{(1)}$ is positive while $u_t^{(2)}$ is negative.

A.4 Validation of (4.3.10) when Mean-Reversion Speeds are Unequal

We substitute the elasticities from (4.3.9) into (4.3.10), and then check directly whether or not the following holds:

$$\frac{S_t}{f_t^{T_1}} e^{-\widetilde{\gamma}(T_1-t)} \frac{Y_t}{f_t^{T_2}} \frac{\widetilde{\gamma}}{\widetilde{\gamma}-\widetilde{\kappa}} \left(e^{-\widetilde{\kappa}(T_2-t)} - e^{-\widetilde{\gamma}(T_2-t)}\right) \neq \frac{S_t}{f_t^{T_2}} e^{-\widetilde{\gamma}(T_2-t)} \frac{Y_t}{f_t^{T_1}} \frac{\widetilde{\gamma}}{\widetilde{\gamma}-\widetilde{\kappa}} \left(e^{-\widetilde{\kappa}(T_1-t)} - e^{-\widetilde{\gamma}(T_1-t)}\right)$$

$$\iff e^{-\widetilde{\gamma}T_1} \left(e^{-\widetilde{\kappa}(T_2-t)} - e^{-\widetilde{\gamma}(T_2-t)}\right) \neq e^{-\widetilde{\gamma}T_2} \left(e^{-\widetilde{\kappa}(T_1-t)} - e^{-\widetilde{\gamma}(T_1-t)}\right) \iff T_1 \neq T_2.$$

Since we assume $T_1 < T_2$, the resulting system is solvable and allows for strategies to attain the required exposures.